BIOMIMICRY AND BIOMIMETIC DESIGN:

IMPROVING THERMOREGULATION OF BUILDINGS THROUGH ROOF DESIGNS IN HOT AND ARID CLIMATES

CAMILLE SEGAERT

MASTER THESIS SUBMITTED UNDER THE SUPERVISION OF

PROF. DR. IR. ARCH. URB. AHMED Z. KHAN

WITH THE ADVICES OF

PROF. DR. IR. ARCH. FILIP DESCAMPS

IN ORDER TO BE AWARDED THE MASTER'S DEGREE IN

ARCHITECTURAL ENGINEERING

BRUSSELS FACULTY OF ENGINEERING

ACADEMIC YEAR 2019-2020

Preface

"This Master's thesis came about (in part) during the period in which higher education was subjected to a lockdown and protective measures to prevent the spread of the COVID-19 virus. The process of formatting, data collection, the research method and/or other scientific work the thesis involved could therefore not always be carried out in the usual manner. The reader should bear this context in mind when reading this Master's thesis, and also in the event that some conclusions are taken on board."

Acknowledgements

Abstract

This master thesis was submitted by Camille Segaert in order to be awarded the master's degree in Architectural Engineering at the Brussels Faculty of Engineering (BruFACe), during the academic year 2019-2020. The title of the thesis reads as follows: Biomimicry and biomimetic design: Improving thermoregulation of buildings through roof designs in hot and arid climates.

The inefficiency of buildings to thermoregulate their indoor conditions is the direct consequence of the rising dependency on mechanical cooling and heating systems used to achieve thermal comfort of their occupants. In hot and arid climate regions, 70 to 80 percent of the electricity consumption is due to cooling energy demand, resulting for some countries in an unusual increase in electricity blackouts observed in the past decades. In the same regions, the roof surface accounts for half of the heat load entering the building and resulting in overheating and discomfort. In nature, thermoregulation is the feature that most closely links the building envelopes we create with biology, whereas nature presents solutions to this very problem through millions of years of evolution.

Consequently, this master thesis explores the potential of biomimetic and thermoregulating roof designs in enhancing energy performance of buildings in hot and arid climate regions. First, the climatic context of the thesis is delineated and a set of biological role models relevant to thermoregulation in architecture assembled. The literature research is completed by an analysis of the weaknesses inherent to existing roof compositions and solar exposition particular to hot climates. Then, an in-depth review of the classical roof typologies found in the literature leads to the conduction of an explorative roof design classification offering an extension of the state-of-the-art on roof typologies with concern for performance and innovative cooling strategies. The identification of these thermoregulating roof typologies is boiled down to three roof classes later further detailed in sub-classes: the protective, selective, and vernacular roof typology. Subsequently, seven case studies relevant to the architectural expression of roof designs, biomimicry, or roof cooling strategies are assessed comparatively through a specific combination of the defined roof typologies incorporated in an embodied performance scheme. Finally, six theoretically promising roof typologies are explored by simulation with *EnergyPlus* and *DIVA for Rhino*, and applied to the flat roof of a typical school building in Egypt. The roof typologies are explored quantitatively in terms of energy demand and temperature of the classrooms and are sub-divided into the *ventilated roof,* the *cool roof* and *cool roof on ventilation cavity*, the *self-shaded roof* and *self-shaded roof on ventilated cavity*, and finally the *vegetated* or *living roof.* From these examples, numerous demonstrate the potential of biomimicry in thermoregulation through roof design. First, the ventilated roof design can be greatly improved by inclination of the surface as thought by the black-tailed prairie dog burrows. Also, the cool roof and the self-shaded roof show the most promising results and are respectively inspired by the light-coloured desert snail and the ribbed desert cactus. Based on additional criteria of cost, availability, maintenance and longevity, the vegetated roof revealed to be overrated performatively compared to the high cost and maintenance need. On the other hand, the cool roof is given a new interest because of its great impact, simplicity and affordability. In the end, a proposal for further research encourages the application of biomimicry in the field of thermoregulation of buildings and building envelopes.

Key words: Architecture, sustainability, biomimicry, thermoregulation, roof cooling strategies, roof classification, Energy Performance of Buildings, EnergyPlus, hot climate.

Table of contents

List of figures

List of tables

List of acronyms

CDD	Cooling Degree Days	**LiDAR**	Light Detection and Ranging
CGI	Corrugated Galvanized Iron sheeting	**NV**	Natural Ventilation
GAEB	General Authority of Educational Buildings	**PV**	Photovoltaic
KCC	Köppen's Climate Classification	**RC**	Radiative Cooling
LCA	Life Cycle Analysis	**SC**	Scenario (followed by a scenario numbering)

Chapter 1

Introduction

This master thesis explores the potential of roof designs as thermoregulation strategy inspired by biological role models in enhancing energy performance of buildings in hot and arid climate regions. In this first chapter, the problem statement introduces the research goals and questions tackled in the research. Then, the research methodology is depicted followed by the master thesis outline.

1.1. Problem statement

In a context of ecological age, concern for energy consumption has risen significantly in the last few decades. Whereas the future is to sustainable solutions, the present construction sector in Europe is still responsible for no less than one third (31%) of the resource consumptions of the continent (SERI, GLOBAL 2000, & Friends of the Earth Europe, 2009). In addition to the material needs for the construction of a building, the operational energy demand represents a high part of its total life cycle energy. In particular, the heating and cooling periods of a building are critical. Today, thermal comfort is achieved by compensation of the outdoor temperature fluctuations with mechanical cooling and heating systems. Historically, awareness of this dependency of generated power emerged with the writings of Olgyay and Banham in the late 1960s and was only addressed worldwide after the energy crises in the 1970s (Abdellfattah Elsayed, 2016). Yet, it is now known that the building envelope is responsible for more than 40% of the heat losses and gains resulting in summer overheating (Barozzi, et al., 2016).

Hot and arid climate regions represent nearly one third (30.2%) of the world's land and are consequently the most widely present climate type according to the Koppen's climate classification (Peel, Finlayson, & McMahon, 2007). Not only hot climate countries experience extreme temperatures and discomfort but they are also subjected to high demands in electricity consumption resulting for some countries in an unusual increase in electricity blackouts in the past decades (EIA, 2015). Above all, cooling systems operation in these cities represents no less than 70 to 80% of the total energy consumption (Dabaieh, et al. 2014). If the problem resides in the building envelope, the high solar position in hot and arid regions results in a proportionally higher solar radiation on the roof. Indeed, the roof accounts for no less than 50% of the heat load on a building (Dilip, 2005). In architecture however, the design of this "fifth" façade is often set aside. In addition to its potential in energy performance, a few architects manage to take a building's architectural expression to another level by enhancing a roof's aesthetic or showing its structural importance. In the end, the scarce literature documentation about roof designs visibly demonstrates the lack in experimentation about this yet worthwhile topic.

Finally, thermoregulation of buildings is what makes the link between the issue of human comfort and the aim for sustainable solutions. In nature, thermoregulation or *homeostasis is the tendency for living organisms to maintain steady conditions*, and as Michael Pawlyn said, "*it is one of the features that most closely link the buildings we create with biology*" (Pawlyn, 2016). Indeed, whereas concerns for

sustainability and building performance are currently growing, nature presents a range of strongly reliable principles that tackle the same problem. Therefore, the idea of using biomimicry to improve questions of thermoregulation in architecture is evident. Biomimicry can be defined as "*the conscious emulation of life's genius*" (Benyus, 1997) or taking inspiration from features, systems, and shapes from nature to improve technologies towards a more sustainable world. As for living organisms, the skin or envelope of a building connects and separates, creates the filter and the interaction between the exterior world of nature and the interior controlled comfort of humans. Through the envelope, heat transfer can occur by convection, conduction, evaporation and radiation. The Three Tier Approach teaches that the first strategy in a hot climate region is to minimize these heat fluxes and keep the building cool by protecting it from heat gains (Khan, 2017). This research should thus also find inspiration in cooling or protecting mechanisms from nature.

Finally, the problem addressed is *the operational energy consumption of buildings in hot climates, tackled by the architectural design of roofs as part of the building envelope through biomimicry of thermoregulation principles.*

1.2.   Research goals

As was mentioned in the previous paragraph, the issue of buildings operational energy consumption is particularly problematic in hot and arid climate countries where extreme temperatures result in high cooling energy demand that is not yet supplied by renewable energy. Also, roofs were identified as the part of the envelope that is most exposed to the sun in these regions with high solar altitude. Consequently, the first research question of this thesis concerns the design problem that resides in roof designs and goes as follows:

What is the role of roofs in thermal regulation in the context of hot-arid climate zones?

To this problem, a design solution is proposed along with the field of biomimicry and thermoregulation. The central question in this master thesis is:

How to develop sustainable, energy-efficient roof design principles and strategies using a biomimetic approach.

As this thesis is submitted in the field of Architectural Engineering, the design solutions analysed in this work will take into account the aesthetics and comfort of use. The potential of roof design as a fifth façade in terms of architectural expression will also be taken into account in the discussion. An additional question arises:

How can attention to roof designs help improve the architectural expression of buildings?

In addition to architecture, questions of cost, availability, maintenance and longevity will play a role in the assessment and validation of the different designs analysed and proposed. In default of performing a Life Cycle Assessment (LCA) on the explored designs, these questions will still be tackled in a qualitative rather than quantitative way through argumentation.

Finally, as a consequence of the lack of literature available on roof designs based on performance and cooling strategies for hot and arid climate zones, a sub-objective was added to the previous research questions i.e. the development of a performance-oriented classification of roof typologies. In other words, *what are the design strategies that can be applied to roofs in a hot and arid climate?* Moreover, *what can be learned about roof designs from case studies and biomimetic concepts?*

1.3.   Research methodology

First of all, the thesis will be based on a broad literature research on the subject of thermoregulation in hot climates, biomimicry, and finally roof designs. This chapter will enable answering the question linked to the design problem and identifying the role of roofs for thermoregulation in hot climates. In terms of biomimicry, this will be the opportunity to identify biological role models that will be useful for inspiration and finally improvement of the solution proposed. Also, levels of biomimicry will be identified in order to understand to which extend examples and proposals used in this thesis are inspired by nature.

From a focused literature research on existing roof typologies, a classical roof classification will be detailing the archetypes currently used to define roof designs. However, a new performance-based classification (taxonomy) will be created exploratively, addressing the energy performance and consequently enabling a more accurate definition and comparison of further case studies and design proposals.

Then, the case study analysis will be performed in an individual and comparative way based on a set of parameters. Here, both unrealized designs and constructions will be analysed with attention to architecture and how roof designs can show great potential to a building's architectural expression. The roof design taxonomy built on in Chapter three will constitute a reference classification able to redefine and compare the case studies in a performative way. If applicable, the level of biomimicry and biological role model used in a reference design will be identified as defined in the literature review. However, the emulation of an organism inherent to biomimetic design requires advanced knowledge in the field of biology. Consequently, although biomimicry is not one of the determining parameters assessing the research outcomes, it will play a consulting role leading the thesis.

Once theoretical argumentation is built, a more empirical approach can be initiated with a research by design methodology in Chapter five. Here, hypotheses based on biomimetic added values will lead to different scenarios that can be simulated and compared in terms of thermoregulating performance. These will thus be evaluated based on performance, but also discussed in terms of maintenance, availability and cost. Conclusions will be delineated and further research advised.

1.4.   Master thesis outline

Following the above-developed research goals and methodology, the thesis is organized into six chapters whereunder the present introduction chapter. A broad literature review is performed and discussed in Chapter 2. Here, the relevancy of biomimicry applied to roofs in hot climate regions is depicted. First, hot climates are characterized as defined by the Köppen's Climate Classification (KCC) and existing thermoregulation strategies in these climates discussed. Then, biomimetic design with its methodology and biological role models for thermoregulation are exposed. Finally, the literature research particular to roofs combined with biomimicry in hot climate regions is presented.

As a result of the lack of literature and existing classification of roof design archetypes relevant to this thesis, an explorative roof taxonomy is performed based on further literature research. This leads to the discussion of relevant case studies in chapter four based on climate, roof design, biomimicry, architectural expression and above all, performance referring to the developed taxonomy. After having pointed out the advantages of existing technologies and designs, a series of design scenarios are proposed based on hypotheses and explored by simulation on EnergyPlus. Finally, the results are evaluated in terms of energy performance and discussed in terms of architecture, cost, longevity and

availability. A comparison between the four design proposals and their design variations is performed at the end of the chapter. Finally, chapter six discusses the objectives and achievements, the limitations and contribution of the thesis, and suggests future research on the subject.
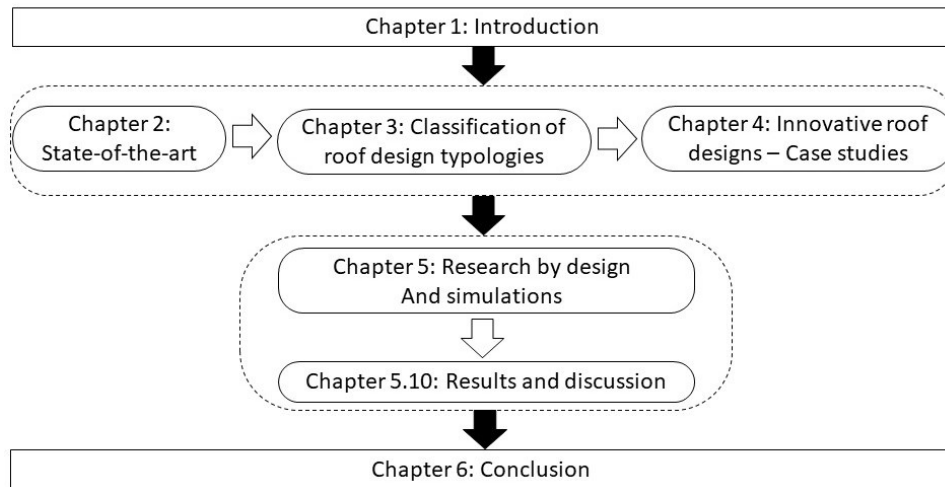
Figure 1: Master thesis outline scheme.

Chapter 2

State-of-the-art

The second chapter provides an overview of the existing literature about building thermoregulation performance improved by roof designs in hot and arid climates using a biomimetic approach. First of all, the context of hot climate is situated and characterized by the KCC and the choice defended by the existing relationship with energy consumption, electricity blackouts and uncomfortable temperatures. Then, the notion of biomimicry is introduced more thoroughly and design approaches defined. When these choices are settled, a state-of-the-art is provided for the existing individual associations between thermoregulation, roof designs and biomimicry in the context of hot and arid climate regions.

2.1. Hot and arid climate

2.1.1. Koppen's classification

The Köppen's climate classification was formulated hundred years ago by Wladimir Köppen and has been verified since then by many successors in the field. The classification is based on a wide range of global data set of long-term monthly measurements, enabling a reliable categorization of regions into five major climate groups defined by both precipitation and temperature thresholds. This way, zones and regions can be assigned to type A tropical, type B arid (hot and dry), type C temperate, type D continental, or type E, the polar climate (Peel, et al., 2007). Each type is then further classified into sub-climate types. The hot and arid climate type B can be subdivided into four arid zones: BWh, BWk, BSh and BSk where the two first letters depend on Mean Annual Precipitation thresholds. The last letter defines whether the climate presents higher mean annual temperatures than 18°C or if the mean temperature drops below 18°C. Although climate type A is not of an arid type and is characterized by high humidity levels (Khan, 2017), the tropical climate zones experience temperatures above 18°C all year long and can be defined as hot climate zones as well. For a more detailed definition of the different sub-climate types, the reader can consult **Appendix A.1**.

When looking at the climate classification map (**Figure 2**), and according to Peel et al. working on the updated Köppen-Geiger climate classification, Africa and Australia are the two continents presenting predominantly a hot and arid climate type (B) with respectively 57.2% and 77.8% of the land surface verifying the criteria. Besides, the hot and arid climate is predominant as it represents nearly one third of the world's land (30.2%) where hot desert climate BWh is the most present type worldwide (14.2%).

In the context of this thesis, the Köppen-Geiger climate classification is a useful tool to determine which climate type the reference examples and case studies experience. Although the focus is laid on hot climate type B, passive cooling strategies applied on roofs will also be of relevance for hot climate type

A as well as for temperate C climates, both having a summer cooling need and therefore presenting relevant building cooling strategies. Whereas hot and humid climates (A) experience stable conditions of warm to hot temperatures, hot and arid climates (B) are characterized by great temperature fluctuations (Khan, 2017). However, as for a tropical climate (type A) the main cooling strategy in bioclimatic design is only to enhance air movement at all times, a broader range of strategies can be explored with the arid climate type (B).
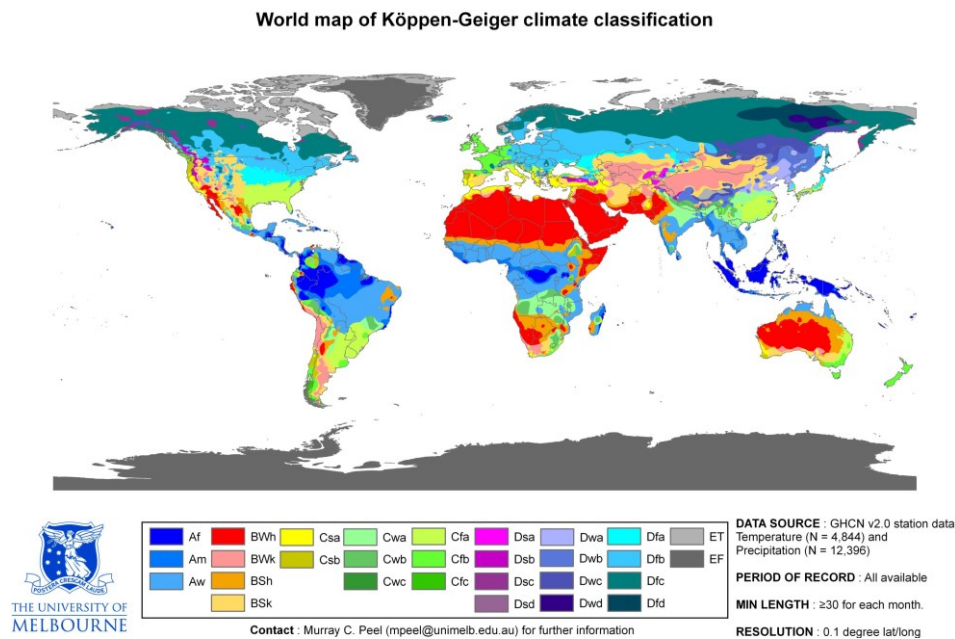
Figure 2: World map of Köppen-Geiger climate classification. (Peel, Finlayson, & McMahon, 2007)

2.1.2. Electricity consumption

Hot climates, both humid and arid, are characterized by a cooling period excessing the heating period (Khan, 2017). Moreover, climate types A and B stand out by a high demand in cooling energy need. In order to illustrate their energy use, **Figure 3** shows the distribution of this cooling demand worldwide in terms of annual Cooling Degree-Days (CDD) set at 18.3°C. It is a measurement for the difference between a day's average temperature and the threshold of 18.3°C, summed to an annual value. Above that threshold, studies have shown that people no longer want to heat their building but rather consider cooling it (Gordon, 2019). According to Mourshed et al., the warmest regions and consequently highest CDD lie between 30° S and 30° N latitudes. Note that the values exceeding 0°C-day (dark blue) and reaching up to 4701°C-days (dark red) coincide with the Köppen-Geiger world map of the two hot climate types A and B situated in between the same latitudes.

Exploring passive means for cooling a building becomes a challenge of great interest when it comes to saving energy consumption. In hot climate regions, cooling systems operation represents no less than 70 to 80% of the total energy consumption of cities (Dabaieh, et al., 2014). Moreover, statistics of the International Energy Agency show an increase in this energy demand of factor eight from 1980 to 2012 in Egypt (EIA, 2015). In the same country, electricity consumption has been increasing much faster than capacity expansions and cities consequently experience an unusual increase in electricity blackouts. These energy shortages combined with energy cost increase lead to an enhancing need for buildings with high energy efficiency and low environmental impact. However, the present buildings rest on excess air conditioning supply to achieve thermal comfort of the occupants, and only when affordable (Abdellfattah Elsayed, 2016).
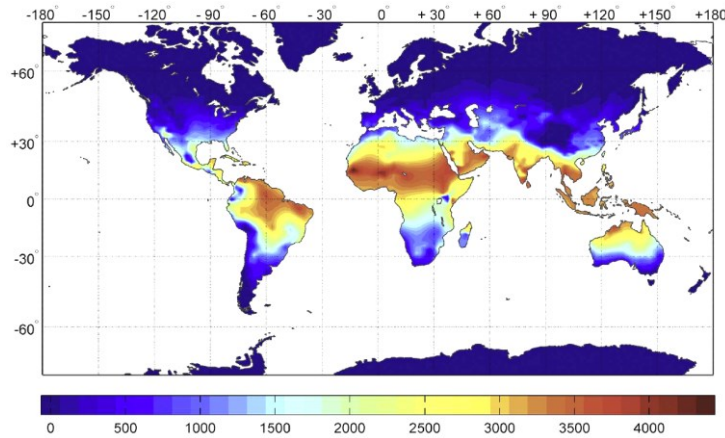
Figure 3: Distribution of annual cooling degree-days at 18.3°C, CDD 18.3 (in °C-day) (Mourshed, 2016).

2.1.3. Low income and discomfort

While addressing passive cooling strategies will improve electricity consumption in developed countries, another consequence will be the very enhancement of the comfort level in low-income countries. Indeed, compensation by mechanical cooling installations will always bring internal temperatures to a comfort level while the effect of efficient design strategies on roofs would have an impact on the living conditions of people who cannot afford these installations. Because *millions continue to live in extremely bad conditions*, it is important to address and improve their indoor environment, health and wellbeing (Butters, 2015). Additionally, according to the International Monetary Fund, these developing countries would be situated in relatively hot climates (UNFCCC, 2017). To support this, one can compare the *World by Income* map of the World Bank (**Figure 4**) with the Köppen's World Map (**Figure 2**) to observe that the relation between both is remarkable in several regions such as Africa and South Asia when represented in blue. This means that while performing research for enhanced building design in hot climate regions, special attention should be given to material costs and minimization of transportation costs through availability and use of local resources.
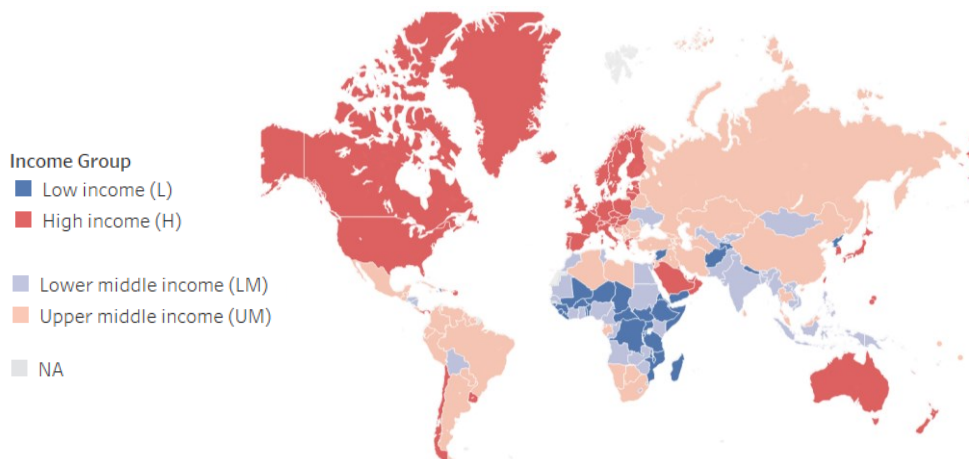
Figure 4: The World by income group. (The World Bank Group, 2020)

In a context of lack in energy amenities and rising costs in energy and fossil fuels, passive, i.e. non-mechanized solutions are to be prioritized since they simply avoid the need for fossil fuels or other bought energy, and present a robust solution with regard to use, operation and maintenance (Butters, 2015). In other words, whereas the world is to technological innovations, the innovative designs proposed in this thesis will be subjected to new criteria of cost, maintenance and longevity.

2.2. Biomimicry

2.2.1. Definition

Biomimicry also referred to as 'biomimetics' or 'bionics' gained interest since its very first introduction by Otto Schmitt in 1969. At that time, it was defined as "the science that studies the replication in human's design of natural methods and processes" (Schmitt, 1969). The word itself originates from the Greek terms "bios" and "mimesis" meaning respectively "life" and "mimicking" (Biomimicry Belgium, n.d.). Since then, definitions have matured and the use of the field has been largely promoted by scientists and biologists. Janine Benyus, founder of the Biomimicry Institute, defined Biomimicry in 1997 as "The conscious emulation of life's genius" (Benyus, 1997). Accordingly, biomimicry resides in taking features, systems and shapes from nature as a source of inspiration in order to improve technologies towards a more sustainable world. Hence, when applying biomimicry, as opposed to bio-inspiration, one has to view and value the natural world as a model, mentor, and measure (Benyus, 1997).

This year more than any year before, citizens all around the world showed their concern by taking part in numerous climate marches. In this context of ecological age, biomimicry represents above all a challenge and an opportunity to lead technology towards a durable future, aiming to erase their actual waste-oriented performance. In a present of rising living standards however, machinery improves human comfort at the expense of the increasing need for energy to power them. It is time to go back to a more sustainable way of thinking and take lessons from the most durable and zero-waste example that nature and eco-systems represent. In fact, nature offers technologies that are operating on free energy, harvest water better than any machinery, regulate their body temperature better than any building and grow their structure based on their very needs. Solutions already exist in the natural world that surrounds us and architecture, like many other fields, should apply the broad range of lessons that nature has to offer.

2.2.2. Biomimetic approaches

Several approaches exist for the application of biomimicry as a design model. First of all, two design strategies can be identified in the literature. In order to develop an innovative design inspired by nature, one can rather start from a design problem or human need and find a solution in an organism or ecosystem tackling the same issues, termed "Design looking to biology" (Top-Down approach), or start from an inspiring organism or ecosystem and find an innovative application for its properties in human designs, named "Biology influencing design" (Bottom-Up approach) (**Figure 5**).

2.2.2.1.   *Top-Down approach*

The first approach encounters several terminologies or variants in the state-of-the-art where the "Design looking to Biology" approach is further referred to as the "Top-Down approach", "Problem-Driven Biologically Inspired Design" and finally "Challenge to Biology" by the Biomimicry Institute (Aziz & El Sherif, 2016). From this range of denominations, one can easily understand how designers look to organisms and nature for solutions. Once they have defined a technical problem, designers can identify organisms or ecosystems that have solved similar problems. The most important aspect of this variant is in fact the knowledge of the researcher about the aims and weaknesses of his design target.

2.2.2.2. Bottom-Up approach

The second strategy is based on an inversed approach compared to the first one, and is referred to as the "Bottom-Up approach" or "Biology influencing design". Similarly, this approach presents a range of synonyms in the literature review. Consequently, "Solution-Driven Biologically Inspired Design" and "Biology to Design" are terms designating the same methodology. Here, the approach depends on previous knowledge of biological research and solutions which could tackle issues that are yet to be identified (Aziz & El Sherif, 2016).

2.2.2.3. Three levels of biomimicry

In addition to this twofold methodology to design with nature, three levels can be identified to biomimicry: the organism level, the behaviour level, and the ecosystem level (Aziz & El Sherif, 2016). First, the organism level illustrates the mimicking of the form of an organism or part of this organism onto a design. Secondly, the behaviour or process an organism adopts to interact with its environment can be reproduced in a design and finally, the most difficult level to mimic is the ecosystem level constituted of complex interactions between processes and organisms. When going further into detail, each level can be undertaken at a certain dimension. Five dimensions further define how nature has been mimicked in a design: by the way it looks (form), what it is made of (material), how it is made (construction), how it works (process) and what its capability is (function) (Aziz & El Sherif, 2016). These levels complete the two strategies. For an example of application of those levels of biomimicry on termite mounds, the reader is kindly requested to consult **Appendix A.2**.

This latter classification in levels of biomimicry will be a way to compare and characterize finalized designs as opposed to what is possible with the Top-Down or Bottom-Up approach which is a methodology or process of design. Designs can arise from nature models but in what way and to what detail extend are they inspired by it?
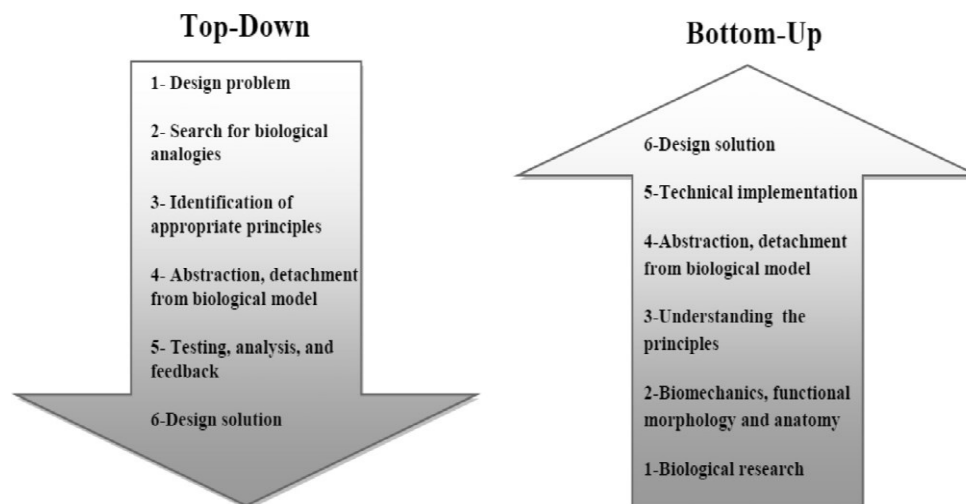
Figure 5: Biomimicry top-down and bottom-up approaches (Aziz & El Sherif, 2016).

2.3. Thermoregulation, roof designs and biomimicry

2.3.1. Thermoregulation and roof design

The thermal transmission and behaviour of a roof under high temperatures are directly related to the identification of weak points and threats delineating the thermoregulating strategies to adopt in hot climates. First of all, solar radiation falling onto a roof surface is partly reflected and partly absorbed. The latter absorbed radiation heats up the surface in combination with the surrounding hot air. Part of the heat is then lost through longwave radiation back to the atmosphere whereas the remaining heat is transferred to the room by conduction (Dilip, 2005). The conduction transfer mechanism becomes the real threat to hot climatic regions when, according to a study held in Orlando in 2016, high temperatures decrease the efficiency of roof insulation materials (Schumacher, et al., 2016). Yet, the external surface of a roof can reach more than 37°C above ambient temperature on a normal sunny day (Dabaieh, et al., 2014).

In addition to the weaknesses inherent to commonly used roof compositions, the horizontal surface would be the element of the building that is most exposed to the sun (Yannas, Erell, & Molina, 2006). When located in arid regions, the roof heated by the sun is responsible for no less than 50% of the heat load into a building (Dilip, 2005). Indeed, the dependency of the inside temperature of a house on the surface temperatures of the walls and roof was confirmed by a research on solar passive techniques for roof cooling.

The solar altitude or elevation that a location encounters will naturally play a key role in the solar radiation a surface is confronted with. Indeed, the more perpendicular the sun is to a surface, the more the sunrays will affect this surface in terms of temperature rise. The necessity of acting on the roof designs in a hot climate in particular rises from the high solar altitude and solar intensity in these regions (Mahmoud Arafa, 2012). Compared to the sun path of Brussels in summer where the sun comes up to 63°, the Egyptian sun rises nearly to 85° in altitude on June 21st (**Appendix A.3**) (Sun Earth Tools, 2009). Moreover, for Egypt and other regions situated between latitude 17 degrees North and 31 degrees North, the solar radiation is distributed over the walls and roof following **Table 1**. Accordingly, the roof receives maximum solar radiation in the summer and still a great amount of radiation in the winter. Therefore, it can be stated that special attention should be given to roofs in regions of hot climate.

	Roof	North	South	East	West
Summer	**48-51%**	3-6%	0-2%	19-20%	19-20%
Winter	**28-34%**	0%	35-44%	14-15%	14-15%

Table 1: The direct solar radiation with roof and wall surfaces equal. For latitudes 17 deg N to 31 deg N. (Gupta)

2.3.2. Architecture and biomimicry

Homeostasis, *the tendency for living organisms to maintain steady conditions, is one of the features that most closely link the buildings we create with biology* according to Michael Pawlyn (Pawlyn, 2011). However, the widespread and practical application of biomimicry in architectural design processes remains largely unrealized (Nour ElDin, et al., 2016). While nature considers the envelope of an organism as a medium, today's designed building envelopes act as barriers to the fluctuating outdoor environment to keep the temperature steady. Indeed, in today's architecture, improvements are made for Passive housing systems where the strategy relies on thermal inertia, enclosing the buildings' interior from the exterior by increasing the insulation and airtightness of the envelope (Passivhaus Institute, 2019).

On the other hand, the field of architecture slowly evolves towards a more sustainable design through the growing energy performance regulation of buildings. In addition to the operating energy, passive design strategies and total LCA gain importance in the building industry. Yet, if one wants to reduce the operational energy needs of a construction, the focus should first be laid on early passive design approaches in order to rely on free energy and minimize the need for resources to run the building. Moreover, researches about more adaptive, flexible and responsive building envelopes based on biomimetic design slowly arise. These find inspiration in organisms' ability to adapt themselves to the outdoor conditions, being able to keep their body temperature at the desired value only by using the accessible free energy of their environment.

2.3.3. Biomimicry and thermoregulation

In both methodologies discussed in **2.2.2** Biomimetic approaches, the main step remains to find analogies between nature and human needs. In the idea of viewing and valuing the natural world as a model, mentor and measure, biological role models have to be investigated for technical application (Benyus, 1997). Therefore, **Table 2** gives an overview of literature findings of thermoregulating properties found in nature and describes the strategies of these relevant organisms to regulate their body temperature or overall surface temperature. Although the literature research has brought up even more examples, the most relevant organisms to the subject of thermoregulation of roofs in hot climates are presented here. Note throughout the examples, that organisms are known to exchange heat by four means: conduction, convection, evaporation and radiation. As such, the following biological role models teach us that conduction of heat can be avoided or minimized through insulation, convective cooling can be enhanced by airflow or ventilation, evaporative cooling can be exploited by introducing moisture on a surface, and radiation can rather be avoided through shading and reflection or used for Radiative Cooling (RC) of surfaces to the atmosphere.

Means of thermoregulation	Biological role model	Description
Self-shading	Cactus	Cooling ribs – Cacti are exposed to a great deal of heat in the desert. Therefore, their surface is equipped with so-called cooling ribs which create alternating shading panes along the surface (AskNature Team, 2017; Tributsch, 1983). These shading panes produce rising and falling air currents, improving air movement and convective cooling. Studies have shown that the total convective loss was about 2.5 times greater than for an equivalent smooth cylinder (AskNature Team, 2017; Lewis & Nobel, 2008).
Minimizing solar radiation	Desert snail	Self-cooling – The cooling strategy of the desert snail *Sphincterochila boisseri* is threefold and allows the organism to survive at temperatures of up to 50°C (AskNature Team, 2016; Riajul Islam & Schulze-Makuch, 2007). First, *shading* of the shell on the ground surface in contact with the snail cools the ground surface, initially at 65°C, down to 60°C. Then, *air insulation layers* introduced by the whorls cool down the temperature further to 50°C on top of the inner volume, where the snail hides. Finally, the outer surface of the shell stays cool thanks to its reflectance capacity of over 90% of the incident radiant energy in the total spectral range of the sun thanks to its *light colour* (AskNature Team, 2016; Schmidt-Nielsen, et al., 1971).
	Tree leaves	Surface Colour – Tree species are adapted to their climate by producing leaves with varying degrees of reflectiveness (AskNature Team, 2017). Dark coloured leaves absorb more heat from the sun than light coloured leaves that reflect excess sunlight. The shading of the ground surface also allows avoiding heat retention of the surface by day and heat rejection by night.

Radiative cooling	Black-tailed Jackrabbit	Oversized ears – The desert Black-tailed Jackrabbit has oversized ears allowing to loss heat by RC to his environment when the surrounding air is cooler than his body temperature (AskNature Team, 2017). By sitting in the shadow, he even achieves RC by day thanks to the large surface of his ears and broad vascularization of them, allowing rapid thermal exchange (Craig, et al., 2008).
Ventilation	Termite mounds	Chimneys – A large variety of nest structures are adapted for ventilation. Enormous chimneys introduce air passages ventilating the mounds (Badarnah, et al., 2010). The shapes of these mounds have been largely studied in the field of biomimicry in the last few years.
	Black-tailed Prairie dog	Bernouilli Principle – Black-tailed prairie dogs in the desert are known for their burrows shaped and oriented respectively according to the Bernouilli principle and wind. Two entrances in the ground are connected and elevated differently. One lower passage is shaped for optimizing air entrance and the other, situated higher, is optimized for air exit using the air velocity differentials along the ground surface that precipitate the air inlet into the ground for ventilation (AskNature Team, 2018).
Thermal mass	Termite mounds	Surrounding earth – Thermal mass in termite mounds enable a stabilization of the temperature thanks to the thermal inertia of the earth surrounding the mounds (Badarnah, et al., 2010).
	Black-tailed prairie dog	Surrounding earth – Similarly, the earth surrounding the burrows of the prairie dog has a beneficial effect on the temperature stabilization (GCP Arquitetura & Urbanismo).
Insulation	Animals	Thick coats with dense hair for one and blubber below the skin for others, insulate animals from summer heat as much as it insulates them from cool winters in other regions (Nour ElDin, et al., 2016).
	Plants	In plants, nature encounters thick external layers and waxy coatings that reduce heat gain. Moreover, leaves cells can absorb and store water creating an insulation layer of another kind (Nour ElDin, et al., 2016).
Evaporative cooling	Human sweating	Sweating – The sweat glands of many mammal aid thermoregulation through evaporative cooling (Nour ElDin, et al., 2016). Indeed, moisture evaporation releases heat and is therefore an efficient heat removal process (Badarnah, et al., 2010).

Table 2: Biological role models for thermoregulation.

Current building designs consider the envelope as a thermal barrier and often seek to avoid any transmission between the indoor and outdoor environment by increasing the insulation of the envelope, making the indoor climate independent of outdoor fluctuations (Pawlyn, 2011). As opposed to this construction strategy, organisms succeed to maintain an adequate balance between heat gains and heat losses to regulate their temperature. This is achieved by adaptive behavioural or physiological means (Badarnah, et al., 2010). In the first case, thermal balance is achieved by varying their body temperatures. These organisms are referred to as ectotherms and count amphibians, most fish, most nonavian reptiles, all aquatic invertebrates, and most terrestrial invertebrates. Endotherms on the contrary, vary their metabolic rate or insulation in a physiological manner. These comprise mammals and birds (Badarnah, et al., 2010). **Figure 6** below illustrates the biological role models in images, and for additional information about them, the reader is referred to **Appendix A.4**.

Figure 6: Biological role models for thermoregulation. *From top to bottom, from left to right*. Desert cactus enhances convective cooling by self-shading. Desert snails minimize solar radiation by colour and shape. Tree leaves minimize solar heating by colour. The Black-tailed Jackrabbit enhanced RC by his large ears. Black-tailed prairie dog burrows enhance passive ventilation. Termite mounds enhance passive ventilation.

2.4.   Conclusion

As has been demonstrated in above paragraphs, the roof is the façade of the building that is most exposed to the sun. This is even more relevant in hot and arid climates where the regions experience a high solar altitude and intensity. Also, one third of the world's land surface is concerned by these extreme temperatures. Additionally, those regions come often together with high cooling demand and consequently a high electricity consumption as buildings mostly operate on mechanical supplies. Issues such as rising electricity consumption come together with increased energy costs and electricity blackouts which are critical in hot and arid climate countries of low-income.

The link between thermoregulation, roof design and biomimicry resides in the design problem as defined in the top-down approach of biomimicry. Indeed, the design problem to resolve through biomimetic design can be stated as the thermoregulation of buildings through roof design in hot and arid climates. Moreover, the search for biological analogies and identification of appropriate principles as a solution to this problem takes advantage of one of the most prominent branches of biomimicry, i.e. thermoregulation. Thermoregulation through building envelopes is indeed the feature of biomimicry that most closely links designed buildings with nature. Therefore, it has great potential for research although the widespread application of biomimicry in architectural design remains largely unrealized at the moment. Moreover, roofs in particular are often set aside from the architectural design and final expression of buildings itself in favour of the vertical façade design. At the end of the state-of-the-art however, the literature research on the topic of this thesis resulted in the observation of a considerable lack of information about roof designs and biomimetic roofs. The scope of research therefore remains open to explorative design proposals in the field.

Chapter 3

A classification of roof design typologies

In this chapter, an attempt is made to fill in the gaps encountered in the literature research about roof designs and related passive cooling strategies. In order to answer the design problem of this thesis, an interpretative work was done by gathering information from papers, examples and case studies to finally define roofs by types and have a better understanding of their distinctive added values and shortcomings.

Research by existing classification however has led to a so-called 'classical' roof taxonomy. By classical is meant that existing classifications of roofs are close to always defined by shape or even "style" differentiation. This is due to the present use of those taxonomies. Indeed, whereas this thesis tackles cooling strategies and performance of roofs, roof typologies are used for purposes as Photovoltaic (PV) panel installation, cellular antenna placement or urban planning depending only on shape, height and inclination. Therefore, the first contribution of the research will be the assessment of the existing thermoregulating strategies on roofs in a clear, explorative performance-based classification. In other words, the explorative roof classification goes one step further than the established archetypes by illustrating roof typologies based on strategies enhancing passive cooling by roof surface, shape or material. The first part of this chapter will discuss in a critical way the establishment of the classical roof taxonomy as found extensively in the literature. The variants of roof typologies defined by shape characteristics will be whittled down to four subtypes of classical roofs. The second part of this chapter addresses the explorative roof classification and three general typologies will be identified: the protective, selective and vernacular roof typology. These will be further subcategorized into several roof design strategies that will be discussed in terms of performance but also cost, maintenance, longevity and availability. Finally, biomimetic strategies are mentioned as relevant biological role models for the different strategies when available in the literature. Here, according to the top-down approach of biomimetic design, solution principles to the design problem of roof designs in hot climates are identified in the form of a taxonomy. Afterwards, a search for biological analogies presents solutions existing in nature as a source of inspiration. Note that this step often requires significant knowledge in biology while in the scope of this research, biological role models were identified with the help of literature and existing research conducted amongst others by entities such as the Biomimicry Institute.

3.1. Classical roof taxonomy

In the literature, one can find a broad range of roof archetypes often classified in terms of geometrical shape. Researches have been conducted by scanning techniques where the classification of roof shapes was achieved based on depth maps or point cloud data collected using a Light Detection and Ranging (LiDAR) system for instance (Zhang & Chen, 2015). In this first study, roofs were classified by "style" and could be regrouped in 13 typologies: flat, shed, gable, hip, pyramid, curved, gambrel, mansard, hex, dome, L-union, T-union, and X-union as shown respectively in **Figure 7** (left). According to Zhang et al., roof types such as flat, gable and hip are the dominant types in every data set. Note that this classification can give rise to different degrees of variation by modifying parameters such as height,

14

dihedral angle with the ground and so on, generating up to or more than hundred thousand synthetic models (Zhang & Chen, 2015).

Roof classifications have also been created for optimal deployment of solar energy through PV panels as their installation strongly depends on size, orientation and also shape of the roofs. Therefore, Mohajeri et al. realized a city-scale roof shape classification for the city of Geneva. In this study, 10.085 buildings were chosen and were assigned to 13 shapes, namely flat, shed, gabled, hipped, gambrel, mansard flat, mansard hipped, cross-hipped, cross-gabled, corner-hipped, corner-gabled, pyramidal, and complex shown in combinations in **Figure 7** (right) (Mohajeri, et al., 2017). The latter typology was also referred to as a 'hybrid' or 'mixture' of several of the above-mentioned roof shapes. One can argue that this classification, as opposed to the one conducted by Zhang et al., already counts variants to flat, hipped and gabled roof types and could as such be further optimized. Moreover, as this taxonomy only refers to typologies present in one city, some typologies are missing such as domed roofs previously mentioned.

Hipped and gabled roofs as well as flat roofs remain the most common roof type encountered in literature. For example, a more recent study using LiDAR combined with satellite images resulted in 8 so-called roof shape 'labels' whereunder variants to flat, hipped and gabled roofs as well as another 'unknown' category referring to the previous used 'hybrid' terminology (Castagno & Atkins, 2018). However, the hipped and gabled roofs are subject to confusion in the systematic classification of LiDAR images as they are very similar in their primary shapes (Zhang & Chen, 2015). Therefore, it would be a relevant improvement to regroup them in one single label for clarity. Yet, geospatial modelling systems study achieved to focus the taxonomy down to three roof types accompanied by a 'complex' or 'hybrid' type regrouping flat roofs, sloped roofs (e.g. gabled or hipped), and domed roofs (Rahmes, et al., 2008).
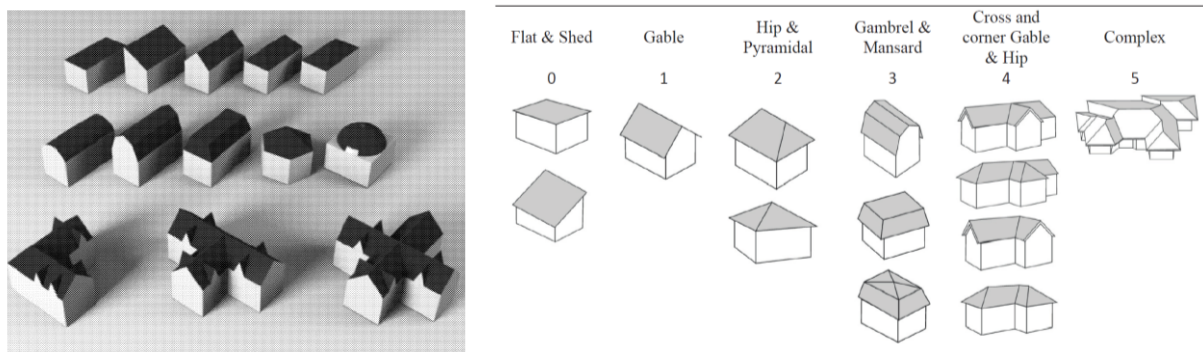
Figure 7: *Left:* Different examples of roof styles capable of recognition. From top to down and left to right: flat, shed, gable, hip, pyramid, curved, gambrel, mansard, hex, dome, L-union, T-union, and X-union (Zhang & Chen, 2015). *Right:* Schematic presentation of different roof-shape classes (Mohajeri, et al., 2017).

Finally, a taxonomy based on this state-of-the-art was realized in the context of this thesis and four main types were identified: flat roofs, sloped roofs, domed roofs and hybrid roof types (**Table 3**). These typologies may further derive into sub-types that will still originate from those four roof classes. By flat roof is meant a slope going up to 10° (Harris, 2000). When slopes exceed this value, pitched-, mono-pitched or shed roofs, as well as hipped roofs and derivates belong to the sloped roof typology. Domed roofs in turn can designate curved roofs such as domes or vaulted roofs and derivates. Finally, hybrid typologies arise from the three earlier classes when used in combination in architectural building designs. LiDAR systems as much as satellite imagery and 3D scanning in other methodologies to these existing classifications result in a range of taxonomies exclusively based on geometrical shapes. Although identifications of these shapes are promising for purposes such as PV panel installation, cellular antenna placement, urban planning, mapping or even disaster preparedness and analysis according to Rahmes et al., there is a great lack in performance assessment of these shapes in terms of solar energy absorption, cooling or heating energy needs and above all, these classifications do not illustrate the state-of-the-art of thermoregulating properties specific to roofs.
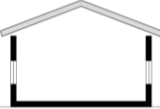
Types	Sub-types			
Archetypes	Flat	Sloped	Curved	Hybrid

Table 3: Classical roof taxonomy

3.2. Explorative roof taxonomy

In the literature, the classical taxonomy of roofs such as discussed in previous paragraph was limiting the research to geometry-based roof typologies. In order to be able to characterize the relevant examples to which this thesis will refer to, geometrically based classification lacks information for performance-based assessment. However, it should be noted that researches are showing interest in going further than geometry to characterize roofs such as the Institute of Photogrammetry and Remote Sensing which performed a roof classification defined by material in addition to shape. The present contribution goes even further by illustrating roof typologies based on strategies enhancing passive cooling achieved by roof surface, shape and material.

Finally, the explorative taxonomy identifies three general typologies that will be further subcategorized into several roof design strategies. For each class, a brief definition of the roof typology is given with some scientific results rising from their state-of-the-art. Additionally, the different solutions are assessed in terms of performance but also cost, maintenance or longevity and availability which are challenges of hot climate building designs previously identified by the literature review in Chapter 2. Finally, biological role models for thermoregulation described in previous chapter are also linked to a technical design problem when relevant for inspiration and finally a possible enhancement of the proposed design.
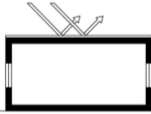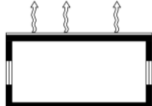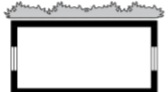
Types	Sub-types			
Protective	Insulation	Mass	Colour	Form
Selective	Wind	Water	Sky	Form
	Living	Operable		
Vernacular	Shape	Material		

Table 4: Explorative roof taxonomy.

3.2.1. Protective roof typology

The first class of this explorative roof taxonomy regroups roof types obeying the first rule of passive design strategies for cooling: heat avoidance (Khan, 2017). Belongs to this class, every roof minimizing heat transmission to the interior space by shading, mass, insulation or by reflection of the solar radiation. Each typology has its positive and negative aspects, assessed by performance but also by cost, longevity or maintenance and availability for the reasons explained previously in the state-of-the-art.

3.2.1.1. *Insulation*

This category promotes the use of an insulation layer to minimize heat transfer from the outer roof surface to the inside space. As detailed in the state-of-the-art of biological role models, both plants and animals present variants to insulating layers occurring in nature under the form of waxy coverings to reduce heat gains for plants, or thick coatings with dense hair and subcutaneous fat layers for animals. Although the application in the natural world is more responsive to climate than static insulation layers in the building industry, thermal insulation has proven to reduce energy use in both cold and hot climates. The more the temperature difference between inside and outside is significant, the more important the role of insulation will be (Yannas, et al., 2006). Its use also increases with extreme climates where the comfort temperature spreads from the outdoor conditions.

Although the actual use of insulation in hot climate and developing countries is not common (Butters, 2015), a study on roof performances for passive cooling in the arid region of Rajasthan, showed its positive impact potential on temperature mitigation (Dilip, 2005). According to the KCC, Rajasthan situated in India indeed experiences a climate B of type BWh, hot and desert. In this study, an insulation layer was applied beneath a roof surface and the overall performance of the roof was compared to the bare roof case in the same climate. According to the results, the roof surface inside the room was reduced from 63.1°C to 51°C thanks to the application of this insulation layer (Dilip, 2005).

However, in a hot climate, it was already stated that the efficiency of an insulation material deceased above 10 to 15°C according to measurements on the R-value and conduction of insulation panels (Schumacher, et al., 2016). Hence, the use of insulation has a positive impact on the thermal transmission of outdoor heat but its overall performance however shows weaknesses. Moreover, in terms of maintenance, note that one would prefer to place insulation internally to a building in order to meet several benefits. Indeed, internal insulation is not exposed to harming wind and rain, and can consequently be simpler in production, lighter, and in terms of cost much less expensive than external insulation panels (Butters, 2015).

Biomimicry	Animal skin fat
Assessment parameters	
Performance	(-) Counters RC (+) Counters conduction

Figure 8: *Left:* Performance scheme of the insulated roof typology (Protective roofs). *Right:* Summary of the analyed roof typology in terms of identified biomimetic role models and relevant assessment parameters.

3.2.1.2. *Mass*

The use of thermal mass in a building provides a stabilizing effect on internal temperatures when outdoor fluctuations occur (Yannas, Erell, & Molina, 2006). In hot and dry regions such as climate type B of the KCC, significant diurnal swings occur and thermal mass will therefore be even more important in these regions (Butters, 2015). This strategy relies on the idea that building elements can represent interim heat

sinks. A wall or roof's ability to store heat is characterized by its heat capacity, expressed in Joule per Kelvin and depends on an element's density, volume and especially its specific heat (in Joule per kilogram Kelvin) (Yannas, Erell, & Molina, 2006). In Europe concretely, traditional architecture has already proven the efficiency of building materials of high thermal mass such as masonry in the stabilization of indoor temperatures. Indeed, this had a positive effect in keeping indoor temperatures below outdoor peaks during daytime in warm summer (Yannas, Erell, & Molina, 2006). Moreover, although one can argue that a certain volume of material is needed, this strategy is very low maintenance for stable performance over a long time period. In nature, this principle has shown its potential in burrows of black-tailed prairie dogs for example, where the surrounding earth mass helps to stabilize the inside temperature of their habitat (AskNature Team, 2018).

Biomimicry	Earth layer of the prairie dog burrows
Assessment parameters	
Maintenance	(+) Low maintenance

Figure 9: *Left:* Performance scheme of the Mass roof typology (Protective roofs). *Right*: Summary of the analysed roof typology in terms of identified biomimetic role models and relevant assessment parameters.

3.2.1.3. Colour – Cool roof

A cool roof is *a roof that reflects most of the incident sunlight and efficiently emits some of the absorbed radiation back to the atmosphere instead of conducting it into the building below* (Garg, et al., 2015). The properties of a cool roof can be achieved by the application of a high albedo or high reflective coating. The higher the reflectance of the surface, the less energy will be absorbed by the roof (Dabaieh, et al., 2014). A simple white paint gives a flat roof the most effective colour, able to reflect up to 80% of incident sunlight (Yannas, Erell, & Molina, 2006). In nature, animals change the colour of their skin from black, when solar absorption is needed to light colours when cooling is needed (Vanaga, 2019). To illustrate this principle, the World Bank conducted a study in India by applying the cool roof principle on two school buildings. Results showed a significant improvement in the comfort levels of the students thanks to the targeted reduction of outdoor and indoor roof surface temperatures resulting in a reduction of the indoor air temperature of the buildings (Garg, et al., 2015). According to Suehrcke et al., cool roofs result in a reduction of heat gains by 30% compared with a bare roof (Garg, et al., 2015; Suehrcke, Peterson, & Selby, 2008). This will also contribute to a reduction of about 10% to 40% in air-conditioning energy for an application in Egypt (Dabaieh, et al., 2014). In the same study, this strategy has proven to be more efficient than insulation or even roof ponds and a ventilated space below the roof as will be developed later in this chapter.

Moreover, compared to other roof types, above its efficient performance, it is also a cost-effective solution according to the World Bank (Garg, et al., 2015). In India, the financial payback period of a cool roof application would be less than 3 years when accounting for a heat flow reduction into the building by 49% in the same research (Garg, et al., 2015; Bhatia, Mathur, & Garg, 2011). In terms of maintenance, a long-term benefit is that the reduction of the roof surface itself leads to an extended life of the roof (Dabaieh, et al., 2014). However, the performance of the cool roof being highly dependent on its surface colour, high maintenance is needed to minimize dust particles settlement. Also, although the lower surface temperature serves a certain mitigation of the heat island effect, reflection of the white surfaces additionally creates glare and visual discomfort for neighbours and taller adjacent buildings (Dabaieh, et al., 2014). Nevertheless, the application of a white paint or coating is easily accessible and applies to both corrugated metal sheeting and flat concrete roofs which are widespread in many hot and arid countries now (Butters, 2015).

Biomimicry	Animals skin colour; desert snail
Assessment parameters	
Maintenance	(-) High maintenance to maintain its cleanness and efficiency
Cost	(+) Low cost

Figure 10: *Left:* Performance scheme of the Cool roof typology (Protective roofs). *Right*: Summary of the analysed roof typology in terms of identified biomimetic role models and relevant assessment parameters.

3.2.1.4. *Form – Ribbed roof*

This typology relies on form to create a new strategy protecting buildings from heating sun rays. More than in other identified roof classes, this strategy relies exclusively on a biomimetic principle. According to the Biomimicry Institute, cactus achieve self-shading in the desert, minimizing heat gains through an increase of 2.5 times the convective loss of a smooth surface (AskNature Team, 2017; Lewis & Nobel, 2008). Note however, that this applies to vertical surfaces or inclinations where ribbed surfaces create shading panes. Indeed, convective cooling occurs only thanks to the rising and falling air currents due to these alternating shading panes (AskNature Team, 2017; Tributsch, 1983). One should be careful in the use of this roof typology and assure a relevant application on roof surfaces following this principle. Nevertheless, if self-shading is verified, this roof typology presents a solution that demonstrates how high-design can offer cheap solutions and enhanced performance as it is not based on mechanized solutions and relies on the interpretation of biological role models.

Biomimicry	Cactus, self-shading

Figure 11: *Left:* Performance scheme of the Ribbed roof typology (Protective roofs). *Right*: Summary of the analysed roof typology in terms of identified biomimetic role models and relevant assessment parameters.

3.2.2. Selective roof typology

As formulated in the design handbook for cool roofing techniques by Yannas et al., the selective environmental function of roofs investigates the *selective* coupling of the roof to heat sinks as main passive cooling strategy (Yannas, Erell, & Molina, 2006). In this case, two free available heat sinks are identified, namely the ambient air and the sky. In every sub-type of this category, the proposed roof design aims at dissipating heat to these heat sinks through for example convective cooling, evaporative cooling or RC.

3.2.2.1. *Water – Evaporative cooling*

In nature, the skin provides a medium between the organism and the surrounding environment which, amongst other particularities, provides thermoregulation by sweating, resulting in evaporative cooling (Badarnah, Nachman Farchi, & Knaack, 2010). Similarly, the present roof typology depicts the use of roof ponds mimicking this cooling strategy. In this system, an exposed layer of water in contact with the building's roof evaporates whereby the surface temperature of the water may be considerably lower than the prevailing air temperature (Pearlmutter & Berliner, 2017). These wetted roofs, providing evaporation

due to unsaturated surrounding air, are even more efficient in arid regions thanks to the higher difference in dry and wet bulb temperatures of the ambient air (Dilip, 2005). In addition to this evaporative cooling, the high heat capacity of the pond provides a stabilizing effect of the inside temperatures (Kharrufa & Adil, 2007). Hence, a study showed that the installation of a roof pond in Baghdad (climate type BWh) resulted in a reduced inside temperature by 3.36°C (Kharrufa & Adil, 2007). Another study performed in hot-dry conditions stated that the roof pond introduced a temperature reduction of up to 10°C compared to a bare roof (Pearlmutter & Berliner, 2017). In the latter, the optimal water depth was defined at a level of 2 to 4 cm.

Although evaporative cooling has proved to be an effective passive cooling strategy for hot and dry climates, a replenishment rate is needed to maintain a constant water level which is a major drawback for regions like Egypt which encounter water shortages (Dabaieh, et al., 2014; Pearlmutter & Berliner, 2017). Moreover, it is not ideal to adopt this roof typology for low-cost buildings as it requires a consequent bearing structure capable of standing the dead load of the water (Dabaieh, et al., 2014). Besides, this system requires regular maintenance and one should be careful for roof leakages in countries where workmanship is inefficient such as it is the case in Egypt (Dabaieh, et al., 2014).

Biomimicry	Human skin, sweating
Assessment parameters	
Maintenance	(-) Difficult to maintain, risk of roof leakage
Cost	(-) Structure needs to support the weight of the water.
Availability	(-) Water scarcity in hot and arid climate regions
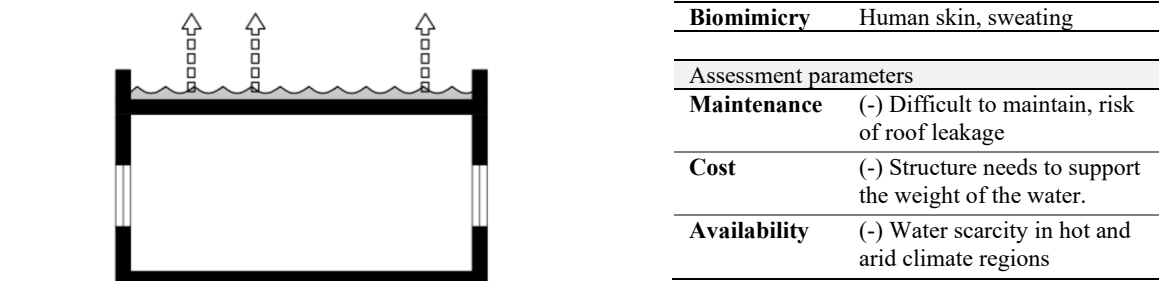
Figure 12: *Left:* Performance scheme of the Pond roof typology (Selective roofs). *Right*: Summary of the analysed roof typology in terms of identified biomimetic role models and relevant assessment parameters.

3.2.2.2.   Wind – Convective cooling

Like nature uses only the energy it needs and relies on free available energy, this roof cooling strategy relies on free available wind to increase the roof's performance (Biomimicry Institute, 2015). By introducing a ventilated airspace below the roof surface, natural convection occurs and drives off residual heat from the roof (Biwole, Woloszyn, & Pompeo, 2008). Double skin roofs are highly investigated especially in hot and dry countries where they seem to be very efficient (Abanomi & Jones, 2005). In both Köppen's climate types A (tropical) and B (hot and arid), this system shows potential in reducing power costs for air conditioning (Biwole, Woloszyn, & Pompeo, 2008). Furthermore, a study held by Biwole et al. has identified several efficiency parameters i.e. the cavity width, the roof inclination and the emissivity of the layers, RC and insulation thickness when coupled to this roof type (Biwole, Woloszyn, & Pompeo, 2008). In the same paper, results state that natural convection is made easier with a higher slope as is predicted by Yannas et al. in their design handbook for roof cooling techniques (Yannas, Erell, & Molina, 2006). Also, one would rather increase insulation thicknesses than the cavity width which is most effective between 6 cm and 10 cm (Biwole, Woloszyn, & Pompeo, 2008). However, the system is still effective with a higher width according to a case study improved by Abanomi and Jones, where the outer roof layer was constructed at a distance of 1 meter from the first layer.

This roof typology stands out from other design strategies for several reasons. First and foremost, wind is a cheap and renewable resource. It is thus cost-effective and has the additional advantage of extending the life span of the main slab by exercising shading for the bottom roof. However, cost-wise, the challenge in developing countries will be the need for a second roof above the existing one to achieve performance. This could be handled by considering the option of creating an additional room between the two roof layers when the cavity width is extended to an entire floor height. Moreover, Butters et al.

point out the interest of installing the cavity layer under the existing roof by placing an insulation layer at a distance of the ceiling and introducing vents in between the two layers (Butters, 2015). Anyway, the pay-back period would be beneficial to evaluate in both cases. Finally, note that wind is low-mai

Biomimicry	Prairie dog, Termite mound
Assessment parameters	
Performance	(+) Very efficient solution
Maintenance	(+) Protects the main slab
Cost	(-) Need for a second roof surface (+) Wind is cheap
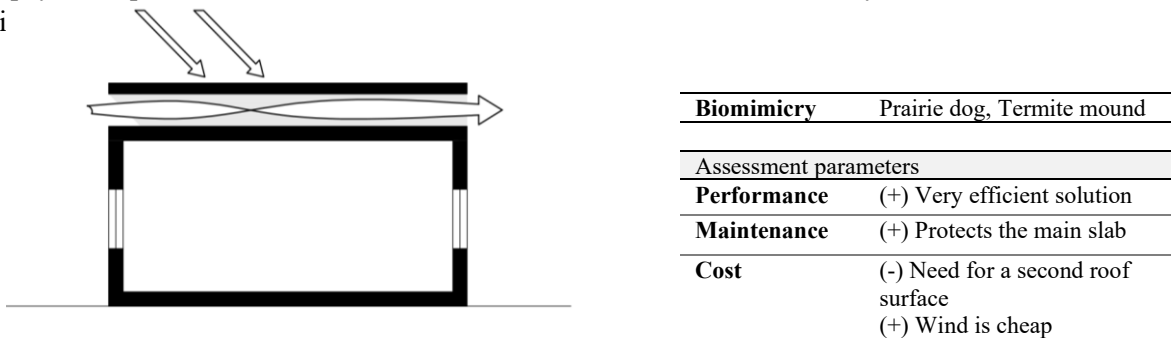
Figure 13: *Left:* Performance scheme of the Ventilated roof typology (Selective roofs). *Right*: Summary of the analysed roof typology in terms of identified biomimetic role models and relevant assessment parameters.

3.2.2.3.   Sky – Radiative cooling

Similarly to the Jackrabbit achieving RC through his oversized ears in the desert, this roof typology relies on a spatial interaction between a roof surface and the sky (Craig, et al., 2008). Because the sky temperature is lower than the surrounding air temperature nearby heated surfaces, the sky is to be seen as the ultimate heat sink to which surfaces dissipate the heat absorbed by the sun on a daily basis (Yannas, Erell, & Molina, 2006). At night, owing to the absence of solar gains heating up the same surface, a net cooling effect is achieved. The performance of a radiative surface is most effective in temperate (climate type C) or Mediterranean climates (type B in the KCC) where larger diurnal temperature swings occur in addition to lower humidity levels with minimal cloud cover (Lu, et al., 2016). Also, surfaces are called good radiators when their inherent emissivity is high. According to Yannas et al., *Emissivity is a measure of the ability of a surface to emit longwave radiation relative to a blackbody, a perfect radiator with an emissivity of 1.0.* Also, most building materials have already a high emissivity near to 0.9 and are thus good radiators. Moreover, the use of coatings that radiate efficiently at low temperatures is a cost-effective solution that results in an improved radiative loss (Gupta). Finally, the roof is the only building element that can be used for RC because of its view to the sky zenith. For the same reason, flat unobstructed roofs perform better than pitched roofs.

Biomimicry	Jack rabbit
Assessment parameters	
Cost	(-) Low cost, Use of a natural passive process
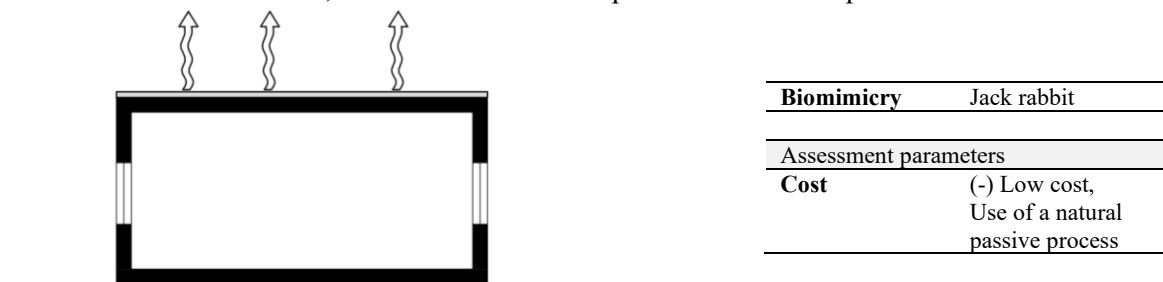
Figure 14: *Left:* Performance scheme of the Radiative roof typology (Selective roofs). *Right*: Summary of the analysed roof typology in terms of identified biomimetic role models and relevant assessment parameters.

3.2.2.4.   Form – Complex surface

Although this roof typology is quite specific, the design principle and idea of introducing a complex, multifunctional surface are relevant to the roof taxonomy. Based on some traditional buildings in India, the entire roof is covered with small closely packed inverted earthen pots. The shape and availability of these pots are remarkable. The arrangement of the pots increases the surface area of the roof for radiation emission and the still air inside them creates an insulative cover to the roof. Besides, this system minimizes shortwave radiation heating the roof by day thanks to the self-shading of the roof. The overall

complexity of the shape impedes heat flow into the building while still permitting upward longwave heat radiation at night (Gupta). This shows how complexity can result in multifunctionality and selective operation. However, the major drawback of this roof type is that the roof is rendered inaccessible and that the close arrangement of the pots makes it difficult to maintain.

Biomimicry	/
Assessment parameters	
Maintenance	(-) Difficult to maintain because of its complex form
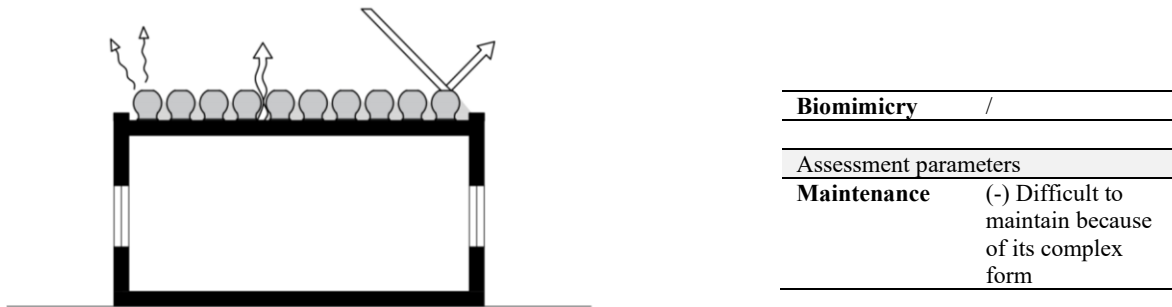
Figure 15: *Left:* Performance scheme of the Complex roof typology (Selective roofs). *Right*: Summary of the analysed roof typology in terms of identified biomimetic role models and relevant assessment parameters.

3.2.2.5. *Hybrid – Living roof*

Living roofs, also referred to as green roofs, represent a hybrid solution of a performative kind. Indeed, the performance of such a system relies on a combination of several above-mentioned strategies. Concretely, heat flux through the roof is reduced by physically shading the roof, increasing the insulation and thermal mass and by promoting evapotranspiration (Oberndorfer, et al., 2007). Also, as opposed to the double layer roof type, if the top layer is replaced by deciduous plants, this permeable layer allows for RC to occur by night (Gupta). On the other hand, the evapotranspiration from the leaf surfaces lowers the temperature of such a cover and can even go below the day time air temperature, resulting in a very cool roof surface (Gupta). According to a study held in Singapore, the performance of a living roof results in a reduction of about 90% of heat transfer compared to a bare reference roof (Wong, et al., 2003). Therefore, living roofs lower the energy demand of cooling systems (Oberndorfer, et al., 2007). Also, a positive impact has been witnessed on the heat island effect. A study in Toronto showed a decrease in the air temperature as great as 2°C in some areas in Toronto when this roof typology is applied to 50% of the roof surfaces in the city (Bass, et al., 2003).

The improvement achieved with green roofs is also due to its ecosystem characteristics inherent to biomimicry or bioengineering as was stated by Oberndorfer et al. Accordingly, *the ecosystem created by a green roof's interacting components mimics several key properties of ground-level vegetation that are absent from a conventional roof* (Oberndorfer, et al., 2007). Note that for the soil-plant system to have a maximum effect on the building interior, the structural bearing system should be closely coupled with the soil. This excludes the use of insulation in addition to this hybrid roof system (Yannas, Erell, & Molina, 2006). Finally, although planted roofs are effective in performance, the major drawback of this typology is that it is an expensive solution (Butters, 2015).

Biomimicry	Ecosystems
Assessment parameters	
Cost	(-) Structure needs to support additional earth layer. (-) Expensive solution
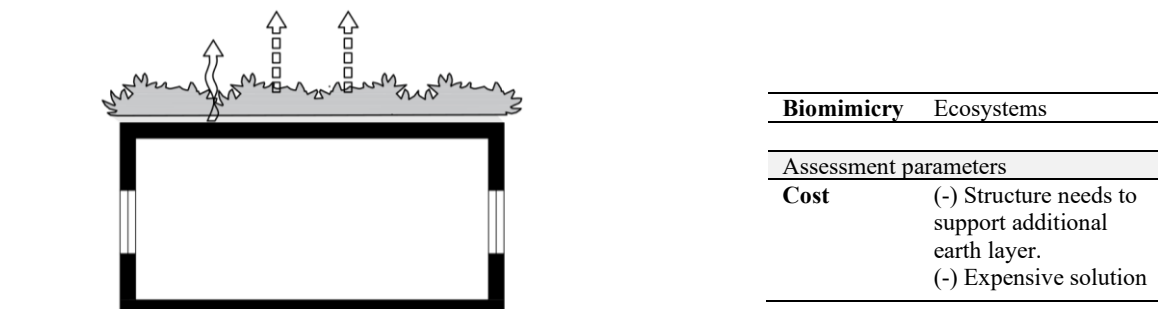
Figure 16: *Left:* Performance scheme of the Living roof typology (Selective roofs). *Right*: Summary of the analysed roof typology in terms of identified biomimetic role models and relevant assessment parameters.

3.2.2.6.   Operable roof

This last roof typology achieves selectivity by changing its state in time. According to a biomimetic research carried by Saalman Craig et al., a contradictory problem inherent to roof cooling techniques exists. The aim of the paper was indeed to achieve a night-time cooling of the roof by coupling its thermal mass to the sky for longwave RC while minimizing its exposure to daytime solar radiation and resulting heating. In order to do that, one solution inspired by nature was to make changes in the time parameter by bypassing the insulation or barrier when it is advantageous to do so (Craig, et al., 2008). Consequently, the design principle of this system is to mount an insulation layer above the roof by day and remove it by night to permit RC (Craig, et al., 2008). A similar alternative is the inexpensive and effective roofing device made of a removable canvas cover (Gupta). However, this roof typology needs a mechanical solution to operate. Non-mechanical solutions on the other hand are more robust with regard to users and are low-maintenance which is preferable (Butters, 2015). One may also state that mechanized solutions often turn out in high tech solutions that are more expensive and less accessible.
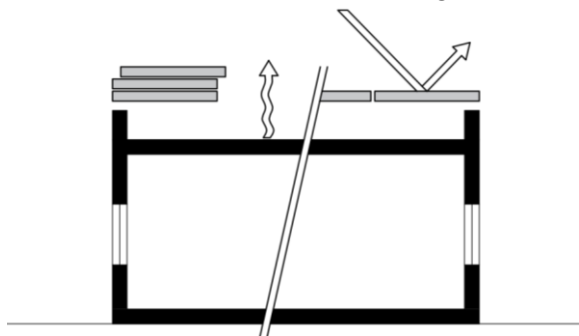
Biomimicry	BioTRIZ matrix of Salmaan Craig
Assessment parameters	
Maintenance	(-) Operable mechanisms require high maintenance
Cost	(-) Expensive solution if high tech solution

Figure 17: *Left:* Performance scheme of the Operable roof typology (Selective roofs). *Right*: Summary of the analysed roof typology in terms of identified biomimetic role models and relevant assessment parameters.

3.2.3.   Vernacular roof typology

This last category explores the vernacular roof typologies with a new perspective. Indeed, shape and material often used in hot and arid climate countries are analysed in terms of performance achieved with these traditional building techniques.

3.2.3.1.   Shape

In vernacular architecture, domed and vaulted roofs have been widely used by architects and builders in hot and arid climate regions in the past. Some researchers assumed that these shapes were adopted for climatic and environmental considerations while others stated that the geometry was stressed out of religious and cultural issues (Tang, Meir, & Wu, 2006). Furthermore, Yannas et al. identified an issue of material availability in hot arid countries that lead to the use of stone as structural component which functions by compression arches (Yannas & Weber, 2014). As opposed to the classical taxonomy developed in the beginning of this chapter, the present explorative taxonomy will guide the shape typology towards performative and physical explanations from the literature.

Regarding thermoregulating performance, buildings with vaulted roofs achieve lower indoor temperatures than flat roofs (Tang, Meir, & Wu, 2006). Unlike flat roofs, curved roofs are partly in the shade for a period of the day (Dabaieh, et al., 2014). Also, a domed or rounded roof absorbs less beam radiation at noon than its corresponding flat roof (Runsheng, Meir, & Etzion, 2002). Indeed, at that time, the temperature of the top of the vault is at the highest temperature similarly to the entire surface of a flat roof. On the other hand, the lowest point of the vault directed parallel to the solar radiation, experiences lower temperatures (Tang, Meir, & Wu, 2006). However, at hours of early morning or late afternoon, the vaulted roof is more exposed than the flat roof, and studies have concluded that curved

roofs absorb overall more solar radiation (Runsheng, Meir, & Etzion, 2002; Tang, Meir, & Wu, 2006). According to the study of Debaieh et al., the efficiency of a rounded roof resides in its larger convection heat-transfer surface, allowing it to be more easily cooled by dissipation to the surroundings (Dabaieh, et al., 2014). Consequently, this roof typology is most suitable for buildings located in hot and dry regions (Tang, Meir, & Wu, 2006).

The efficiency of a vaulted or domed roof is highly dependent on a geometrical parameter called the half rim angle of a vault. The lower the half-rim angle, the closer a dome or vault shape is to a flat roof and the same applies to their respective performances. Recent simulation tests have concluded that a vault of half-rim angle 70° with additional application of high albedo coating resulted in a reduction of cooling hours by 53% (Dabaieh, et al., 2014). Also, the higher the angle of the half-rim, the greater the surface of the roof leading to an increase in the cooling load through the roof if air-conditioning is installed. The study of Tang et al. therefore recommended a half rim angle between 50° and 60° to satisfy the needs in both non-air-conditioned and air-conditioned buildings (Tang, Meir, & Wu, 2006). They also recommended a vault orientation to be north-south facing. North-south facing vaulted roofs as opposed to east-west facing vaults absorb somewhat smaller amounts of beam radiation (Runsheng, Meir, & Etzion, 2002).

Vernacular	Domes, vaults
Assessment parameters	
Performance	Performance by shape only
Cost	High design for cheap solutions
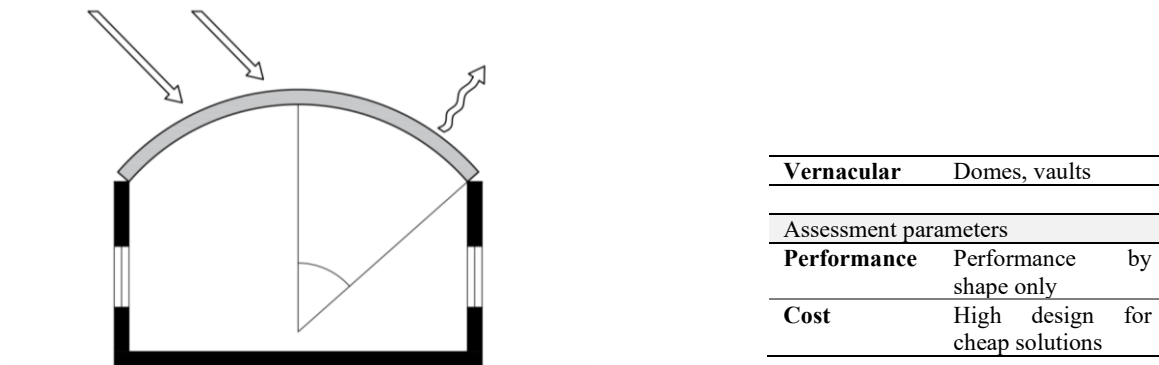
Figure 18: *Left:* Performance scheme of the Curved roof typology (Vernacular roofs) with half rim angle indication. *Right*: Summary of the analyzed roof typology in terms of identified biomimetic role models and relevant assessment parameters.

3.2.3.2. Material

The material used for roofing often depends on availability, cost and longevity. However, these parameters do seldom serve the energetic performance of a building. The relative effect of various building elements with regard to passive cooling strategies has seldom been experimented and elucidated (Butters, 2015). Illustratively, millions of low-income dwellings in hot climate regions have uninsulated roofing made of Corrugated Galvanized Iron (CGI) sheeting as shown in **Figure 19**, although it causes extremely poor indoor conditions in summer and winter (Butters, 2015). Metallic roofs are also very common in farm buildings, animal sheds, industrial and even residential buildings in most of the developing countries (Dilip, 2005). However, metal roofs are popular in hot climates for other reasons. The high temperatures and intense sun are especially damaging to roofing materials and cause them to break down, crack, curl, dry out and become more susceptible to leaks and wind damage whereas metal sheeting is more durable and lasting regarding solar radiation (Classic Metal Roofing Systems, 2011).

Other materials of the traditional architecture however differ from metal sheeting. Indeed, classical vaults are nowadays made of reinforced concrete and could be replaced by bricks to offer cheaper solutions. Some materials as wood however are not available locally in hot countries and its use would be less durable due to the transport engendering also additional costs to the construction (Yannas & Weber, 2014). As a performance effective alternative to CGI sheeting, Butters recommended the use of micro concrete roof tiles which *although relatively expensive can still be far cheaper than CGI sheeting, in addition to being climatically much better* (**Figure 20**) (Butters, 2015).

Figure 19: Examples of CGI sheeting in hot climates. *Left*: Typical rural house construction in Tanzania. *Right*: Typical slum housing with CGI roofing, Capetown, South Africa. (Butters, 2015)

Figure 20: Microconcrete (MCR) roof tiles produced on site, cheaper than CGI sheets; here also with a ventilated roof. Architect Chris Butters. (Butters, 2015)

Longevity, cost and availability are thus parameters that can lead to a choice of material or another, depending on the climate, location and purpose of the construction element. Ideally, a balance between those parameters and performance should be achieved in order to lean towards a sustainable solution. For example, while timber is a less conductive material than steel, it is also less available in hot and arid climate countries and when used outdoors its longevity is quite poor due to the pathologies this material is subjected to. On the other hand, steel creates very poor indoor conditions because of its low thermal inertia and high conductivity of daytime solar radiation but is highly available in hot and dry countries, which consequently reduces transportation costs and emissions, while being more resistant to hot outdoor conditions. In the end, alternative assemblies of materials representing distinct advantages for roofing introduce sub-scenarios to every typology discussed above which are more likely to be assessed in terms of availability, cost and LCA.

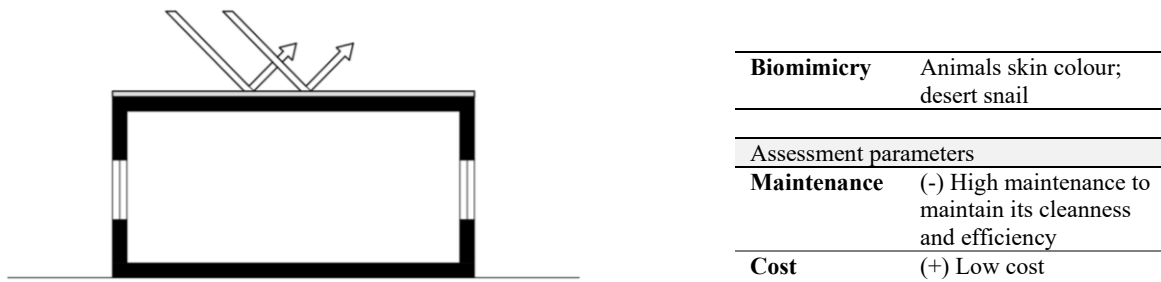| Vernacular	CGI sheeting
Assessment parameters	
Maintenance	(+) Resists to high temperatures
Availability	(+) Locally available in hot climate countries
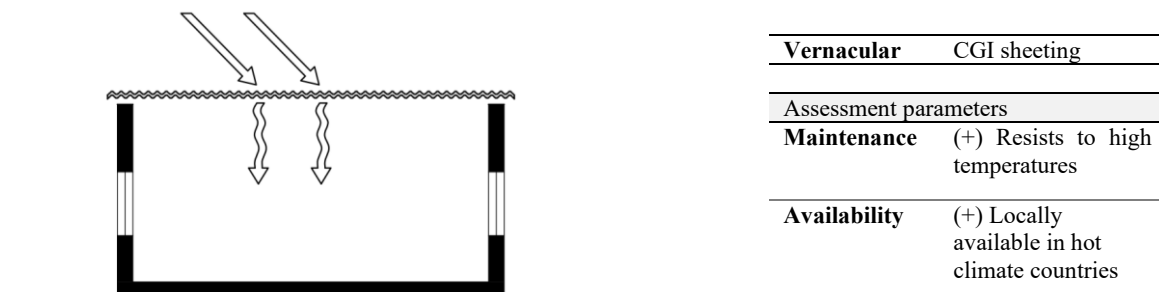
Figure 21: *Left:* Performance scheme of the CGI sheeting roof typology (Vernacular roofs). *Right*: Summary of the analysed roof typology in terms of identified biomimetic role models and relevant assessment parameters.

Chapter 4

Innovative roof designs – Case studies

*In this chapter, case studies were chosen for their relevance to the context of hot climates, the architectural expression of innovative roof designs, interesting cooling strategies achieved through roof thermoregulation, or even inspiration from biological organisms. Based on the developed explorative roof design taxonomy in Chapter 3, identified roof typologies will be illustrated in an adapted performance scheme showing the combined cooling strategies proper to each case study. The climate type of each location will also be identified by the KCC presented in Chapter 2 for comparison between similar climate regions and joined cooling strategy. From the same chapter, the levels of biomimicry are used to define to what extent the case studies are inspired by nature when applicable. For additional documentation of the case studies, the reader can consult **Appendix B**.*

4.1. Building designs and constructions

4.1.1. Louvre (Abu Dhabi) – Jean Nouvel

The Louvre Abu Dhabi was designed by the French Pritzker Prize winner architect Jean Nouvel and is situated along the sea, on the Saadiyat island of Abu Dhabi (Fisher & Craig, 2017). The museum is a relevant case study both because of the correspondence with the Köppen's climate type addressed in this thesis (BWh) and the importance of the roof in the architectural expression of the project as well as in its passive cooling performance. Indeed, the performance of the roof is important for shallow morphologies such as a museum building as the roof represents a great surface compared to the vertical walls and is therefore the element that is most exposed to the sun. Moreover, while the white buildings composing the plan are designed in a very sober way, the architectural statement relies on the complexity of the 180-meter span shallow dome built over them. As it filters the natural light through a seemingly random but highly controlled pattern of steel elements, the dome offers this unique and dramatic lighting experience by creating a delicate and changing "rain of light" beneath it (**Figure 22**). Designed for the United Arab Emirates, the design would finally have to reflect the building's own era and the local traditions of the host country while showing a dialogue between the cultures of East and West (Grange, 2014).

Figure 22: *Left*: View of the dome from inside (ArchDaily 2017). *Right*: View of the Louvre from the outside (Bianchini 2019).

From the pattern of the roof structure, one might recognize the play of light also suggested by the claustra lattice or Mashrabiya of the local culture. On the other hand, Grange (Grange, 2014) and other references talk about the pattern giving the same vision through the canopy as through interwoven palm leaves, a traditional roofing material in the Emirates. Yet, the Atelier Jean Nouvel practice mentions that the inspiration of the entire structure was driven by the geometry of the Dragon Blood tree precisely (**Figure 23**). This tree, found in Yemen, is able to harvest dew from fog and gave them an insight into how a dew-harvesting structure might look on a micro-scale (Fisher & Craig, 2017). In terms of the *levels of Biomimicry* defined earlier, the dome would thus mimic the Dragon Blood tree on an *organism level* and by *function*. In other words, the building functions like the tree in a larger context; it is able to harvest dew from fog. The dome also looks like a dew-harvesting structure and was therefore also mimicked on the *organism level* by *form*.
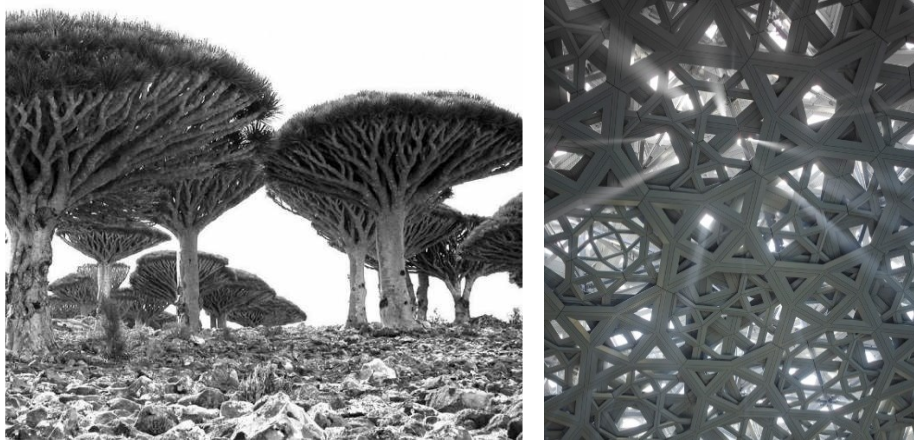
Figure 23: *Left*: Dragon Blood trees found in Yemen (Fisher & Craig, 2017). *Right*: View on canopy of the Louvre Abu Dhabi from beneath (ArchDaily, 2017).

When analysing the present case study based on the above-elaborated roof design classifications, the present roof complexity can be defined by a combination of identified roof typologies. First, if the performance of the roof had not been more important in this project, the *Classical roof taxonomy* would define the building as a combination of a *flat* and *domed* roof typology based on simple morphological characteristics. However, the shallow dome design goes far beyond shape and demonstrates thereby the interest of the extended explorative roof taxonomy. Hence, by a close collaboration between architects, engineers, and experts of diverse fields, the *classical* dome became what they call an "environmentally informed envelope design" (Imbert, et al., 2012). The dome shape is composed of no less than ten layers of cladding that are added to a double skin structure to attain a balance between radiant heat, luminance and light 'dappling' while assuring its structural function (**Figure 24**) (Fisher & Craig, 2017).
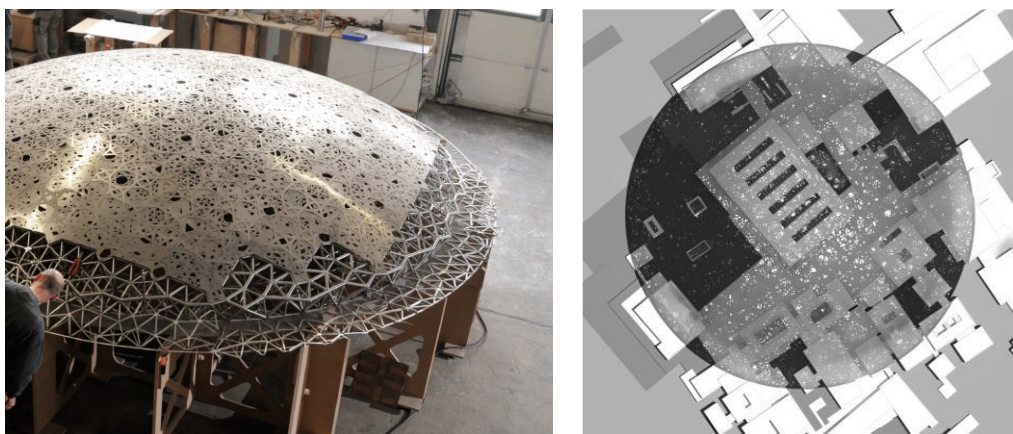
Figure 24: *Left*: Prototype scale 1:33 of the roof and cladding layers (Koren, 2017). *Right*: Overall translucency map with resulting shadow effect beneath the dome (Fisher & Craig, 2017).

In fact, several performative roof typologies can be recognized in the combined roof cooling strategies adopted by the designers and are summarized in **Figure 25**. First, the *vernacular roof typology* accounts for the dome shape referring to the Arabic vernacular architecture. Then, the *protective roof typology* explains how light-reflecting materials in pale colours used for the cladding send solar heat back rather than absorbing it. Moreover, the material choice of Aluminium and stainless-steel results in an effective night-time RC, which was defined as a *selective roof typology* in the explorative taxonomy. Besides, as the temperature of the roof surface drops down compared to the ambient temperature, the designed cladding is able to produce condensation like the earlier mentioned Dragon Blood tree. Dew is formed at a scale of no less than 60,000 litres for 250,000 square meter cladding under clear night skies (Fisher & Craig, 2017). Finally, the dome being open and permeable, wind flows freely under the dome and in between the flat roofs of the museum, creating a cooling Natural Ventilation (NV).

Figure 25: Performance scheme of the Louvre Abu Dhabi roof based on the developed explorative roof taxonomy. Combination of typologies 1, 2 and 3: *1. Protective roof typology*: Colour – Cool roof. *2. Selective roof typology*: Wind – Convective cooling, Water – Evaporative cooling, Sky – Radiative cooling. *3. Vernacular roof typology*: Shape – Dome.

4.1.2. California Academy of Sciences (San Francisco) – Renzo Piano

The California Academy of Sciences is situated in San Francisco and is exposed to dry and warm summers as defined by the Köppen's climate type CSb. Designed by Pritzker prize winner architect Renzo Piano, the building was completed in 2008 as reconstruction after a devastating earthquake damaged the original building in 1989 (D+H Mechatronic AG, 2013). In addition to the great recycling of the demolition materials, the project's performance strategies earned the academy the LEED Platinum prize accolade, giving it the title of the largest public building in the world to achieve platinum certification (Reid, 2009).
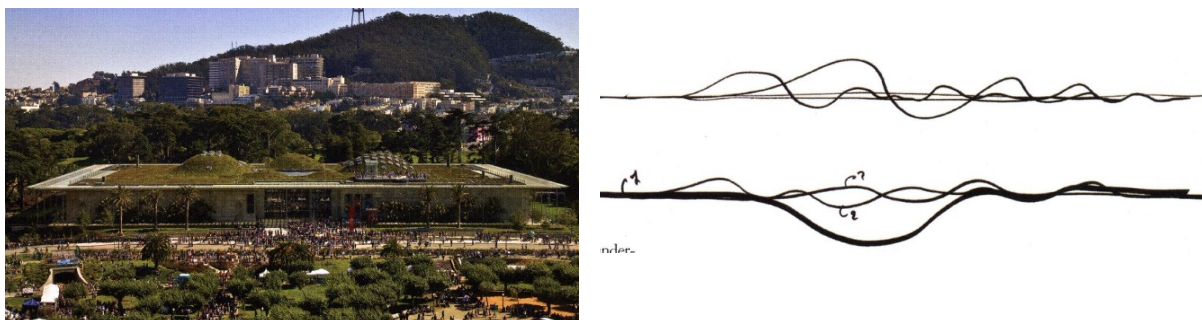
Figure 26: *Above*: Renzo Piano's original sketch for the 'living' roof (McIntyre, 2009). *Below*: View on the building in its hilly context (McIntyre, 2009).

The roof in particular became the main architectural gesture of the project. Indeed, the very first conceptual sketch of the architect showed a topography profile drawn out of single lines, referring to the Seven Hills of the city (**Figure 26**). Located in an iconic park, the main concept was, in Piano's words, to "Lift up a piece of the Golden Gate Park landscape and put whatever was needed underneath it" (Pearson, 2009). More than just a reference to the sinuous context, the roof was seen as an opportunity to add quality and purpose to the building itself. Therefore, the fifth façade gave place to a green roof with deep soil to welcome over 1.7 million native plants and all kinds of insects and birds (Reid, 2009). The geometry of the roof itself offered the possibility to reflect and adjust its height to the program below. Consequently, two spheres housing a planetarium and a rainforest exhibit are echoed in the roof geometry by two outstanding domes (**Figure 27**). The resulting morphology of the roof can be defined by the *classical roof taxonomy* as assigned to the curved roof typology, in a hybrid way as it combines two domes and sinuous geometries. Indeed, the view of Olaf de Nooyer –partner in the Renzo Piano Building Workshop– confirms that "Certain elements do not fit under a flat roof" (Reid, 2009).

Figure 27: *Left*: Observation deck on the roof with visitors. *Right*: Glazed dome housing the planetarium (McIntyre, 2009).

Once again, performance of the building and roof are of great importance for this project as museums typically operate in a tight range of parameters regarding temperature and humidity to preserve the displayed artifacts qualitatively. The main strategy the designers opted for was intelligent NV, using natural airflow that appears due to different dimensions of the curved roof constructions, domes and façade elements. No less than 720 ventilation drives and 40 controllable roof flaps above the two domes are connected to the Building control centre to pop open in reaction to internal and external climate data (D+H Mechatronic AG, 2013). When the skylights are open in different configurations and with changing opening angles, passive cooling is managed by night-time ventilation when very warm days occur, by stack effect releasing excess hot air through the roof and by cross-flow effect on windier days. With this technology, the building's interior spaces are kept cooler by approximately 5.6°C than would a traditional roof (Reid, 2009). According to Arup –Sustainability-consulting services of the project– the NV combined to the shading and heat recovery are responsible for 30 to 35% energy savings compared to California's already strict requirements (Pearson, 2009).

Finally, the performance strategies adopted in the design of the California Academy of Sciences are summarized in **Figure 28** based on the *explorative roof taxonomy*. First, the main architectural gesture concerns the living roof of the building, accounting for evaporative cooling as explained in the *selective*, *living roof typology* of the taxonomy. Then, insulation made of upcycled blue jeans was used to assure a minimized thermal transfer of the hot summer environment like in the *protective roof typology* (Pearson, 2009). Finally, wind-driven ventilation passing through the roof flaps accounts for a s*elective, ventilated roof typology* variant, although this is not due to the performance of the roof itself but rather to electronically connected openings regulating the air inlet and are therefore not represented in the taxonomy-based scheme hereunder.

Figure 28: Performance scheme of the California Academy of Sciences roof based on the developed explorative roof taxonomy. Combination of typologies 1, and 2: *1. Protective roof typology*: Insulation. *2. Selective roof typology*: Hybrid – Living roof.

4.1.3. Gando Primary School (Gando) – Kéré Architecture

The Gando primary school was completed in 2001 by the office Kéré Architecture and won several sustainability prices whereunder the Global Award for Sustainable Architecture in 2009 and the Aga Khan Award for Architecture in 2004 (Kéré Architecture). The project is located in Burkina Faso which has a hot and arid steppe climate (BSh in the KCC) where the cooling strategies consequently prevail. Also remarkable is that within the local architecture, many houses are constructed with CGI roofs that absorb the heat from the sun, making the interior living space intolerably hot (Kéré Architecture). This issue however was handled differently by the architect of this project. Indeed, Francis Kéré designed a similarly CGI roof and pulled it away from the main volume, letting air ventilate the space between roof and ceiling (**Figure 29**). The project also stands out because of the intention of the architect to involve members of the community in the construction process, to adopt simple construction methods and to efficiently use local materials as constituents for the building. Kéré states "This is our working method and this is how I define sustainable", talking about his architecture, indeed often defined as social architecture that considers both ethics and aesthetics (Lepik, 2017).

Figure 29: Gando Primary School (Kéré Architecture).

Francis Kéré studied engineering in Europe but had always been a child growing up with many challenges and few resources (Kéré Architecture). In the same way, this very first project evolved from a long list of parameters including cost, climate, resource availability, and construction feasibility. As illustrated by the performance scheme in **Figure 30**, the design can be redefined in terms of performance, based on a combination of earlier identified roof typologies from the *explorative taxonomy*. The primary

school is arranged in three separate classrooms positioned in a row. The roof is composed of a lightweight CGI roof similarly to the typology discussed in the *vernacular roof typologies* in terms of material, and is then raised at a distance of the ceiling by an open steel rebar structure resembling the *selective and ventilated roof typology* (Hanley, 2012). The walls of the classrooms are made of clay using the traditional building material in the shape of modern, structurally more robust bricks. Also identified in the explorative taxonomy as *protective roof* this time, clay provides *thermal mass* to stabilize the fluctuating outside temperatures and has the advantage to be available and easy to produce (Kéré Architecture).
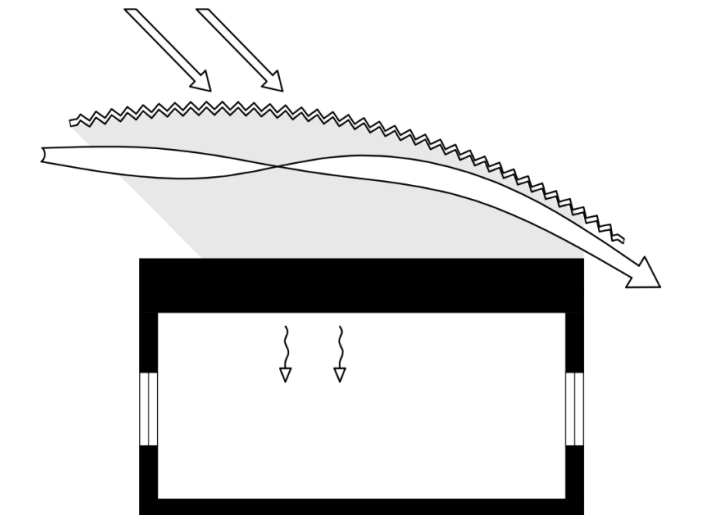
Figure 30: Performance scheme of the Gando Primary School roof based on the developed explorative roof taxonomy. Combination of typologies 1, 2 and 3: *1. Protective roof typology*: Mass. *2. Selective roof typology*: Wind – Convective cooling. *3. Vernacular roof typology*: Material – CGI sheeting.

In contradiction to the often poorly lit and ventilated schools in Burkina Faso, the Gando primary school was designed to provide NV in a simple and efficient way, and consequently discard air conditioning equipment (Lepik, 2017). On hot days, cooling breezes flow in through colourful steel window shutters that were made by local metalsmiths (Slessor, 2009). The excess hot air of the interior spaces is drawn up through the perforated vaulted ceiling and dissipated into the roof space by stack effect (**Figure 31**) (Slessor, 2009). The difference in temperature between the interior and exterior is immediately felt. The roof separated from the ceiling allows the heat to escape and the cantilever extension of it provides additional shading and rain protection of the clay walls (Kéré Architecture). Finally, the orientation of the building was also thought of by closing it to the dusty winds of the east and opening it to western breezes (Hanley, 2012).
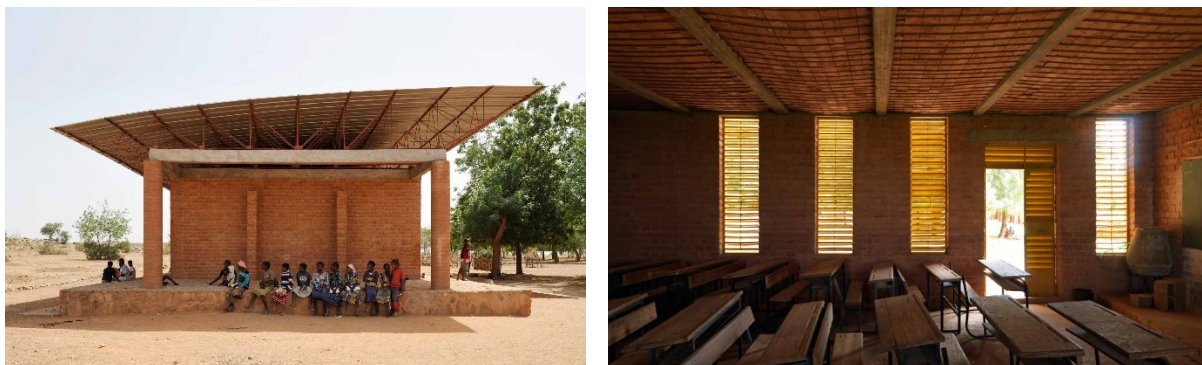
Figure 31: *Left*: Gando Primary School short facade view with uplifted roof. *Right*: Interior of classes and view on ceiling and shutters (Kéré Architecture).

4.1.4. Votu Hotel (Brazil) – GCP Aquitectura & Urbanismo

The Votu Hotel is a project located along the Algodões beach in South Bahia (Brazil) and is implemented adjacent to a tropical forest full of valuable fauna and flora (Araujo, Haddad, & Garcia). Due to the hot and humid climate of Brazil, climate type Af according to the KCC, thermoregulation will become important to maintain the comfort of the hotel's clients. The GCP Architects also wanted to minimize the impact of the construction on the surrounding nature and included consideration of a certified biomimicry specialist, Alessandra Araujo, from *Biomimicry 3.8* (Araujo, Haddad, & Garcia). Therefore, this case study is interesting because it is an example of biomimetic thermoregulation design, more specifically taking inspiration of black-tailed prairie dogs and the Saguaro cactus to enhance the thermoregulation of bungalow complexes in a hotel.

Figure 32: *Left*: Rendered view on the bungalows of the Votu Hotel. *Right*: Inside view of the concrete structure. (Delaqua, 2018)

Unfortunately, humans have already had a massive impact on the landscape of the project's surroundings. Less than 5% of the original forest cover remains while 40% of its plants and 60% of its vertebrates are unique in the world (Woolley-Barker, 2017). This awareness is the reason why, in this project in the tropical forest of Brazil as well as all over the world, biomimicry is increasingly considered. In this project, Alessandra Araujo took inspiration from nature's lesson on the *ecosystem level* (*Levels of Biomimicry*), explaining the importance of being "resource-efficient" by creating cycles and managing the water resources. Indeed, the biologist working on the project envisions that cities would function as forests with interdependent nutrient cycling (Future Architecture). Moreover, on the *organism level*, the bungalows mimic the native mangroves and *Restinga* forest trees by *form* and rest on stilts similarly to the trees (**Figure 33**) (Woolley-Barker, 2017). This way, the 1,603 square meter project does not interfere with the topography nor the rainwater flow of the environment.
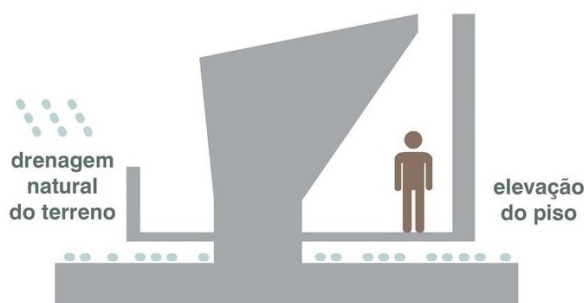
Figure 33: *Left*: Scheme of the stilted bungalows for rain flow (GCP Arquitetura & Urbanismo). *Right*: native Restinga forest trees (Woolley-Barker, 2017).

Knowing the cooling strategies will be important for the comfort of the guests, the architects aimed at minimizing the usage of air conditioning and electricity consumption. First, the main strategy for NV was identified as inspired by the black-tailed prairie dogs (**Figure 34**). As extensively explained in the biological role models of thermoregulation, this specie lives in desert burrows which help them thermoregulate their body temperature (AskNature Team, 2018). According to the *Levels of Biomimicry,* this phenomenon was transferred to the roof system on a *behaviour level*, mimicking the *process*. Accordingly, the building works in the same way as the burrows of the Black-tailed prairie dog would, by careful orientation, shape, material properties and NV. First, the thermal mass obtained by the soil layer all around the tunnels was translated into a massive concrete structure combined with a roof garden (**Figure 32**). Then, the principle of airflows from the prairie dogs was achieved by inclining the roof and orienting the low point towards the prevailing eastern wind. When the air approaches the roof, the wind is entering openings between the top of the wall and the low part of the roof, ventilating the space inside the bungalows effectively (**Figure 34**) (Araujo, Haddad, & Garcia).
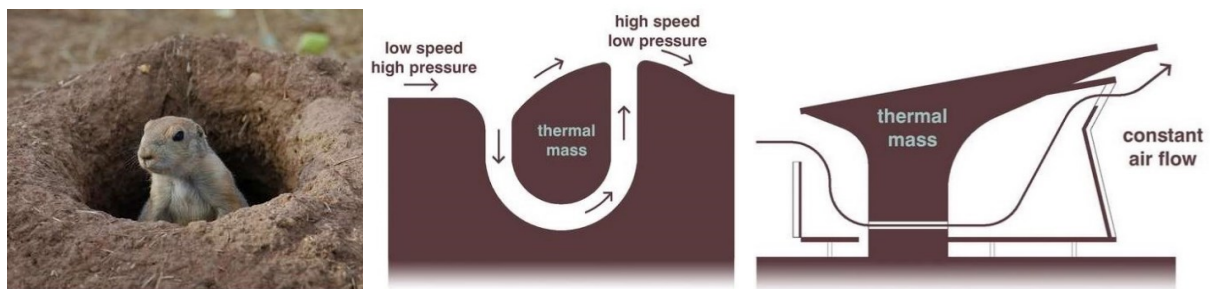
Figure 34: *Left*: Black-tailed Prairie Dog. Centre: Bernoulli Principle of the burrows. *Right*: Transfer design of the bungalows. (Araujo, Haddad, & Garcia)

Another cooling strategy is derived from the self-shading capacity of the desert Saguaro Cactus (**Figure 35**) (Araujo, Haddad, & Garcia). This organism was also mimicked on a *behaviour level* for its *process* as the building envelope works in the same way the Cactus would regarding the solar radiation: by specific shape and form. Mentioned previously as a relevant biological role model for thermoregulation, this organism has long spines and accordion-like folds mitigating the extreme desert temperatures and exposures (Woolley-Barker, 2017). This principle was transferred to the design of the Votu Hotel bungalows through the introduction of slatted wood on their facades (Araujo, Haddad, & Garcia).
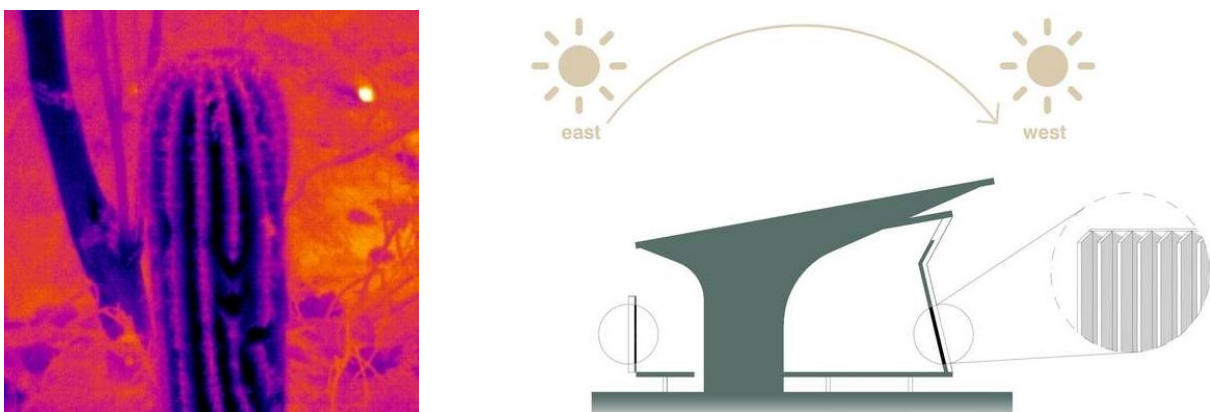
Figure 35: *Left*: Heat along the cooling ribs of Saguaro Cactus (AskNature Team, 2017). *Right*: Scheme of transfer design to slatted wood facades (Araujo, Haddad, & Garcia).

Finally, the combined performative roof typologies cited above are represented schematically in **Figure 36**. In terms of *protective roof* strategies, ribbed surfaces are applied to the vertical planes of the bungalows and additionally, mass is introduced with the concrete core as sketched in the section. From the *selective roof typologies*, one can recognize the ventilated roof combined with the living roof

typology. From the *classical roof taxonomy*, the shape of the bungalows can be characterized by a *sloped* roof typology and more particularly a mono-pitched roof. Note that this latter definition is seemingly less complete than through the explorative roof typologies.
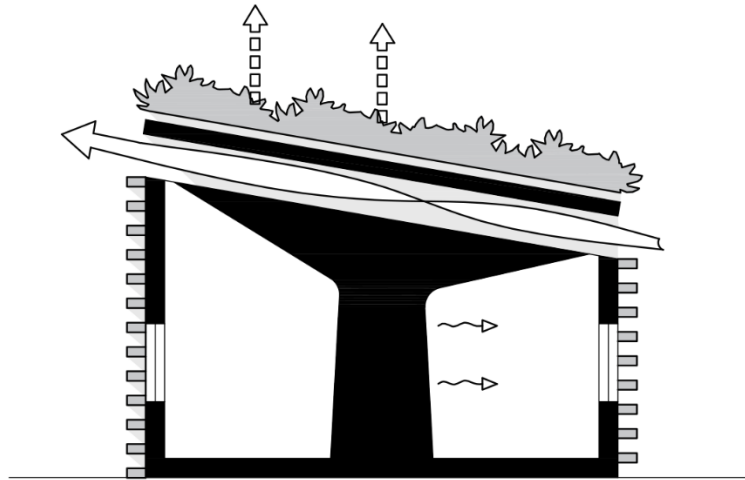
Figure 36: Performance scheme of the Votu Hotel roof based on the developed explorative roof taxonomy. Combination of typologies 1 and 2: *1. Protective roof typology*: Mass, and Form – Ribbed roof. *2. Selective roof typology*: Wind – Convective cooling, Hybrid – Living roof.

4.1.5. Esplanade - Theatres on the Bay (Singapour) – DP Architects

The Esplanade and Theaters on the Bay (**Figure 37**) is an international design competition project won by DP Architects and Michael Wilford & Partners for the design of what is now known as one of the busiest Arts Centers in the world (Verma, 2017). After its opening in October 2002, the New York Times referred to the project with the sentence "who could forget a building that is so, well, prickly?" (Wayne, 2002). This illustrates how iconic the roof shell design became to the Singaporean people who now refer to their Performance Arts Centre as "#mydurian". The new landmark indeed resembles the Durian fruit from Southeast Asia which has a spiky husk similar to the shading system of the two rounded envelopes covering the main performance venues of the Centre (DP Architects Pte Ltd., 2020). Even though this envelope was rather designed in a biomimetic way or for purely practical reasons, this case study is an example of roof design that drove the project towards a timeless identity by its shape and of which the shading system acts as a passive cooling strategy in a hot tropical rainforest climate (Af by the KCC).

Figure 37: View on one of the two rounded envelopes of the Performing Arts Centre, Singapour (Hwang, et al., 2015).

When the project was completed, people gave the building the spontaneous nickname of the "Durian" because of the aspect resulting from the shading devices surmounting the two glazed domes (**Figure 38**). In terms of *levels of biomimicry*, the building would be mimicked on an *organism level* by *form* as it resembles the shape of the fruit. The fruit is oblong in shape and has creamy flesh protected under its spiky husk that is savoured in items ranging from ice cream to pizza (Verma, 2017). The New York Times seemed to justify the resemblance as a way of not only representing the governor's hope that Singaporeans will develop their taste for the arts, but that the rest of the world will acquire a taste for Singapore (Wayne, 2002). However, although the project is the subject of several biomimetic references (Hwang, et al., 2015; Parametric House, 2019), others say that the architects did not intend to look like the durian fruit but that it simply seemed the most interesting way of doing sunshades (Verma, 2017).
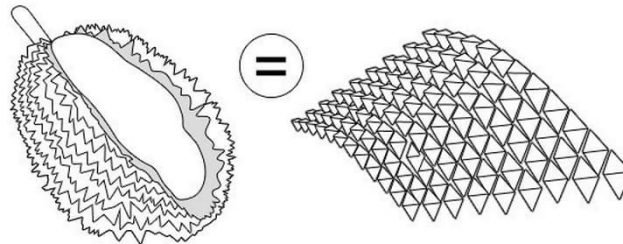
Figure 38: Biomimetism of the envelope (right) resembling the Durian plant (left) (Parametric House, 2019).

From the *classical roof taxonomy*, the building's design clearly arises from a *dome*-shaped roof typology. However, the two 40 meters spanning domes made of lightweight superstructure should once again be assessed on a more performative aspect as it goes beyond the classical geometry. The curved space-frames forming the dome are fitted with triangulated glass and covered by a system of champagne-coloured sunshades folding around the domes (T.Y. Lin International Group, 2020) (Anderson, 2012). The impact of these 7,000 aluminium sunshades on the thermoregulating performance of the envelope can be determined by referring to the *explorative roof taxonomy* and the *cool*, light-coloured roof typology reflecting the solar heat. The overall performance of the roof design is illustrated in **Figure 39**. The sun shading lattice gradually transforms in shape and orientation to adjust to the sun's angle and position during the day, in a responsive way (Parametric House, 2019). To do so, a complex geometry analysis via computer modelling was performed, enabling the calibration of the shields (Parametric House, 2019). By tracking the sun path of the equatorial climate, analysis showed an almost exactly east-west orientation that finally determined the exact shape and depth of the louvers (Parametric House, 2019). The result is a unique roof design giving out light at night and offering an internal architectural experience and a dramatic, ever-changing mesh of dappled sunlight and shadows (Anderson, 2012).
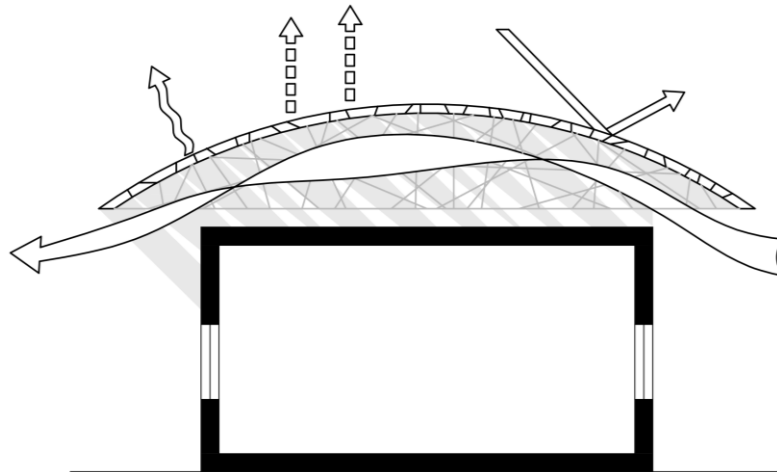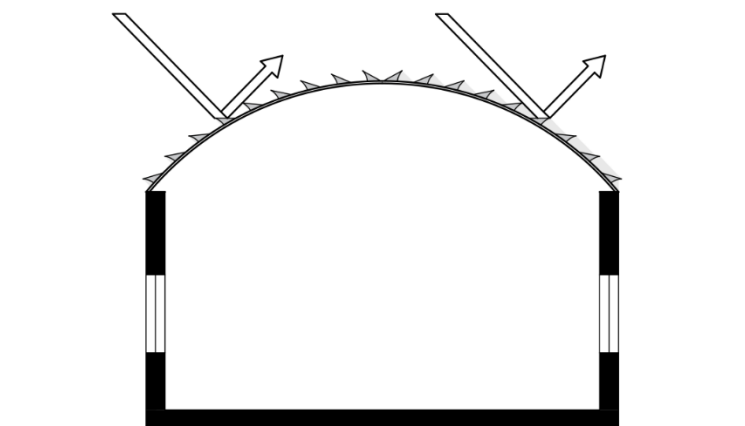

Figure 39: Performance scheme of the Theaters on the Bay roof based on the developed explorative roof taxonomy. Combination of typologies 1 and 3: *1. Protective roof typology*: Colour – Cool roof, Form – Ribbed. *3. Vernacular roof typology*: Shape – Dome.

4.1.6. Rafflesia House (Kuala Lumpur) – Zoka Zola Architecture

The Rafflesia House is one of the six winning designs for the Bird Island Zero-Energy Home competition held in 2007 (Zoka Zola, 2007). Eight design offices from all over the world proposed projects reflecting the competition brief calling for innovative and extraordinary designs that would contribute to the legacy of contemporary architecture. The site of the project is situated in the middle of the tropical Sentul Park in Kuala Lumpur, Malaysia, experiencing a tropical rainforest climate Af according to the KCC. The whole project showcases an integrated design in a singular context (**Figure 40**), achieving thermal comfort by balancing the openness of the building towards the outside, with the shelter that the building provides from the outside elements like plants, creatures, rain, sun, wind and heat (Zoka Zola, 2007). In order to allow species to develop around the construction, a minimal footprint became an important feature of the project and the floor was therefore elevated from the ground by twelve columns (**Figure 41**, Right) (5osA, 2009).

Figure 40: *Left*: View from the centre of the Rafflesia house, on the courtyard. *Right*: Plan of the project (Zoka Zola, 2007).

One of the challenges in such a setting was to work in harmony with the environment, use renewable materials, achieve a zero-energy balance and even comprise water recycling features (Zoka Zola, 2007). Following the *levels of biomimicry*, this project would mimic *ecosystems* on a *process* level; The building works in the same way as an ecosystem. Indeed, it recycles water, uses renewable materials, and achieves a zero-energy balance. On the other hand, the shape of the house would also look like the native Rafflesia flower (**Figure 41**), the largest flower in the world growing in the rainforest of Malaysia (Zoka Zola, 2007). If this *level of biomimicry* concerns *form* at the *organism level* (the building looks like the flower), the architects of the project however state that the resemblance was unintentional and that biomimicry was not its initial design strategy.

Figure 41: *Left*: the native Rafflesia flower of the Malaysian rainforests (Zoka Zola, 2007). *Right*: Rafflesia house, on stilts for minimal footprint (Archello, 2020).

The climate of Kuala Lumpur was extensively analysed for solar orientation, wind directions and rainfall to take the best of those surrounding conditions with regard to energy and comfort (Zoka Zola, 2007). According to the paper of Chris Butters –*Enhancing Air Movement by Passive Means in Hot Climates*– the main cooling strategy in such hot and humid climates will be the extensive use of air movement to achieve thermal comfort despite the hot temperatures (Butters, 2015). Indeed, contrary to the arid climate strategies referred to in this thesis, the present case study features a hot tropical climate design where NV is enhanced through wall shape, wall openings and a roof buffer space. Firstly, the alternating convex and concave walls of the envelopes accelerate the air movement and direct them towards the open windows and doors. The stilts of the house offer access for ventilation in the central courtyard. Also, the shielding of the wind by itself was minimized by elevating one part of the house higher than the other (**Figure 41**, Right). Finally, the roof design was conceived with an air space between the top and lower roof to insulate the house from solar heat gains, similarly to the strategy detailed in the *ventilated roof typology* of the *explorative taxonomy* (**Figure 42**). The interstitial space is 50 cm high and about 6 m deep to offer a sufficiently ventilated space to reject overheated air. Note that this value is higher than the cavity heights recommended by roof cooling researches discussed in Chapter 3, but lower than the space provided in the Gando Primary School. Additionally, low energy fans in the ceiling of the rooms remove exhaust air from indoor spaces to the latter roof space and consequently pull fresher air into the room (**Figure 43**). This combined strategy is predicted to offer enough cooling to achieve the necessary comfort and make the air-conditioning supply useless (Zoka Zola, 2007).

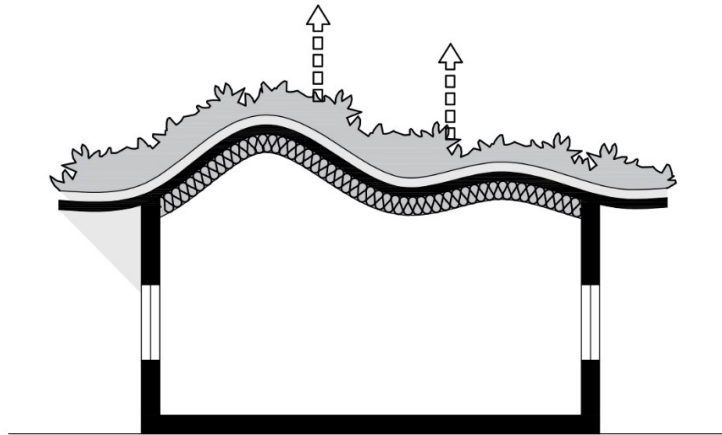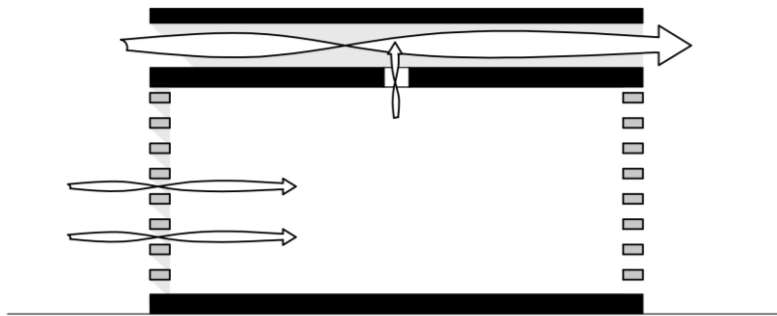**Figure 42**: Performance scheme of the Rafflesia House roof based on the developed explorative roof taxonomy. Combination of typologies 1 and 2: *1. Protective roof typology*: Form – Ribbed. *2. Selective roof typology*: Wind – Convective cooling.
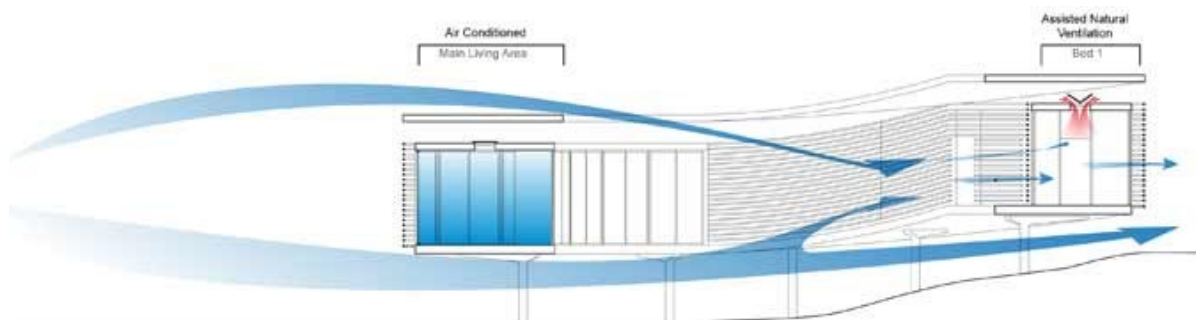
Figure 43: Natural ventilation strategies. *Blue*: Ventilation through the concave envelopes and below the stilts. *Red*: Exhaust air fans and interstitial roof ventilation (Zoka Zola, 2007).

4.2. Concepts and speculations

4.2.1. Roof system from BioTRIZ methodology – Saalman Craig

When searching for more speculative or conceptual biomimetic approaches for roof structures in hot climates, one cannot bypass the research of Environmental Technology engineer Salmaan Craig about a roof system based on the BioTRIZ tool methodology (**Figure 44**) (Craig, 2020). Together with David Harrison from the School of Engineering and Design of Brunel University, and Andrew Cripps and Daniel Knott from Buro Happold Ltd in London, Salmaan Craig worked on a paper demonstrating the access to biological strategies that the so-called *TRIZ contradiction matrix* offers for solving contradicting engineering problems (Craig, et al., 2008). This matrix is a tool made up of several opposing features that will point out a handful of principles that have been found to resolve a complex problem. This paper more specifically subjects a case of roof structure design in hot climates to the tool because of the contradictions inherent to the design optimization. Indeed, the insulation of standard roofs has a major issue that, although it stops the sun and convection from warming up the building, its closed character lacks interaction with the sky to enable RC. The aim is thus to find a nature-based solution, mimicked on any useful *level of biomimicry*, that enables inside accumulated heat to escape while avoiding outside heat to enter and heat the building (Craig, et al., 2008).
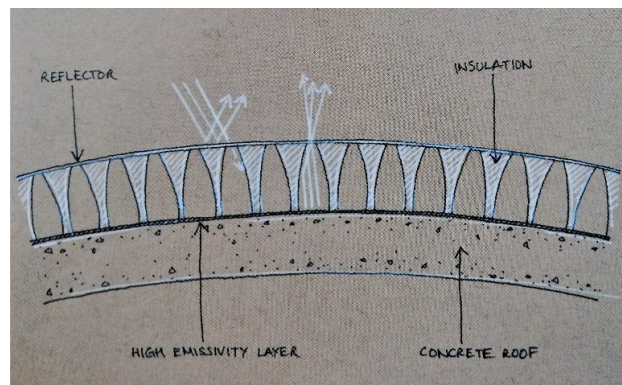
Figure 44: Roof structure conceived by Salmaan Craig with the BioTRIZ method (Pawlyn, 2016).

In hot climates, to save energy for cooling, buildings should be designed to cool down passively faster than they heat up. The passive strategies then become three-fold; the envelope should prevent heat gains, maintain cool air and reject excess heat into available heat sinks. One important and free available heat sink at all times is the open sky which is often at a lower temperature than the ambient air at ground level. The sky emits longwave infrared radiation downwards and the building emits longwave infrared radiation upwards. When the latter outweighs the former, net RC occurs (Craig, et al., 2008). In addition to that, the sun has a harmful heating effect by emitting shortwave radiation towards the roof. For a more detailed explanation of the thermal interactions of a roof with the sun, sky and ambient air, the reader is referred to **Appendix B.7**. Therefore, an optimal solution to achieve RC would be to counter shortwave radiation of the sun, while enabling longwave radiation from the building to escape. This spectral selectivity is already found in vernacular architecture in hot climate zones through the use of white paint or washes on massive buildings. White reflects the majority of shortwave radiation but lets longwave radiation pass. A direct biological analogue of this principle would be in the leaves, birds' eggs, and desert snail shells that reflect most of the near-infrared component of sunlight, countering partially the sunlight's thermal load (Craig, et al., 2008). Consequently, the building mass should be decoupled from the sun and the ambient air convection and conduction, but coupled to the sky in a more efficient way than 'standard' roofs do today.

Amongst other suggestive inventive principles to solution the contradictory problem of the coupling to the sky, the TRIZ matrix proposed changes in the structure to achieve longwave transparent insulation (Craig, et al., 2008). Salmaan Craig interpreted this result as offering longwave radiation a clear pathway by introducing voids through the insulation, bottom to top. A honeycomb structure was considered as a compatible example and was further investigated. The model is shown in section on **Figure 45** and represents a four-layer prototype composed of a shortwave reflector on the outer layer, a honeycomb insulation, a high emissivity layer or radiator, and a thermal mass layer like concrete on the inside. **Figure 46** also links these strategies with the developed explorative roof taxonomy. If RC is to occur in this situation, it is more likely to occur at night. When the radiator (c) is cooler than the mass (d), heat conducts upwards through the mass to the radiator. The radiator can reject his heat to the sky because the honeycomb (b) and the convection guard (a) let longwave radiation pass (Craig, Harrison, Cripps, & Knott, 2008). In the other direction, the honeycomb counters conductive transfer from the outside to the inside like standard insulation layers. The convection guard also arrests convection to transfer heat from the outside to the inside. Note that the concept will be successful if the night time cooling exceeds the day time heating (Craig, et al., 2008).

(a) **Shortware reflector / longwave transmitter / convection guard** - e.g. thin white tile

(b) **Honeycomb** – insulates from ambient heat gain, but allows longwave radiation to pass

(c) **Radiator** - e.g. concrete surface painter black

(d) **Thermal mass** - e.g. concrete
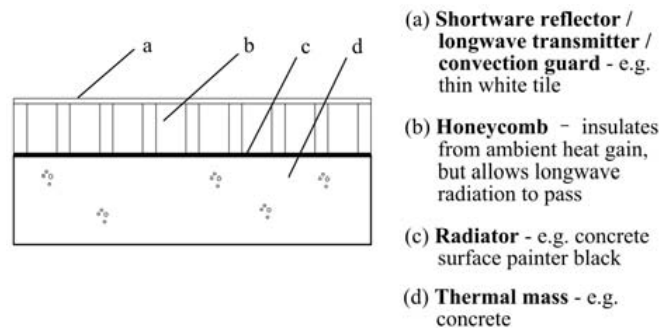
Figure 45: A cool roof for hot countries (not to scale) (Craig, et al., 2008).
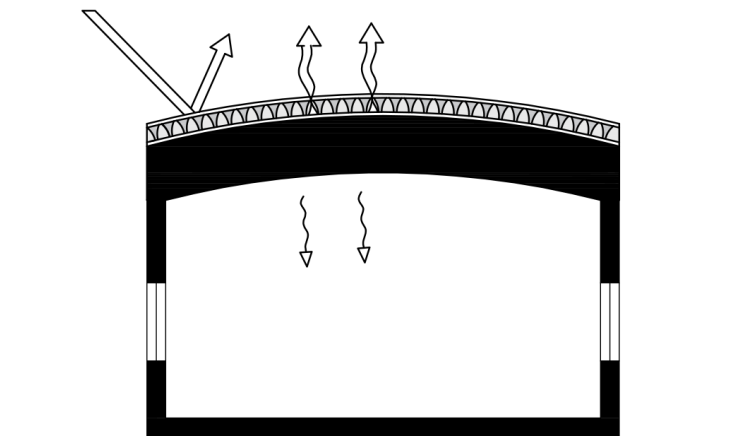
Figure 46: Performance scheme of the roof system from BioTRIZ based on the developed explorative roof taxonomy. Combination of typologies 1 and 2: *1. Protective roof typology*: Insulation, Mass, and Colour – Cool roof. *2. Selective roof typology*: Sky – Radiative cooling.

The analysis was performed for a one-year time-lapse using weather data from Riyadh, Saudia Arabia as a hot climate, more precisely defined by the KCC as belonging to a hot and arid desert climate type BWh. The model also simulated a white surface with an 80% shortwave reflectance (Craig, et al., 2008). Afterwards, the results were compared to a "standard roof" made up of 0.3 m of concrete painted white, indicative of the vernacular of Middle Eastern regions. The comparison is shown in **Figure 47** for two hot days in August. One can see that the difference stands out at night where a dip in temperature occurs on the outer surface of the 'new' roof. This temperature fall happens thanks to the more closely coupling to the sky and is translated into extra cooling (Craig, et al., 2008). On the inner surface, the new roof stays a few degrees cooler than the standard roof. **Table 5** shows more precisely how temperatures vary

thanks to the honeycomb. When the mean temperatures of the midpoints of the concrete masses are compared, it can be seen that the new roof stays 4.5°C cooler. More importantly, the new roof is 2.4°C cooler than the average ambient temperature while the standard roof stays above ambient temperature by 2.1°C. Finally, since the surface temperature never goes above the ambient temperature, it was concluded that the cooling period is on average longer than the heating period, which is a success (Craig, et al., 2008).

(a) Upper surface mass temperatures

(b) Lower surface mass temperatures
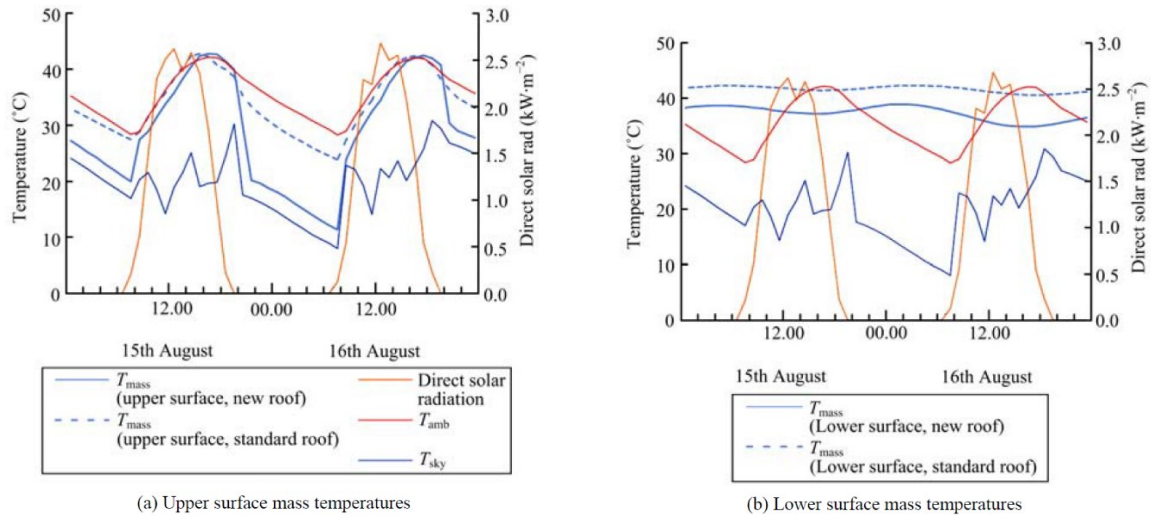
Figure 47: Performance estimation of the "standard" roof and "new" roof in Riyadh, Saudi Arabia (Craig, Harrison, Cripps, & Knott, 2008).

	T_{sky} (°C)	T_{amb} (°C)	Solar rad[*] (kWh·m^{-2})	Standard roof, T_{mass}(°C)			New roof, T_{mass}(°C)		
				Upper	Middle	Lower	Upper	Middle	Lower
Mean Max	21.9	31.7	2.4	32.2	31.5	31.9	32.0	29.1	28.3
Mean	11.7	25.6	0.63	24.2	27.7	31.2	19.6	23.2	26.9
Mean Min	4.1	19.0	0	17.1	24.4	30.7	8.0	17.7	25.8

[*]Direct only, annual total = 5494.2 kWh·m^{-2}.

Table 5: Performance of the "standard" and "new" roof over a whole year in Riyadh, Saudi Arabia, as modelled in TRNSYS (Craig, Harrison, Cripps, & Knott, 2008).

Before focusing on the honeycomb solution, the paper developed three other research fields that are worth mentioning in the context of roof design optimizations for hot climates (Craig, et al., 2008). Firstly, a change in space or interaction on a broader level than the subsystem was suggested. This can be interpreted with the example of the desert Jack Rabbit that feeds under open shade. His vascularized ears can reject heat to the open sky even in day time thanks to the protection from the sun by shading. Therefore, an external shading that follows the sun or even a well-placed tree could give a roof system enough open shading to enable daytime RC. Secondly, changes in time parameter suggested bypassing the insulation or barrier when it is advantageous to do so, for example at night. The roof system could thus have some removable insulation or flip round to expose the mass at night. Finally, a change in energy suggested adaptive structures. Thermal expansion is one interpretation given by the tool and suggests using thermal expansion or contraction of a material, or several with different expansion coefficients, to create some useful movement or some sort of deployable structure. These adaptive mechanisms could connect and disconnect the mass to the sky depending on the ferocity of the environmental heat sources like surface pores could close when it gets too hot (Craig, et al., 2008).

Chapter 5

Research by Design and simulations

*In Chapter 3, an explorative roof taxonomy was developed in order to expand the existing classification towards a thermal performance criterion. In Chapter 4, this taxonomy was applied to existing buildings and concepts demonstrating the potential of the new typologies compared to the limited existing archetypes in defining innovative roof designs through a combination of roof cooling strategies. Whereas the previous chapters were theoretically developed based on scientific results from the state-of-the-art of individual roof typologies, the present chapter explores by design and simulations the most promising roof typologies identified from the taxonomy, the case studies or biological role models in a quantitative way. To do so, four roof designs will be explored by simulation and compared to a reference scenario in terms of energy, temperature and discomfort to identify their advantages and weaknesses when subjected to the same conditions. Several designs are also further investigated for optimization with design variations as illustrated by the chapter outline in **Appendix C.1**. At the end of the chapter, the six roof design scenarios are compared to one another and conclusions are made in terms of energy and temperature, but also in terms of costs, availability, maintenance and longevity.*

5.1.   Energy Plus Simulation

EnergyPlus^{TM} is a building energy simulation program based on fundamental heat balance principles used by engineers, architects and researches to model both energy consumption and water use in buildings. In this chapter, the energy consumption of a design model is calculated based on input parameters defining among others heating and cooling schedules, ventilation, lighting, occupancy, material constituents and climate data for environmental conditions. The program basically reads input and writes output text files that will be interpreted for each scenario. The simulations calculate temperature and energy gains and losses for variable running periods (year, June, one day in June) and determined time steps (hourly, daily, monthly). For the 3D modellisation of the reference building, *Rhinoceros 5* is used and linked to *EnergyPlus v8.4.0* by a *Grasshopper* plug-in called *DIVA for Rhino*. Depending on the design proposal and feasibility, the roof surfaces are modified rather in the 3D model, or later by modification of the generated .idf file in the EP-Launch of EnergyPlus.

The precision of the results simulated by this program is directly dependent on the chosen input parameters and accuracy of the 3D model compared to the existing building in terms of material composition, orientation of the building, sizes, etc. In this chapter, several parameters had to be taken as default values, or estimated with the available documentation of the studied building. However, if these are chosen well, the program itself is reliable and very close to reality as it has been subjected to many verification and validation processes.

5.2.   Design questions

The design questions will be useful for the focus of the research. Indeed, by defining clear questions and objectives to the simulations, output parameters can be defined. The reference scenario is the opportunity to assess the present state and performance of the numerous and typical school buildings in the hot and arid climate of Egypt. The energy consumption for cooling, the temperature of the classrooms, and the discomfort experienced in those schools will be the focus of the research in order to be improved by the proposed roof designs developed in this thesis. Moreover, it will also be the occasion to validate the assumptions made in the literature research.

The questions to be answered through the experiment on Scenario (SC) 0 are:
1.   *What is the energetic performance of a typical Egyptian school building?*
2.   *What is the maximum temperature of the roof surface in the hottest months?*
3.   *Is the surface of the roof indeed more exposed than the façades in the hot and arid climate county?*
4.   *What is the level of discomfort of the students in the Egyptian schools as designed today?*

Furthermore, the different roof designs proposed later in this chapter will focus their discussion on:
1.   *What is the (quantitative) performance of the proposed roof design in terms of cooling and total energy consumption, surface and air temperatures, and comfort of the occupants?*
2.   *How can each explored roof typology be optimized and what are the points of attention influencing the design?*
3.   *Which solution stands out in terms of performance, and in terms of cost, availability, maintenance and longevity?*
4.   *Do the simulation results confirm the potential of the developed explorative roof taxonomy?*

5.3.   Scenario 0: Reference design

In this part, the reference scenario is introduced to set a base case on which further roof typologies will be applied and the results compared and discussed.
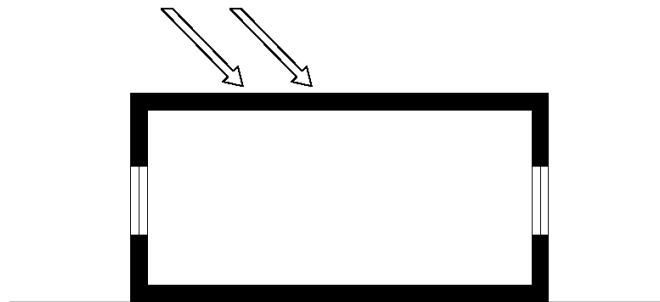
Figure 48: Performance scheme of the reference roof design. SC 0.

5.3.1.   Location and climate

The location that meets the requirements for the defined scope of the thesis is Egypt. As mentioned in the state-of-the-art, the country is located in a hot desert climate according to the KCC and experiences cooling needs and excess energy consumption resulting in electricity black-outs. Moreover, Egypt is part of the low-income group as defined by the World Bank and adds the challenge of cost to the research. In the EnergyPlus simulation, the weather data of the Cairo International Airport is used (**Appendix C.2**). Amongst others, the latitudes, longitudes, monthly temperatures, humidity, solar irradiance and wind speeds are measured in a weather station and referenced in the Climate Design Data

2009 ASHRAE Handbook. Accordingly, the summer period in Egypt is defined from May to July, and winter from November to January. In the summer, the average high temperature of Cairo ranges from 18.3°C in the morning to 34.1°C around 3 PM. The maximum dry bulb temperature occurs on June 7th and reaches 43.0°C. The annual average wind speed at the International Airport is 3.4 m/s although this average reached 8 m/s in the paper of Debaieh et al. for Cairo. The direct solar radiation is the highest in June and the lowest in January. The annual global average solar radiation in Cairo is 5.3 kWh/m². Finally, According to the ASHRAE adaptive comfort model Standard, comfort levels in Cairo range between 19.6°C and 29.0°C (Dabaieh, et al., 2014).

5.3.2. Shape and function

First of all, in the scope of this master thesis, the roof design should have a great impact on the building thermoregulation and the shape of the simulated model should therefore reflect the added value of the design. For example, a building that has several levels and a small roof surface will have a small roof to wall ratio and the design of the roof will have less impact than for the walls. Consequently, the model should be relevant for this purpose. Secondly, as the period of solar heating of a horizontal surface such as roofs coincides with a daytime occupation, the research should focus on sectors such as workplaces or schools. Moreover, in Egypt, schools represent a broad sector of construction with about 15 600 schools all around the country. More importantly, thermal comfort plays a major role in the educational building sector, especially in hot and arid climates where design has a big impact on interior temperature and therefore on the well-being and concentration of the pupils (Saleem, et al., 2015). However, this building sector in Egypt does not have a small roof-to-wall ratio as these constructions typically are elongated in plan and count at least three levels above ground. Consequently, it would be more interesting to make use of exclusively the upper level of a typical educational building typology for the simulation model. Finally, a typical educational building should be used as a base case model in order to be relevant to the research. In 1992, Egypt experienced a considerable increase in demand for educational buildings and the General Authority of Educational Buildings (GAEB) was established by the government to design new schools that have been copied as typology all over the country. These schools relied on infiltration air of cross-ventilation with ceiling fans to achieve thermal comfort. However, as they have been copied regardless of the climate variation in the different regions, the project resulted in uncomfortable interior conditions within the classrooms i.e. heat stress, lack of adequate ventilation, glare and exposure to excess solar radiation (Saleem, et al., 2015). Therefore, a GAEB educational building is an excellent case study for improved thermal performance of a typical building in Egypt.

5.3.3. Simulation model

5.3.3.1. Case study

The research will base its input parameters and geometry on a coherent case study responding to the climate, shape and function discussed above. The Assiut Prototype Distinct Language School is a public primary school built in 2009 belonging to the GAEB (Saleem, et al., 2015). This school has consequently been designed based on the prototype architectural system as for the typical schools all over the country. The building is elongated in plan and counts five stories for a total surface of 3168.37 m². Each floor counts five classrooms reaching a total of 24 classrooms throughout the school. The façade is made of construction materials that are conventional according to the Egyptian Code for Buildings (Saleem, et al., 2015). As detailed in **Table 6**, the external walls are made of 25 cm red brick with interior finishing while the floors and roof are made of a 12 cm concrete slab with interior finishing and additional sand brick and tiles. Windows have also glass specifications detailed in **Table 7** and the glazing type used is a 6 mm single clear layer glazing with aluminium frames. These will be the construction layers of the simulation model of the present reference design.

Material	Thickness [mm]	Density [kg/m³]	Conductivity [W/mK]	Specific heat [J/kgK]
External wall from outside to inside (U-value = 1.58 W/m²K)				
Plaster (light)	25	2300	1.3	840
Mortar	20	2800	0.88	896
Brick	250	1500	0.85	840
Roof from outside to inside (U-value = 1.92 W/m²K)				
Mosaic tiles	30	2100	1.4	800
Mortar	20	2800	0.88	896
Sand brick	60	2200	1.83	712
Reinforced concrete	120	2300	1.9	840
Mortar	20	2800	0.88	896
Plaster (light)	25	2300	1.3	840
Intermediate floors (U-value = 1.14 W/m²K)				
Ceramic tiles	25			
Mortar	20	2800	0.88	896
Sand brick	60	2200	1.83	712
Reinforced concrete	120	2300	1.9	840
Mortar	20	2800	0.88	896
Plaster (light)	25	2300	1.3	840

Table 6: Case study Assiut prototype distinct language school. Built in 2009. Construction materials of the reference design. (Saleem, et al. 2015)

Material	Category	SHGC	LT	U-Value [W/m²K]
Glazing				
Clear 6.4 mm	Single	0.71	0.65	5.76

Table 7: Used Glass specifications. SHGC = Solac Heat Gain Coefficient. LT = Light Transmission. (Saleem, et al., 2015)

Due to a lack of documentation about the building geometry itself, the simulation model as shown has been reconstructed based on a 3D view and given surfaces of windows and total floor area. Finally, the building is approached to measure 45 meters by 13.80 which results in floor surfaces of 621 m² and a total floor area of 3105 m² which is close to the 3168.37 m² announced in the case study itself. In **Figure 49** below, one can compare the documented three-dimensional view with the actual reference design built in *Rhinoceros 5*. The windows are partly operable on a surface of 1.50 m to 1.20 m as is mentioned in the case study and their total surface is approached by a 2.80 m by 1.70 m rectangular window frame. All the input parameters and assumptions made for the simulation are based on the knowledge of this typical school building in Egypt and are discussed in the following paragraphs. For additional pictures of the classrooms and these windows, the reader is referred to **Appendix C.2**. The Grasshopper script of the simulation model is also available in **Appendix C.3**.
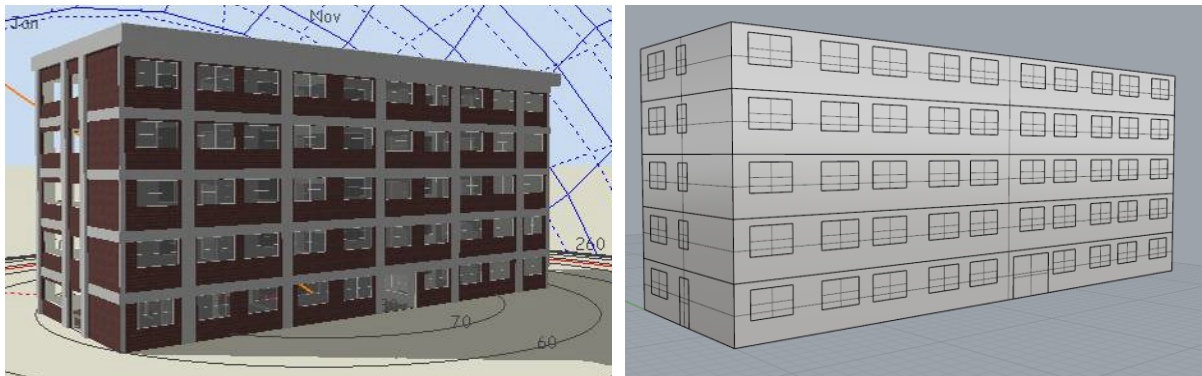
Figure 49: *Left*: Reference case model in Design Builder given in the Case study documentation (Saleem, et al. 2015). *Right*: SC 0. Simulation model of the reference design in Rhino 5.

5.3.3.2. Input parameters

Schedule, occupancy and infiltration
The occupancy rate will be taken as 1.1 m² per pupil (or 0.909 person/m²) as expressed in the case study documentation (Saleem, et al., 2015). Note that this value is a lot lower than in the USA, where 2.15 m² per pupil is taken into account. This means that pupils have less individual space in a typical primary school in Egypt. As the reference building is a school, the simulation will be performed in a schedule of working days. However, although the scholar period of Egypt goes from September 15th until June 30th, the program doesn't allow to simulate results over two years i.e. from the 9th month to the 6th month of the year. Therefore, the simulations will be performed over the entire year. Yet, as the hottest month is June and the occupants have school until the last day of that month, the analysis on the cooling period is still relevant. Moreover, the performance assessment of the roof designs will be more complete for further application to other purposes.

Infiltration and ventilation
As windows are single glazed and poorly constructed, very high levels of permeability occur on both long sides of the building. An infiltration rate of 0.5 ach/h is considered as was given. This value takes into account the operability of the windows when the classrooms are occupied. Mechanical ventilation is not provided but ceiling fans create air movement which will have a positive impact on the comfort of the occupants. However, no input parameter enables us to take this into account as it is neither NV nor mechanical ventilation where air is refreshed.

Internal gain
In the case of primary school buildings, one can assume that less to no computers are needed for the pupils and the *Equipment Total Heating Energy* is therefore assumed to be neglectable. The main internal gains come naturally from the people releasing metabolic heat, i.e. the *Zone People Total Heating Energy*. Moreover, as the occupancy of the classrooms in public schools of Egypt are relatively high, this value will contribute considerably to the overheating of the classrooms. Finally, the artificial lighting will also contribute to the heat gains of the rooms, i.e. the *Zone Lights Total Heating Energy*. The classrooms are provided with four groups of three 1200mm T8 lamps which represent a wattage of 192 Watt (16W per lamp) per classroom, or 1,71 W/m² of heat gains (Saleem, et al., 2015; Philips, 2019).

Temperature setpoints
According to the previous climate analysis, the comfort levels in Cairo lay between 19.6°C and 29°C. These values are consequently taken as setpoint temperatures for the simulation model. This means that when the temperature rises above 29°C, mechanical cooling is turned on and when it goes below 19.6°C, heating is needed. These setpoints have thus a direct impact on the total heating and cooling energy needs of the building.

Thermal zone
In EnergyPlus, a thermal zone has to be defined where the thermal conditions and balance with external temperatures will be calculated by the software. Here, the zone of interest will be the last level of the building. By considering only the last floor, the impact of the roof on the indoor conditions will be considerably higher. According to the following basic formula (**5.2.3.2.(1)**) of roof-to-wall ratio, the ratio goes from 0.3 in the case of the whole building to 1.5 for the last level alone. The connection of this thermal zone to the lower levels of the building is taken into account by defining the floor as an adiabatic surface. This means that no heat will be transferred between two adjacent levels as they behave the same way with respect to the outdoor conditions and experience the same temperature fluctuations.

$$\frac{Roof\ surface}{External\ wall\ surface} = Roof\ to\ wall\ ratio \qquad (\textbf{5.2.3.2. (1)})$$

5.3.3.3.   Output parameters and hypotheses

Energy

In order to assess the energetic performance of the reference building and thereby answer the first design question, an energy balance or Sankey diagram will be simulated for the cooling period of June, being the hottest month of Cairo in Egypt. The balance will be formed by gains and losses that are equilibrated by the cooling energy to keep the temperature at a comfort level (**Table 8**).

Parameter	Output parameter in EnergyPlus	Gain	Loss
People internal gain	Zone People Total Heating Energy [J]	Gain	
Lighting internal gain	Zone Lights Total Heating Energy [J]	Gain	
Windows	Zone Windows Total Heat Gain Energy [J]	Gain	
	Zone Windows Total Heat Loss Energy [J]		Loss
Opaque Surfaces	Zone Opaque Surface Inside Faces Total Conduction Heat Gain Energy [J]	Gain	
	Zone Opaque Surface Inside Faces Total Conduction Heat Loss Energy [J]		Loss
Infiltration	Zone Infiltration Total Heat Gain Energy [J]	Gain	
	Zone Infiltration Total Heat Loss Energy [J]		Loss
Cooling Energy	Zone Ideal Loads Zone Total Cooling Energy [J]		Loss

Table 8: SC 0. Output parameters for the energy balance of the reference design. Monthly simulation for the month of June.

Furthermore, the energy demands will be simulated for the entire cooling and heating period to understand the importance of the cooling energy compared to the heating energy in hot and arid countries.

Parameter	Output parameter in EnergyPlus
Cooling Energy	Zone Ideal Loads Zone Total Cooling Energy [J]
Heating Energy	Zone Ideal Loads Zone Total Heating Energy [J]

Table 9: SC 0. Output parameters for the cooling and heating energy needs of the reference design. Simulated in monthly values for the entire year (January 1st until December 31st).

Temperature

First, the envelope of the typical school building will be assessed based on the air temperature inside the classrooms in function of the climate and outdoor temperature. This will be performed on a monthly basis for the period of occupancy, while the temperature setpoints are set on. Therefore, this does not indicate if overheating occurs but gives a first insight into the behaviour of the envelope.

To understand the influence of the roof designs proposed in further scenarios, the inside and outside surface temperatures of the roof will be analysed. The aim of this research is of course to diminish the surface temperatures of the roof by design proposals. Also, in this reference scenario, the outside surface temperature of the roof will be compared to the temperatures of the facades to confirm the hypothesis that the roof surface will be more exposed to heat than the vertical façades in the hot and arid country. To do so, and to answer design questions 2 and 3, the following output parameters will be simulated over the entire school period, on a monthly basis:

Parameter	Output parameter in EnergyPlus
Outside air temperature	Zone Outdoor Air Drybulb Temperature [°C]
Inside air temperature	Zone Mean Air Temperature [°C]
Outside surface temperature	Surface Outside Face Temperature [°C]
Inside surface temperature	Surface Inside Face Temperature [°C]

Table 10: SC 0. Output parameters for the air and surface temperature calculations. Simulated on a monthly basis for the entire year (January 1st until December 31st).

Discomfort

In this section, the cooling (and heating) setpoints will be set off. This will help understand the risk of overheating and the level of discomfort that is experienced when no cooling mechanism equilibrates the gains due to solar heat, people and lighting equipment. First, overheating will be measured with hourly values over the hottest month (June) of the year. Then, the hours of discomfort according to the ASHRAE 55, will be evaluated daily over the same month. As was stated in the literature research in Chapter 2, Egypt experiences summer discomfort due to a lack in cooling amenities and excess heat stress. This will therefore constitute the hypothesis that should be verified through this simulation.

Parameter	Output parameter in EnergyPlus	Simulation
Hours of discomfort	Zone Thermal Comfort ASHRAE 55 Simple Model Summer Clothes Not Comfortable Time [hr]	Daily
Inside air temperature	Zone Mean Air Temperature [°C]	Hourly

Table 11: SC 0. Output parameters for the evaluation of discomfort in the classrooms of the reference scenario. Simulated over the entire year (January 1st until December 31st).

5.3.4.   Results and discussion

5.3.4.1.   *Energy*

First of all, the energetic performance of the typical school building in Egypt can be assessed with a simple heat flux equilibrium during the hottest month of the cooling period of Cairo. The so-called Sankey Diagram is illustrated in **Table 12**. The difference between the total heat gains and losses are compensated by a cooling energy need that equilibrates both sides. On one hand, the detailing of the heat gains shows the importance of the people internal gains mainly due to the high occupancy of pupils per classroom. Also, gains through the large windows are consequent as well as the ones through the walls and roof (opaque surfaces). On the other hand, NV through the operable windows (here the infiltration losses) has a beneficial compensation role resulting in a reduction of the total cooling energy needed. Finally, the balance shows an equilibrium around 27.50 kWh/m².

Energy Balance Cooling period, June	Gains [kWh/m²]	Losses [kWh/m²]
Internal gains (People)	12.53	
Internal gains (Lighting)	0.38	
Windows	6.28	2.04
Opaque Surfaces	8.44	3.25
Infiltration	0.18	2.92
Cooling energy		19.29
Balance	27.80	27.50

Table 12: Sankey diagram of the cooling period of June. Energy balance gains – losses. Monthly value simulation. SC 0.

The annual energy needs result directly from the sum of the heating and cooling energy use for the entire year. As expected for a hot and arid climate region, **Table 13** shows that the cooling energy exceeds the heating energy by nearly a factor ten. The design proposals in this chapter will aim to minimize this cooling energy need and finally the total energy consumption of the school building.

Annual Energy needs Academic year	
Annual Cooling Energy [kWh/m²]	100.33
Annual Heating Energy [kWh/m²]	12.82
Total Annual Energy	113.15

Table 13: Annual Cooling and Heating energy need. Annually value simulation.

The distribution of these annual values over the months of the year are illustrated graphically in **Figure 50**. The maximum monthly value for cooling energy reaches 21.25 kWh/m² whereas the maximum heating value reaches 5.43 kWh/m². For detailed results of SC 0, the reader is referred to **Appendix C.5**.
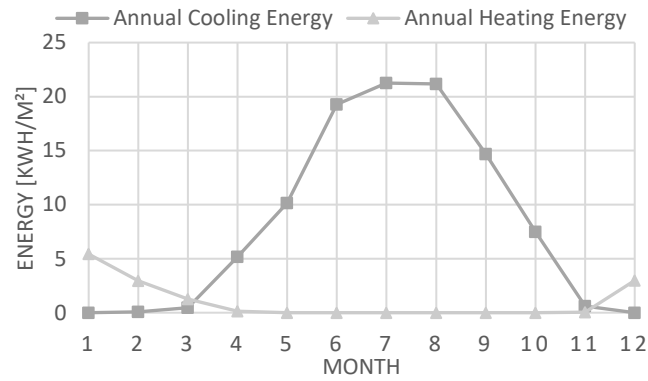
Figure 50: Graph of the annual cooling and heating energy need of the reference building distributed over the year. SC 0.

5.3.4.2. Temperature

From the temperature results in **Figure 51**, several questions from paragraph **5.2** can be answered. First of all, the left graph shows the behaviour of the envelope as buffer between the indoor air temperature and the outdoor dry-bulb air temperature. Indeed, the temperature inside the classrooms is higher but also more constant than the outdoor environment. Note that mechanical cooling and heating are also keeping the temperatures between comfort levels i.e. between 19.6°C and 29°C as defined for Egypt. Moreover, the results show the average roof surface temperature exceeding the outdoor hottest month temperature by 7.3°C. Finally, the right graph of **Figure 51** compares the surface temperatures of the roof surfaces to the south-facing wall and confirms that the roof reaches much higher temperatures and is therefore seemingly more exposed to sun radiation. The highest temperature difference is reached in July with a gap of 6.3°C. Therefore, improving the roof design has great potential in reducing temperatures and energy consumption compared to vertical façades.
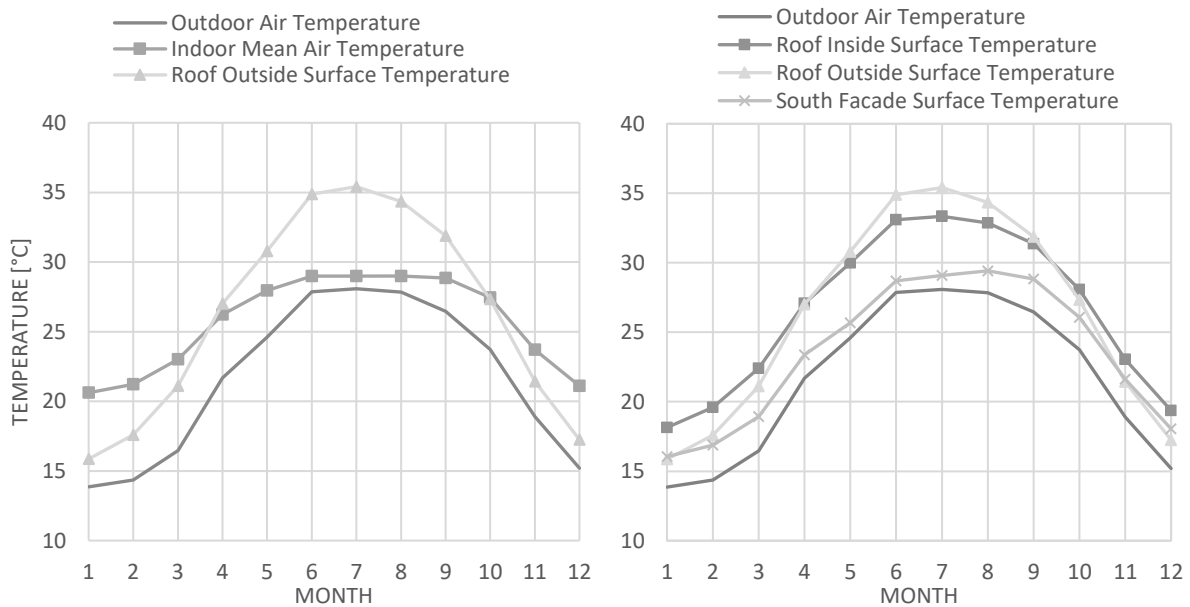
Figure 51: Monthly temperature values. Monthly simulation. Cooling On. *Left*: Indoor Air Temperature and Roof Surface Temperature. *Right*: Surface Temperatures.

5.3.4.3. Discomfort

For this part of the performance analysis of the building, the mechanical cooling schedule is set off. This means that inside temperatures will not be cooled down when they exceed 29°C. The hours of discomfort shown in **Figure 52** correspond to the number of hours per day that the indoor temperature exceeds this setpoint and causes discomfort for the occupants. In the hottest month of June, the average discomfort

hours reach 10 hours per day when the pupils are at school i.e. five days per week. Although the temperature probably still exceeds this comfort level in the weekend, no discomfort is experienced as the classrooms are not occupied. The level of discomfort in typical school buildings with no cooling amenities are thus consequent in cities like Cairo and confirm the issue of the hot and arid climate countries.
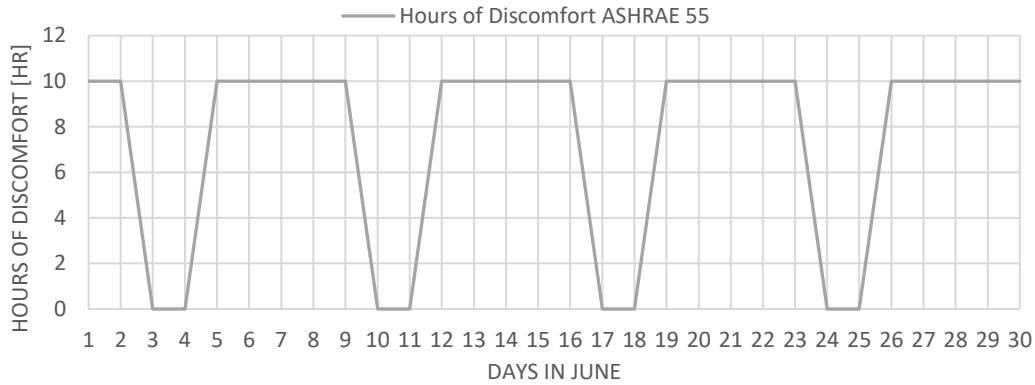
Figure 52: Graph of the number of hours of discomfort in the classrooms distributed over the days of June. Daily simulation. Cooling schedule Off. SC 0.

The risk of overheating can also be illustrated in temperature when the cooling systems are set off. For June, **Figure 53** shows that the air temperatures inside the classrooms range between 27.8°C and 40.7°C. Most of the time however, the temperatures exceed 29°C.
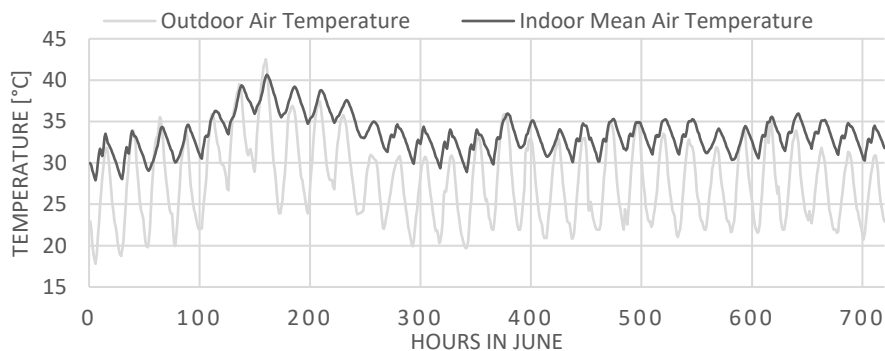
Figure 53: Risk of overheating. Indoor Mean Air Temperature. Cooling Setpoint Off. Hourly value simulation. June. SC 0.

A closer look at the temperature tendencies can also be taken on the hottest day of the year to visualize the peak values of the roof and indoor air temperature when no cooling is used. The roof surface temperature on that day reaches 55.3°C when the outdoor air temperature is at a temperature of 41.7°C around 2 PM. The peak temperature inside the classrooms however occurs at 4 PM that day, with a value of 40.7°C.
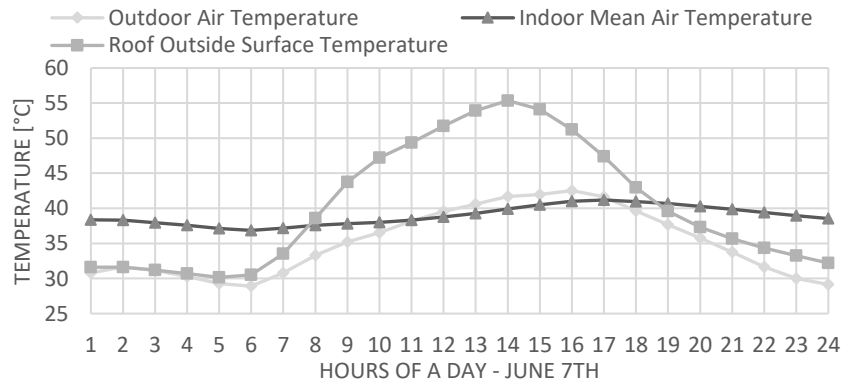
Figure 54: Graph of the roof and air temperature tendencies on June 7th. Hourly value simulation. Cooling setpoint Off.

5.4.   Scenario 1: Naturally vented cavity

The first improvement that will be explored by design is the application of a naturally vented roof. As seen in paragraph **3.2.2.2** of the developed selective roof taxonomy, this strategy is of great interest because of the use of wind which is a renewable and cheap passive cooling system. It is also low-maintenance and effective in performance according to the literature research.
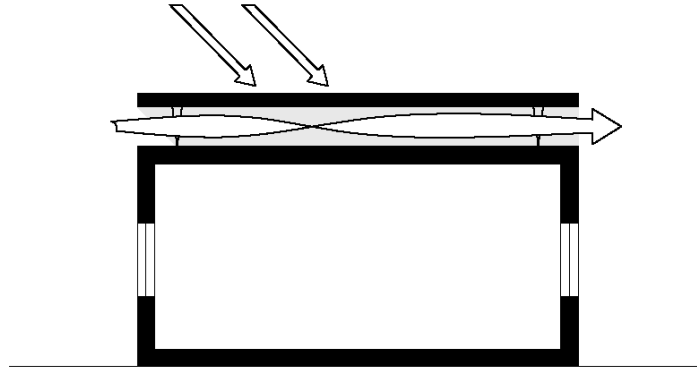
Figure 55: Performance scheme of the ventilated roof design. SC 1.

5.4.1.   Simulation model

The expected effect of the ventilated space on the indoor conditions of the building can be simulated through EnergyPlus by the input object "SurfaceProperty:ExteriorNaturalVentedCavity" introducing a so-called opaque multi-skin exterior. In this case, the cavity acts as a radiation and convection baffle separating the exterior environment from the outside face of the underlying heat transfer surface. The outer surface or "baffle" is, in contrary to the underlying mass surface, considered as a layer of very low (neglected) heat capacity and which is sufficiently thin and high-conductivity to assume a single temperature.

5.4.1.1.   Input parameters

Exterior baffle material
The baffle, or second roof above the vented cavity, is considered to be made of a thin precast concrete panel. As opposed to the CGI sheeting, concrete is less conductive but has a higher emissivity which means the panel will encounter lower temperatures than with CGI. Moreover, concrete panels are used more extensively in the past years in hot and arid countries and are thus available in these regions as explained in point **3.2.3.2** of the vernacular roof typologies. This material is characterized by a thermal emissivity of 0.90 and a solar absorptivity of 0.72 (Marceau & VanGeem, 2008).

Summary of SurfaceProperty:ExteriorNaturalVentedCavity parameters
The following table shows the parameters used for the simulations in EnergyPlus. Three cavity thicknesses will be evaluated for further optimization of the design: 10 cm, 50 cm, and 270 cm. The area fraction of openings is dependent on the total roof surface and height of the baffle on the perimeter where wind flows through. The effectiveness for perforations with respect to wind depends on the geometry of the openings (higher values correspond to higher wind flow) and was taken higher than the default value to take into account the fully open character of the cavity. This parameter typically ranges between 0.05 and 0.65 with a default of 0.25. Therefore, the increase by 0.10 should be taken carefully but improves the design by an increased mass flow rate through the cavity. To consult the detailed definitions of these parameters as defined by the U.S. Department of Energy, the reader can consult **Appendix C.4** (Figure C - 5).

Parameter	Units	Value	Comment
Area Fraction of Openings	-	0.019	Thin cavity
		0.095	Thin cavity 2
		0.511	One level
Thermal Emissivity of Exterior Baffle Material	-	0.90	Precast concrete
Solar Absorptivity of Exterior Baffle	-	0.72	Precast concrete
Height Scale for Buoyancy Driven Ventilation	m		Depends on inclination and cavity height
Effective Thickness of Cavity Behind Exterior Baffle	m	0.10	Thin cavity
		0.50	Thin cavity 2
		2.70	One level
Ratio of Actual Surface Area to Projected Surface Area	-	1	Flat surface
Roughness of Exterior Surface	-	Medium Rough	Default
Effectiveness for Perforations with Respect to Wind	-	0.35	
Discharge Coefficient for Openings with Respect to Buoyancy	-	0.65	Default

Table 14: Input parameters SurfaceProperty:ExteriorNaturalVentedCavity. SC 1.

5.4.1.2.   Output parameters

For the vented cavity, several output parameters inherent to the cavity and baffle heat (and mass) balance can be simulated by EnergyPlus. These results will help to understand the behaviour of the vented roof typology. In addition, the output parameters selected for the reference scenario will also be calculated in this case in order to be able to compare the results with the initial situation and assess whether or not this is an improvement in terms of performance. For more information about the parameters explained briefly below, the reader is referred to **Appendix C.4** (Figure C - 7).

Baffle heat balance

In the simulation, the baffle is subjected to different heat transfer mechanisms and a resulting heat balance as shown in **Figure 56**. The heat balance on a control volume that just encapsulates the baffle surface will enable the determination of the baffle temperature $T_{s,baff}$ afterwards.

The heat balance on the baffle surface's control volume is:

$$q''_{\alpha sol} + q''_{LWR,Env} + q''_{conv,Env} + q''_{LWR,cav} + q''_{conv,cav} + q''_{source} = 0$$

Where the q variables are the thermal flux exchanges inherent to respectively the solar radiation, radiation to the outdoor environment, convection with the outside air, radiation to the outside face of the underlying roof surface, convection with the cavity air and heat in case of the presence of a heating source like a PV panel. All terms are positive for net flux to the baffle.

Finally, the temperature of the baffle can be calculated as such:

$$T_{s,baff} = \frac{(I_s\alpha + h_{co}T_{amb} + h_{r,atm}T_{amb} + h_{r,sky}T_{sky} + h_{r,gnd}T_{amb} + h_{r,cav}T_{so} + h_{c,cav}T_{a,cav} + q''_{source})}{(h_{co} + h_{r,air} + h_{sky} + h_{r,gnd} + h_{r,cav} + h_{c,cav})}$$

Where I_s is the incident solar radiation [W/m²], α is the solar absorptivity of the baffle, h_r are the linearized radiation coefficients, h_{co} the convection coefficients and T the temperatures of the ambient air, the sky, the outside face of the underlying heat transfer surface and the cavity air.
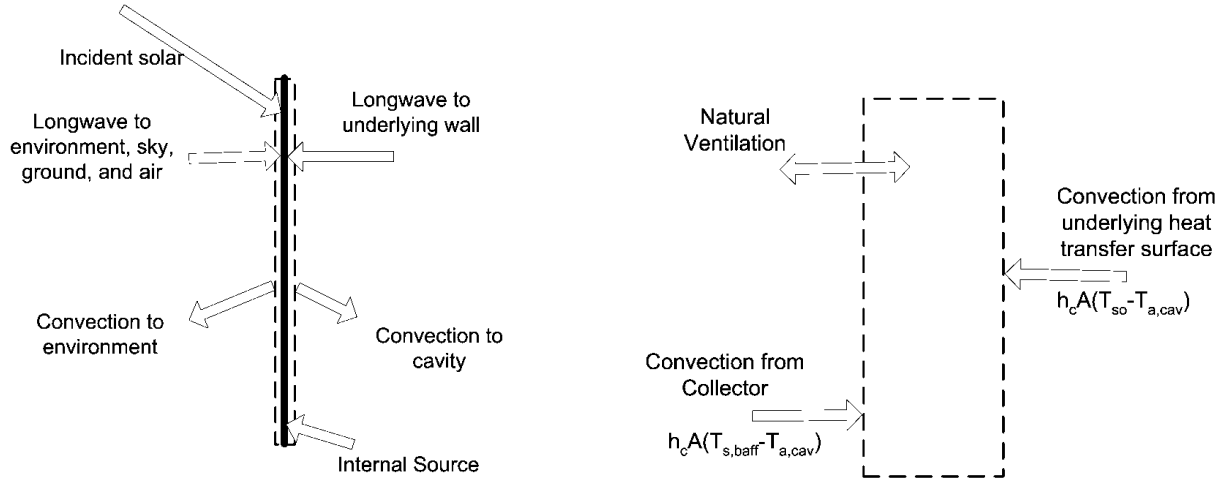
Figure 56: *Left:* Baffle surface heat balance. Heat balance on a volume that encapsulates the surface. *Right:* Cavity air heat balance. (U.S. Department of Energy, 2020)

Cavity heat balance

The cavity is the volume of air between the baffle and the underlying heat transfer surface. The temperature of the cavity $T_{a,cav}$ is determined by first determining the heat balance on a control volume of air as illustrated in **Figure 56**.

The heat balance resulting from the different heat transfer mechanisms is defined by the following relation:

$$Q_{vent} + \dot{Q}_{co} + \dot{Q}_{c,baff} = 0$$

Where Q_{vent} is the net rate of energy added from NV, where outdoor ambient air exchanges with the cavity air. $\dot{Q}_{co}$ is the net rate of energy added by surface convection heat transfer with the underlying surface. $\dot{Q}_{c,baff}$ is the net rate of energy added by surface convection heat transfer with the collector.

Finally, the temperature of the cavity can be calculated as follows:

$$T_{a,cav} = \frac{(h_{c,cav}AT_{so} + m_{vent}c_pT_{amb} + h_{c,cav}AT_{s,baff})}{(h_{c,cav}A + m_{vent}c_p + h_{c,cav}A)}$$

Where m_{vent} is the air mass flow from natural forces [kg/s] which depends on wind velocity, effectiveness of the openings, orientation and the density of air.

5.4.1.3.   Hypotheses

The hypotheses on the results of this design would be the following. First, a decrease of the exterior roof surface or outside face of the surface underlying to the cavity is expected. This would be achieved by a dual effect of, on one hand, the shading of the baffle on the roof and on the other hand, the evacuation of excess heat of the cavity by convection due to wind and buoyancy. However, the double roof layer through which the wind should flow has a minimum depth of 13.80 m which is a lot deeper than for the case studies explored in Chapter **4.1**. In the end, the decreased roof surface should result in a decrease in indoor temperature and therefore indirectly decrease the cooling energy need of the building. On the other hand, the losses through the roof will perhaps also be reduced by the buffer space and additional layer.

5.4.2.   Variation of the design

Intuitively, the first variation of design necessary to this research will be the optimization of the cavity height in terms of *performance*. Back to the selective roof typology of ventilated roofs in paragraph **3.2.2.2**, different opinions were highlighted. Whereas according to Biwole et al., the double skin width should be over 6cm and below 10cm, the Rafflesia House case study in **4.1.6** was designed with a 50cm cavity height and the Gando Primary School in **4.1.3** with an even greater value. Here, the simulations were performed for three values namely 0.10 m, 0.50 m, and 2.70 m (**Table 14**).

The design could also be enhanced by taking lessons from the black-tailed prairie dog as a biological role model enounced in Chapter **2.3.3**. This animal is known for its effective use of wind as renewable energy for NV of his habitat. He uses the pressure differences of air velocity dependent on the height from the ground, governed by the Bernouilli's principle, to enhance the wind flow ventilating his burrows. Based on this principle, it is interesting to quantify the effect of inclination of the cavity and openings towards the wind. Physically, from the ExteriorNaturalVentedCavity component of EnergyPlus and its input parameters, it is clear that the inclination will affect the buoyancy variable positively which will increase the airflow through the cavity.
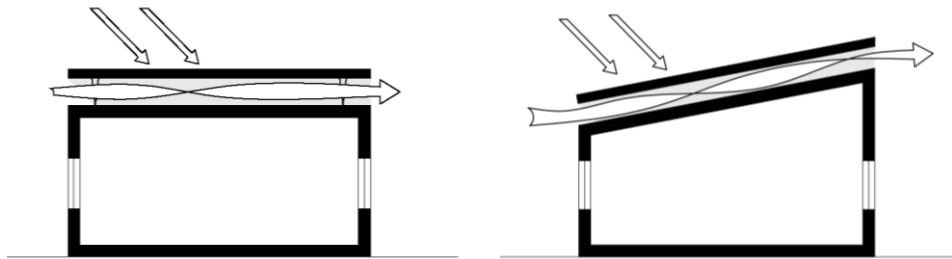
Figure 57: *Left.* Performance scheme of the base case of the ventilated roof typology. *Right.* Performance scheme of the design variant by inclination of the ventilated roof typology by 10°.

However, a range of other parameters should come into consideration to characterize the ventilated roof typology. First, *cost* introduces a new design variant whereby the "cavity thickness" is used as an additional habitable space giving an architectural purpose to the second roof. Nevertheless, the efficiency of a cavity of 2.70 m will probably be minimized as the geometry is closer to the reference scenario without ventilated roof. Also, a bearing structure is needed to sustain the upper roof surface at a distance of the initial one. However, this structure is not taken into account in the simulation where the second roof is directly considered at a distance from the existing roof. For the choice of this material, *availability* should come into consideration. However, *availability* of material can affect the *performance* of the design. Indeed, although steel is a good choice for its availability and bearing characteristics, steel is a highly conductive material. Therefore, whereas the baffle counters direct solar radiation and space counters conduction of the heated surface towards the interior of the building envelope, the structure itself will create a weak point of conduction from the exposed surface to the actual roof of the building. This illustrates that performance, cost and availability should find a consensus in further research in order to optimize roof designs.
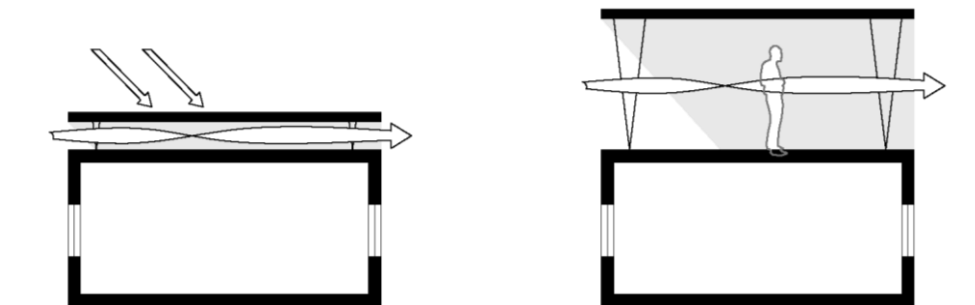
Figure 58: *Left.* Performance scheme of the base case of the ventilated roof typology. *Right.* Performance scheme of the case of elevated second roof for added usable space.

5.4.3.   Results and discussion

5.4.3.1.   *Energy*

With the ventilated roof typology, a reduction of 7.20% can be achieved for the annual cooling energy demand of the building. When this cavity is inclined by 10°, this reduction can reach improved values of more than 16%. From the simulation results of the design variations proposed above, **Table 15** shows that smaller cavity thicknesses are seemingly more efficient for cooling and total energy consumption. Indeed, although the values for a 50 cm and an entire level height are quite similar, an improvement is witnessed for smaller cavity widths. When these are inclined by 10° however, the difference between the 10 cm and 50 cm cavity are less consequent. This would probably be due to the influence of the buoyancy effect for inclined ventilation where pressure differences play a key role in air flow rate. In the inclined SC 1Aa and 1Bb, the buoyancy factor doesn't differ as much and minimizes the influence of the cavity thickness itself compared to SC 1A, 1B and 1C without inclination.

Annual Energy needs Academic year	SC 0	SC 1A 10cm	SC 1B 50cm	SC 1C 270cm	SC 1Aa 10° 10cm	SC 1Bb 10° 50cm
Annual Cooling Energy [kWh/m²]	100.33	93.11	94.39	94.67	84.15	84.99
Annual Heating Energy [kWh/m²]	12.82	9.22	8.99	8.95	13.36	13.14
Cooling energy reduction [%]		**7.20%**	**5.92%**	**5.64%**	**16.13%**	**15.29%**
Total Annual Energy	113.15	102.33	103.39	103.62	97.51	98.14

Table 15: Annual Cooling and Heating energy need compared to the reference scenario. Annually value simulation. SC 1. *SC 1A*: Vented Cavity thickness of 10cm. *SC 1B*: Vented cavity thickness of 50cm. *SC 1C:* Vented cavity thickness of 2,70m. *SC Aa:* Inclined vented cavity by 10° and thickness 10cm. *SC Bb:* Inclined vented cavity by 10° and thickness 50cm.

From the distribution curves of the monthly cooling and heating energy needs (**Figure 59**), it is clear that improvement of the design by inclination of the ventilated roof is preferable than decreasing the cavity width. Indeed, the annual cooling energy need is only slightly mitigated by decreasing the cavity thickness whereas the inclination of a 10 cm cavity revealed the efficiency of the biomimetic solution inspired by the black-tailed prairie dog and the positive effect of the buoyancy on ventilation.
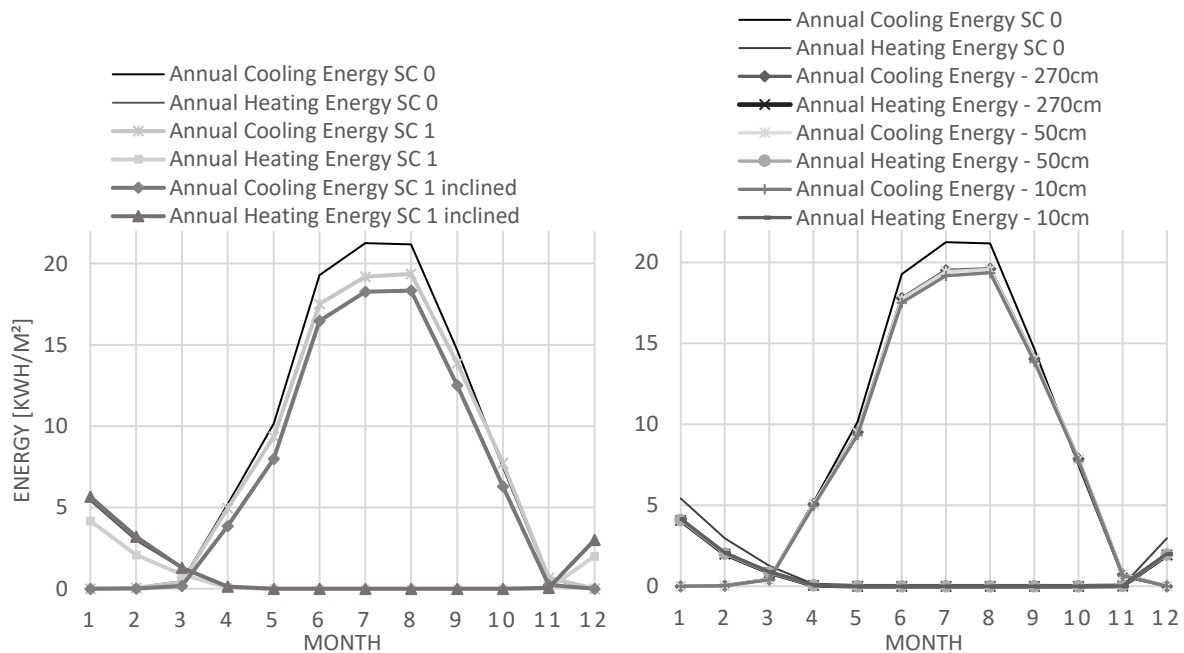
Figure 59: Graph of the annual cooling and heating energy need of the ventilated roof typology distributed over the year. *Left:* Improvement by inclination of a 10cm cavity, SC 1A and 1Aa compared to the reference scenario. *Right:* Effect of the cavity thickness, SC 1A, 1B and 1C compared to the reference scenario.

5.4.3.2. Temperature

First of all, the behaviour of a ventilated cavity can be illustrated by the surface and air temperatures of the different components of the roof design. The left graph of **Figure 60** illustrates the buffer effect of the second roof (baffle) on the surface temperature of the existing roof. Indeed, the roof surface temperature decreases by 1.24°C in summer and stays warmer in winter. This way, the temperatures are less extreme and need less compensation by energy consumption. On the right graph however, the effect of the cavity air on the indoor air temperature is illustrated. The cavity air temperature is higher than the outdoor air temperature as it is heated by the hot baffle surface. The importance of air ventilation to release excess heat becomes evident. Note however that the summer air temperature results are not representative in this case because the space is cooled down mechanically and kept below 29°C.
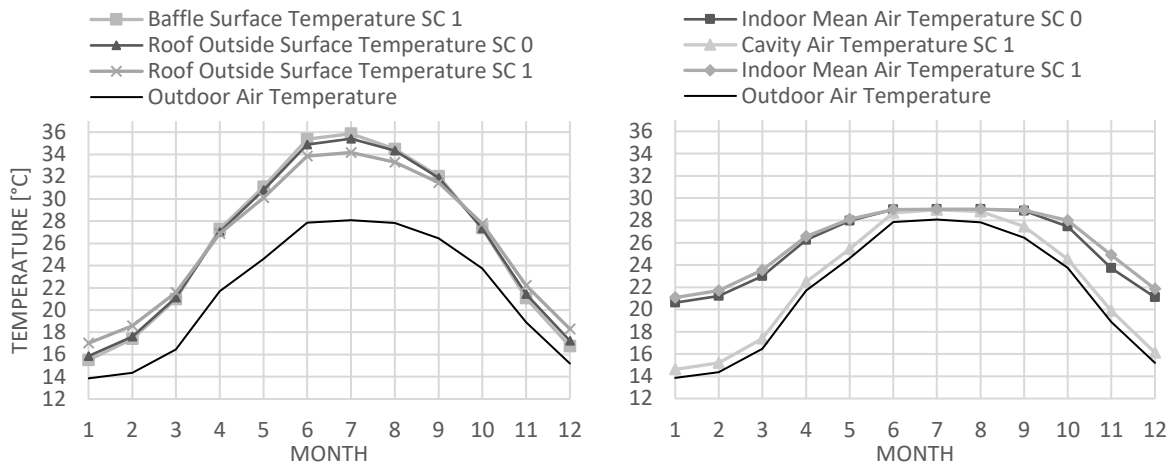
Figure 60: Monthly temperature values. Monthly simulation. Cooling On. *Left*: Roof and Baffle Surface Temperature. *Right*: Drybulb Air Temperatures. SC 1A, 10cm cavity thickness.

According to the simulations, the roof temperature decrease achieved by the different cavity heights are less important with higher widths. A vented cavity of 10 cm, 50 cm and 270 cm respectively cool down the surface by 1.24°C, 1.08°C and 1.04°C. On the other hand, the surfaces stay warmer in the winter with a higher baffle position, respectively by 1.16°C, 1.25°C and 1.27°C. Note that the mass flow rate still increases with higher cavity thicknesses as can be consulted in **Appendix C.5** (Table C - 3). Finally, the inclined vented cavity improves the design and cools the roof surface down by another 1.76°C, or a total of 3.0°C compared to the reference scenario. Note that the higher baffle heights let more solar radiation reach the lower roof surface because of the open height on the sides. A potential improvement would be to introduce overhangs by extending the baffle on the perimeter. However, this is not possible in simulation due to the restrictions inherent to the *ExteriorNaturallyVentedCavity* component of EnergyPlus.
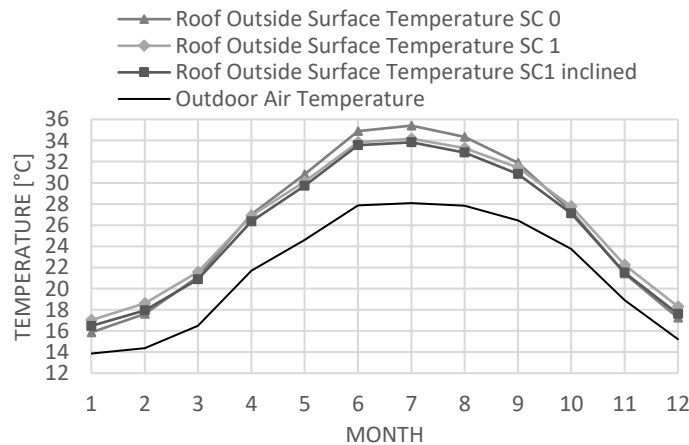
Figure 61: Monthly temperature values. Monthly simulation. Cooling On. Roof surface temperature improvement with vented cavity SC1A and inclined vented cavity SC 1Aa, compared to the reference scenario.

5.4.3.3. Discomfort

When the cooling setpoint is set off, the real behaviour of the ventilated roof design can be illustrated (**Figure 62**). On the hottest day of June, the second roof surface reaches extremely hot temperatures of up to 60.0°C. The baffle is here approached by a highly conductive single layer with a relatively high solar absorptance of 0.72 which means the surface heats up very fast when subjected to high solar radiation. Both the roof surface and the indoor air temperatures are very high when not cooled and reach respectively peak values of 45.8°C and 40.5°C inside the classrooms around 3 PM.
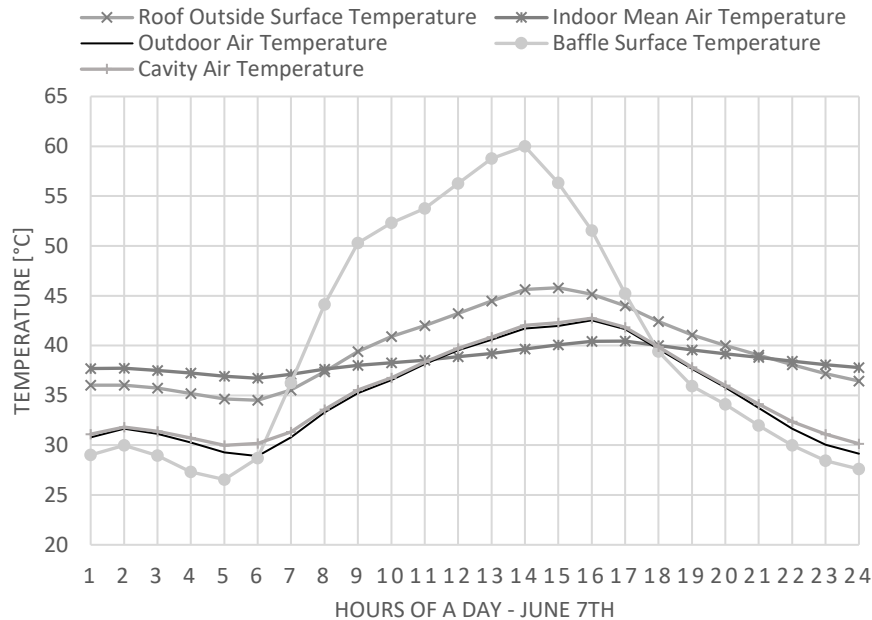
Figure 62: Hourly Temperature values for June 7th. Cooling setpoint Off. SC 1A 10cm vented cavity.

Furthermore, the simulation results show that the inclined variant of the ventilated cavity of 10 cm width cools the roof surface temperature down by another 1.03°C between respectively 13.20°C (SC 1A) and 14.23°C (SC 1Aa) temperature reduction. When the whole month is taken into account, **Figure 63** illustrates that the decrease in indoor air temperature obtained is 1.99°C for the vented cavity of 10cm, and 2.48°C for the same, inclined vented roof system. When the cooling system is Off, results show once again the advantage of the inclined design variation.
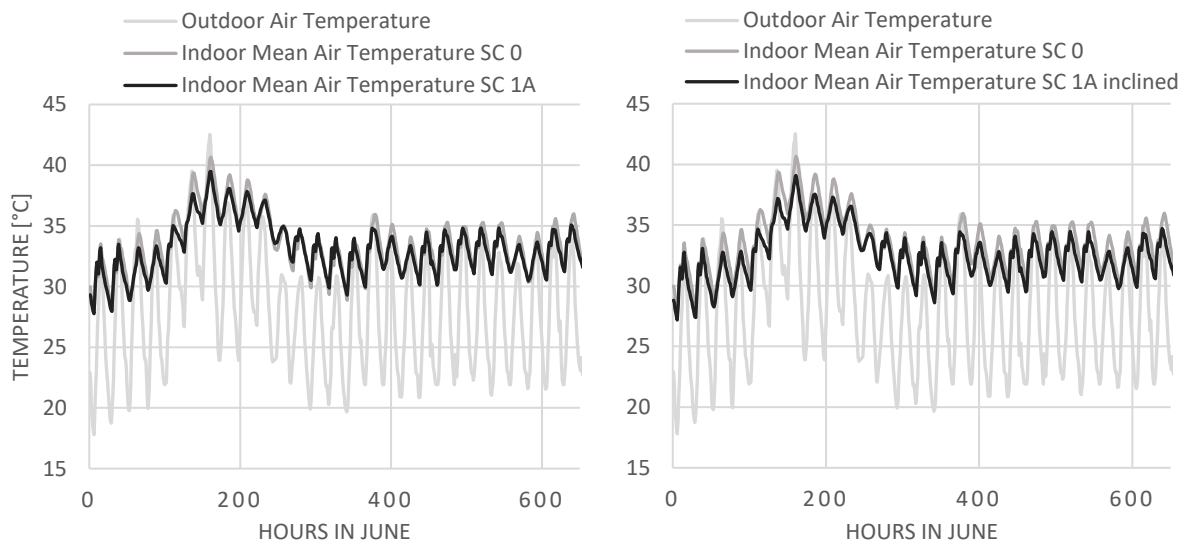
Figure 63: Risk of overheating. Hourly values for the month of June. *Left*: Indoor Air Temperature of Sc 1A. *Right*: Indoor Air Temperature of SC 1Aa.

5.5. Scenario 2: Cool roof

In nature, tree leaves have varying degrees of reflectiveness according to their climate and desert snails survive desert temperatures thanks to their white and reflective outer shell surface. The selective cooling strategy depicted in **3.2.1.3** of the explorative roof taxonomy shows that white paint with high albedo values works as a barrier to longwave solar radiation and lets shortwave radiation to the sky pass through. In the present chapter, the effect of this strategy on thermoregulation of buildings will be assessed by simulation and comparison to the reference scenario.
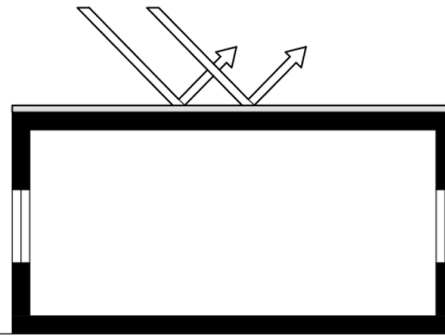
Figure 64: Performance scheme of the cool roof design. SC 2.

5.5.1. Simulation model

The simulation model of this design will be based on the reference scenario where a cool white roof coating will be applied on the exterior surface of the roof. Hence, the mosaic tiles of the outer roof layer that had initially a thermal and solar absorptance will change surface characteristics to that of a white coating. The thermal characteristics of the underlying layers will not be modified and stay valid.

5.5.1.1. *Input parameters*

The cool roof coating used for the simulation is a *cool white roof coating based on styrene acrylate copolymer and cement* that is characterized by a good cooling effect resulting from its high reflective property and integrates also good mechanical properties and water tightness necessary for roof surface application and durability (Xue, et al., 2015). Theoretically, the coating has an emissivity of 0.88 and a solar reflectance of 0.82 close to the 0.90 of the outer shell surface of the *Sphincterochila boisseri* or desert snail. However, these values are valid for a new and clean surface whereas dust particles affect the solar reflectance of the white coating. The research of Xue et al. tested the optical characteristics of the product and its dirt resistance under artificial accelerated weathering. Consequently, the solar reflectance decreased up to 0.63 corresponding to a solar absorptance of 0.37 which will be more accurate for the assessment of the cool roof design in service (**Table 16**). By this simple method, the temperature of the roof surface should decrease considerably in the simulation model as it will absorb less solar radiation than with the initial 0.70 solar absorptance.

Parameter	SC 0 – Reference	SC 2 – Cool roof
Thermal absorptance *Tabs*	0.90	0.88
Solar absorptance *Sabs*	0.70	0.37

Table 16: Input parameters related to the cool white roof coating application. SC 2 – Cool roof.

5.5.1.2. *Output parameters and hypotheses*

The same output parameters than the reference scenario are retrieved from the EnergyPlus simulation. The following hypotheses are made for the results.

Energy   The total cooling energy should decrease considerably because of the direct effect of the white coating on the surface temperature of the roof that absorbs less solar radiation

due to its low solar absorptivity.

Temperature   As said before, the roof surface should decrease with the solar absorptivity of the new surface. This would presumably affect positively the indoor air temperature.

Discomfort   As a direct impact of the possible temperature decrease, the hours of discomfort and risk of overheating should be minimized compared to the reference scenario.

5.5.2.   Results and discussion

5.5.2.1.   *Energy*

The effect of the whitewash on the roof surface can be discussed through the Sankey diagram of the heat fluxes illustrated in **Table 17** below. The differences in the opaque surface heat gains and losses are solely due to the roof design as this is the only parameter that changed compared to the reference building. Note that the high emissivity causes an increase in the heat losses through the roof and that the lower solar absorption resulted in nearly a factor 2 reduction of the heat gains through the surface.

Energy Balance Cooling period, June	Gains [kWh/m²]		Losses [kWh/m²]	
	SC 0	SC 2	SC 0	SC 2
Internal gains (People)	12.53	12.53		
Internal gains (Lighting)	0.38	0.38		
Windows	6.28	6.66	2.04	1.63
Opaque Surfaces	8.44	**4.26**	3.25	**5.74**
Infiltration	0.18	0.18	2.92	3.26
Cooling energy			19.29	**13.03**
Balance	27.80	**24**	27.50	**23.66**

Table 17: Sankey diagram of the cooling period of June. Energy balance gains – losses compared to the reference scenario. Monthly value simulation. SC 2.

This greatly improves the annual cooling energy need as it is reduced by nearly 35% (**Table 18**). However, the increase in heat losses through the roof surface witnessed above also increases the heating energy need. The sum of both effects still results in a positive decrease in the total yearly energy demand. **Figure 65** representing the monthly distribution of the cooling energy need is very representative of the improvement achieved by the cool roof design with a witnessed reduction of 6.49 kWh/m² for the hottest month of the academic year (June).

Annual Energy needs Academic year	SC 0	SC 2
Annual Cooling Energy [kWh/m²]	100.33	**65.73**
Annual Heating Energy [kWh/m²]	12.82	19.72
Total Annual Energy	113.15	85.45

Table 18: Annual Cooling and Heating energy need compared to the reference scenario. Annual value simulation. SC 2.
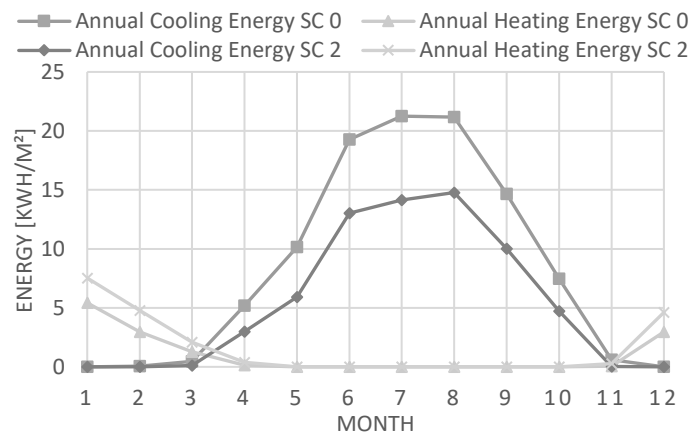
Figure 65: Graph of the annual cooling and heating energy need distributed over the year. SC 2 compared to SC 0.

5.5.2.2. Temperature

For this scenario of cool roofs in particular, the temperatures of interest will be the roof surface temperatures. As illustrated in the left graph of **Figure 66**, the roof outside face temperature decreases considerably all year long, with a peak difference of 4.6°C in summer. On the right, the indoor air temperature tendencies show that although summer temperatures still reach the setpoint of 29°C, the indoor air temperatures show a positive decrease.
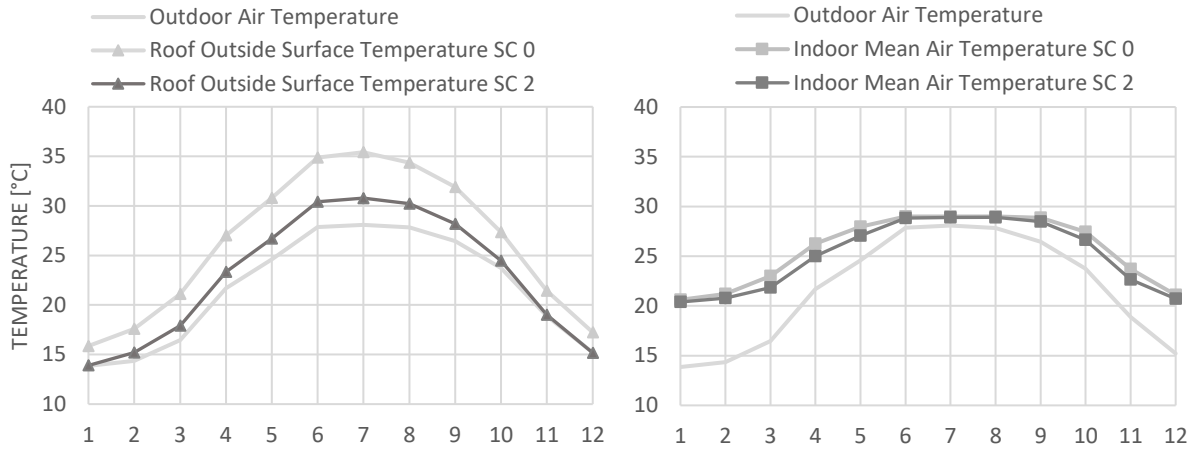
Figure 66: Monthly temperature values. Monthly simulation. Cooling On. *Left*: Roof Surface Temperature of SC 2 compared to SC 0. *Right*: Indoor Air Temperatures of SC 2 compared to SC 0.

5.5.2.3. Discomfort

When the cooling energy does not compensate for the peak temperatures in summer, the classrooms reach uncomfortable temperatures and peak values are reached in June. However, with the application of a cool roof design, a visible improvement rises from the hourly simulation results for indoor air temperature (**Figure 67**). Indeed, a temperature reduction of up to 3.5°C is obtained by the use of the cool roof typology. However, the hours of discomfort are still similar to the reference scenario as the temperatures still exceed 29°C during the school hours.

When one takes a closer look at the hourly simulation results for the warmest day of June (**Figure 68**), both the roof surface temperatures and indoor air temperatures drop below the initial situation. The cool roof design follows the outdoor temperature curve more closely than before and the surface is cooled down by a significant 8.9°C.
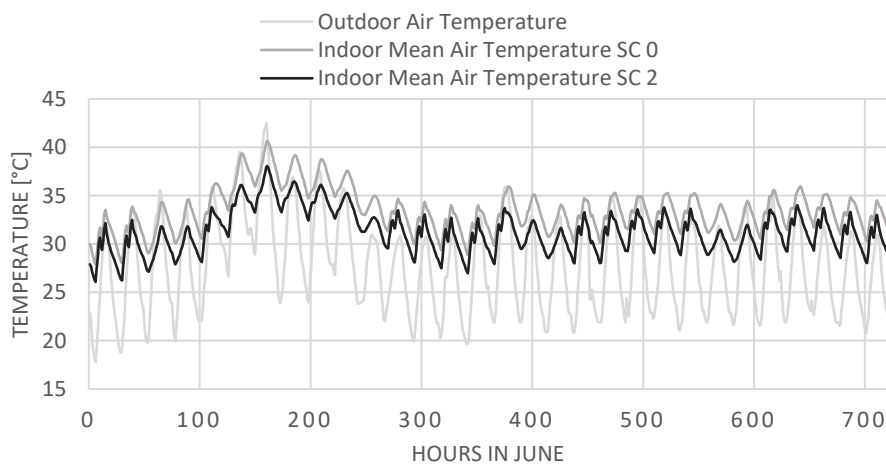
Figure 67: Risk of overheating. Indoor Mean Air Temperature with Cooling Setpoint Off. Hourly simulation. June. SC 2.
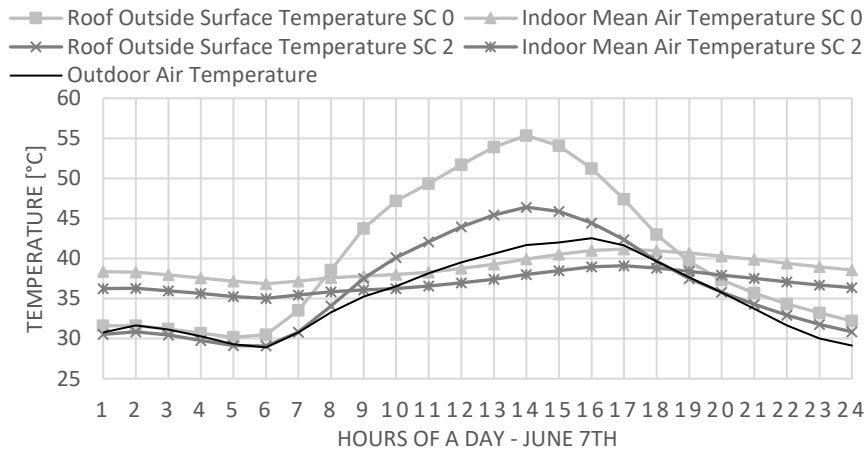
Figure 68: Graph of the roof and air temperature tendencies on June 7th. Hourly value simulation. Cooling setpoint Off. SC 2.

5.6.   Scenario 2.1: Cool roof on naturally vented cavity

Because SC 1 (naturally vented cavity) presented various advantages already extensively analysed in paragraph **3.2.2.2** of the explorative roof taxonomy, it is of interest to quantify its performance when combined with another strategy. In this sense, the present research by design enables us to go one step further than the theoretical classification of the independent strategies. SC 2.1 can be seen as a design variation of SC 2 by combination with SC 1.
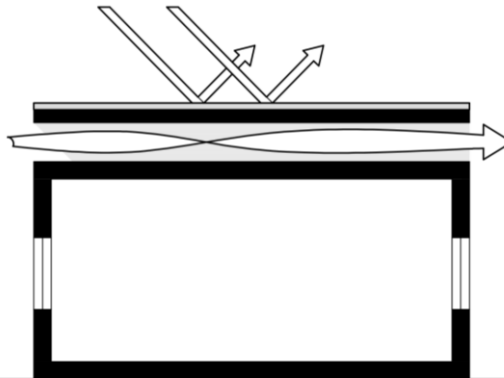
Figure 69: Performance scheme of the combined cool roof and naturally vented cavity as roof design strategy. SC 2.1.

5.6.1.   Simulation model

For this simulation, the properties of white paint will be applied on the upper surface in visible contact with the sky and solar radiation, i.e. the second roof or so-called *Baffle*. Similarly to SC 1, the reference scenario is taken as a base file where a ventilated cavity component is added to the roof in a second phase. Here, the characteristics of the baffle and cavity can be specified.

5.6.1.1.   Input parameters

The input parameters are the same as for SC 1 despite the solar properties of the baffle material. The differences with SC 1 are shown in **Table 19**.

Input parameter	Value SC1 Concrete	Value SC2.1 White coating
Thermal Emissivity of Exterior Baffle Material	0,90	0,88
Solar Absorptivity of Exterior Baffle	0,72	0,37

Table 19: Input parameters of SC 2.1 compared to SC 1. Baffle thermal emissivity and solar absorptivity.

5.6.1.2.   Output parameters and hypotheses

The same output parameters as for SC 1 will be selected. This means values of baffle and cavity temperatures will be calculated. The idea will be to assess the combined effect of SC 1 and 2, and understand the place that each cooling strategy takes when installed together. The hypothesis is not that the two effects will be summed up, but that each strategy will be responsible for a percentage of the total benefit of the design. From there, other combined strategies that exceed the possibilities of the program used for the simulations could be theoretically approached.

5.6.2.   Results and discussion

5.6.2.1.   Energy

The application of a highly reflective layer on the second roof surface of a ventilated roof illustrates the positive impact of the combined use of two previously analysed roof cooling strategies. Indeed, the effect of the cool roof typology on the cooling energy need is remarkable from SC 1 to SC 2.1 (**Table 20**). On the other hand, adding a ventilated cavity to SC 2 is not interesting for cooling energy as SC 2.1 is less efficient than SC 2. However, if the total energy need is regarded, the combined strategy is advantageous compared to both the ventilated and the cool roof strategy thanks to the positive effect of SC 1 on the heating energy need.

Annual Energy needs				
Academic year	SC 0	SC 1	SC 2	SC2.1
Annual Cooling Energy [kWh/m²]	100.33	93.11	65.73	66.77
Annual Heating Energy [kWh/m²]	12.82	9.22	19.72	13.33
Total Annual Energy (TAE)	113.15	102.33	85.45	**80.10**
Reduction cooling energy		7.20%	**34.49%**	33.45%
Reduction total energy		9.57%	24.48%	**29.21%**

Table 20: Annual Cooling and Heating energy need compared to the reference scenario. Annually value simulation. SC 2.1.

On a monthly distribution (**Figure 70**), this combined design shows a decrease of the cooling energy by 7.50 kWh/m² for the month of July. However, this curve is not much different from the white roof solution without vented cavity which is more the case for the heating energy curve as the values in **Table 20** announced.
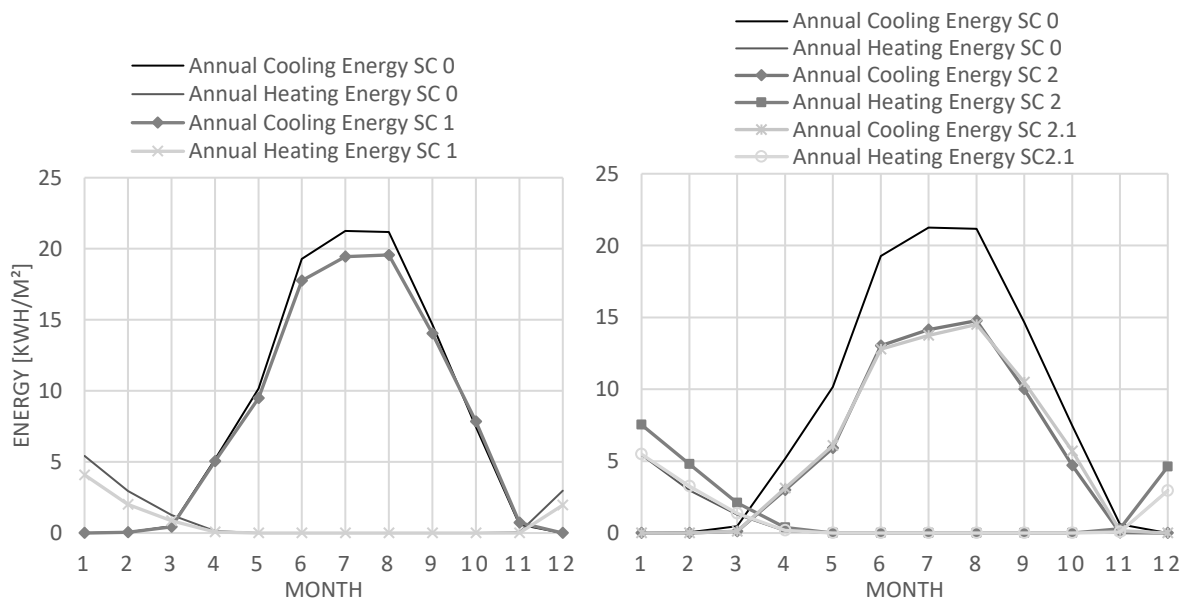
Figure 70: Graph of the annual cooling and heating energy need distributed over the year. *Left:* SC 1 vented cavity compared to the reference scenario. *Right:* SC 2 and 2.1 compared to the reference scenario.

5.6.2.2. Temperature

To understand the improvement between SC 1 and 2.1, baffle temperatures and underlying roof surface temperature are compared for both scenarios and illustrated in **Figure 71**. The application of the white paint on the second roof surface has a consequent cooling effect on the baffle surface temperature of no less than 5.1°C. Also, the roof surface temperature has decreased by 3.6°C. Scenario 2.1 can thus be interpreted as a consequent improvement of the ventilated cavity roof typology, by application of a cool roof layer on the outer roof surface.
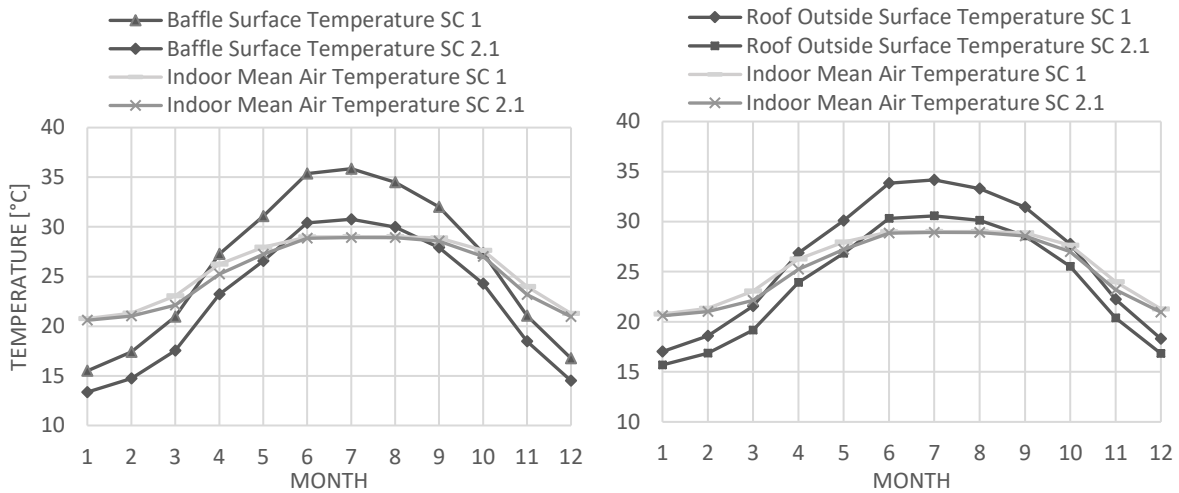
Figure 71: Monthly temperature values. Monthly simulation. Cooling On. *Left*: Baffle Surface Temperature of SC 2.1 compared to SC 1. *Right*: Roof Surface Temperatures of SC 2.1 compared to SC 1.

5.6.2.3. Discomfort

Compared to the reference scenario, a maximum temperature reduction of 4.5°C is achieved with the ventilated cool roof (SC 2.1) for the summer month of June. Compared to the cool roof in SC 2, the range of fluctuation is lower and more stable thanks to the buffer effect or inertia given by the cavity. Compared to SC 1 which achieved a reduction of 2.0°C of the indoor air temperature (**0**), the present hybrid solution results in a more than doubled effect.
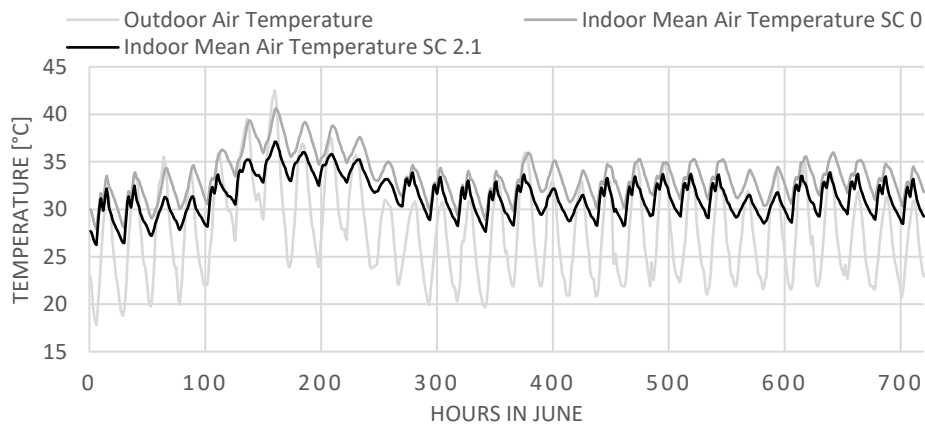
Figure 72: Risk of overheating. Indoor Mean Air Temperature with Cooling Setpoint Off. Hourly value simulation. June. SC 2.1 (cool roof on ventilated roof) compared to SC 0.

62

5.7.   Scenario 3: Self-shading

The ribbed surface of the desert *Saguaro* cactus was identified by the Biomimicry Institute as being a thermoregulation strategy amongst nature that cools down the organism in hot and arid climates by form. Further in this thesis, the strategy was theoretically applied to roofs as a possible roof cooling strategy named self-shading. This was already applied to walls in the case study discussed in **4.1.4** for the Votu Hotel in Brazil. In this chapter, the strategy of self-shading will be quantified for roofs and compared to the reference scenario.
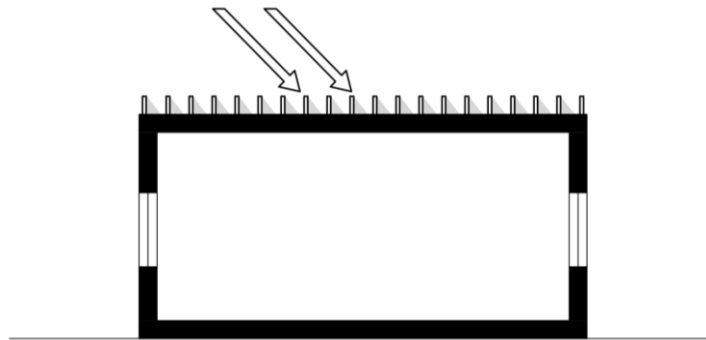
Figure 73: Performance scheme of a self-shading roof form. SC 3.

5.7.1.   Simulation model

5.7.1.1.   modelling

The shading geometry will be modelled as a lattice of shading panes of a certain height, orientation and number. For the purpose of this research, two orientations will be compared in terms of the efficiency achieved to shade the roof surface. Hence, one longitudinal and one transversal orientation of the lattice will be simulated. The effect of the height of the shading devices could also be explored although it is evident that the higher the shading, the better the roof will be shaded and will consequently be cooler. Unfortunately, the iteration of such parameters is not possible through EnergyPlus without a fastidious manual methodology.
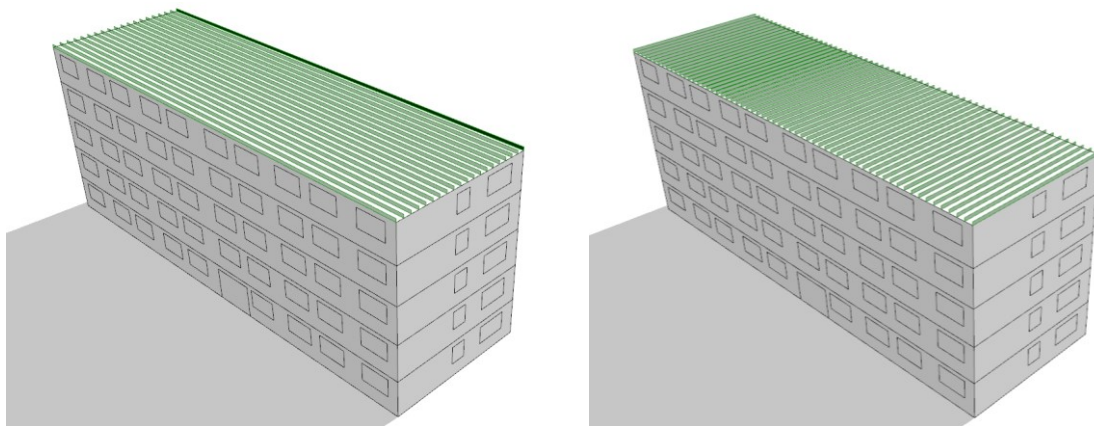
Figure 74: Simulation model of the shading lattice of the self-shading roof typology. SC 3. *Left*: longitudinal configuration of the lattice. *Right*: Transversal configuration of the lattice.
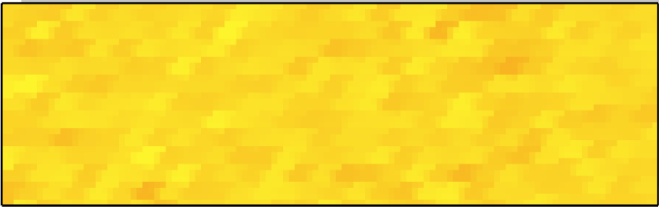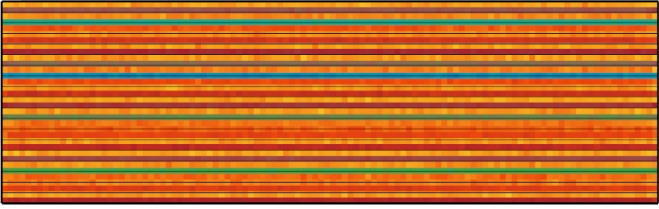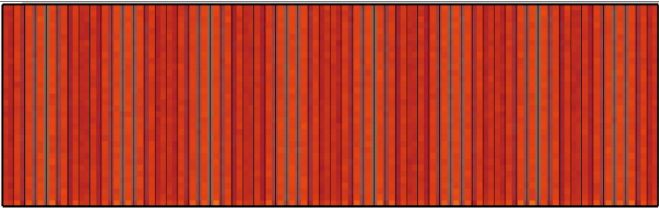
5.7.1.2.   Input parameters

Once again, the same input parameters are selected for the thermal zone definition and materials. For the lattice which is the particularity of this scenario, a default height of 30 cm was chosen for the shading panes and a distance of 75 cm in between each panel is valid for both lattice orientations. This

configuration is parametrically defined in grasshopper and could be changed easily. To consult the Grasshopper script used to model the shading lattice, the reader is referred to **Appendix C.3**. However, each configuration needs one simulation in EnergyPlus which is not parametrical, as explained before. Finally, note that with this sequence the roof is made inaccessible which is probably the main drawback of this scenario.

5.7.1.3. Radiation on roof surface

A first way to predict the impact of the shading lattice on the roof surface temperature is by simulation of the yearly solar irradiance on the surface for each orientation and compare it to the existing situation. For the Grasshopper script of the grid simulation, the reader is referred to **Appendix C.3**. The results are shown in **Table 21** below.

Scenario	Render of the yearly solar irradiance of the roof surface	Minimum	Maximum
SC0		1853.9 kWh/m²	1956.6 kWh/m²
SC3 longitudinal		471.7 kWh/m²	1884.3 kWh/m²
SC3 transversal		1065.4 kWh/m²	1737.2 kWh/m²

Solar Radiant Exposure [kWh/m2]   0   1950

Table 21: Results of the DIVA simulation of yearly solar irradiance of the roof surface. Comparison of SC 0 and two orientations of SC 3.

The two configurations of lattices minimize the solar irradiance of the roof, which announces a beneficial effect on the roof surface temperature, indoor temperatures and consequently on the energy need of the building. When the two configurations are compared to each other, one can see that the longitudinal lattice reduces the minimum solar irradiance up to 471.7 kWh/m²/year, which is also visible in blue and green on the grid render. However, yellow is still visible and corresponds to the high values of 1884.3 kWh/m²/year. On the other hand, the transversal lattice shows a better decrease in the maximum solar irradiance (red) but a higher minimum value than the longitudinal lattice on the green zones of the render.

5.7.1.4. Output parameters and hypotheses

The same output parameters as the reference scenario will be selected. This will enable a clear comparison of the two scenarios in terms of energy, temperatures and comfort.

Energy   The effect of the lower roof surface irradiance should have a positive impact on the total energy need of the building.

Temperature   Special attention will be given to the roof surface temperature in order to validate the positive impact of the shading lattice. Compared to the preliminary simulation of solar irradiance, the material properties of the roof will be more precisely defined and the values of temperature will be more accurate.

Discomfort   For the same reasons as above, the comfort level of the occupants should be enhanced and the risk of overheating minimized by this strategy.

5.7.2.   Results and discussion

5.7.2.1.   Energy

In terms of annual energy demand of the school building, the roof typology based on self-shading is a promising design strategy. Indeed, based on the EnergyPlus simulation results below, this solution can save up to 32% of cooling energy. However, the orientation of the cooling ribs has an influence on the efficiency of the solution. Compared to the longitudinal lattice presenting a 32% cooling energy saving, the transversal configuration enables a lower 12,2% reduction. Hence, the design with the longitudinal lattice orientation provides the best results for cooling and total energy demand optimization.

Annual Energy needs			
Academic year	SC 0	SC 3A	SC 3B
Annual Cooling Energy [kWh/m²]	100.33	88.13	**67.94**
Annual Heating Energy [kWh/m²]	12.82	13.89	16.66
Total Annual Energy	113.15	102.02	**84.60**

Table 22: Annual Cooling and Heating energy need compared to the reference scenario. Annually value simulation. SC 3. Variants of SC 3: the transversal lattice orientation (3A) and the longitudinal orientation (3B).
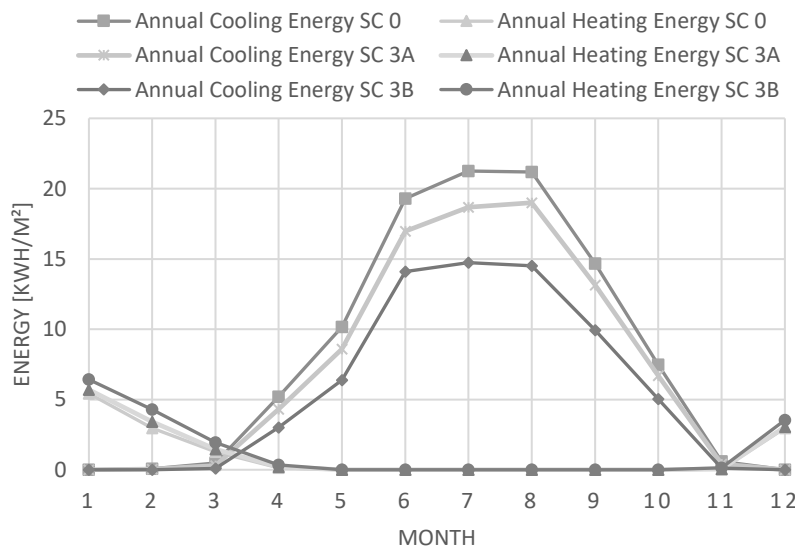
Figure 75: Graph of the annual cooling and heating energy need distributed over the year. SC 3A and 3B.

5.7.2.2.   Temperature

In terms of temperature improvement, SC 3B stands out again with its longitudinal lattice configuration. The roof surface temperature is indeed respectively lower for the longitudinal configuration and transversal configuration as was expected from the surface irradiance simulation in **5.7.1.3**. Consequently, by adding a surface lattice on the roof according to the ribbed roof typology, the surface temperature decreases up to 1.6°C first, and when oriented in a more optimal direction decreases up to 4.3°C. This demonstrates the importance of the orientation for the present roof design.
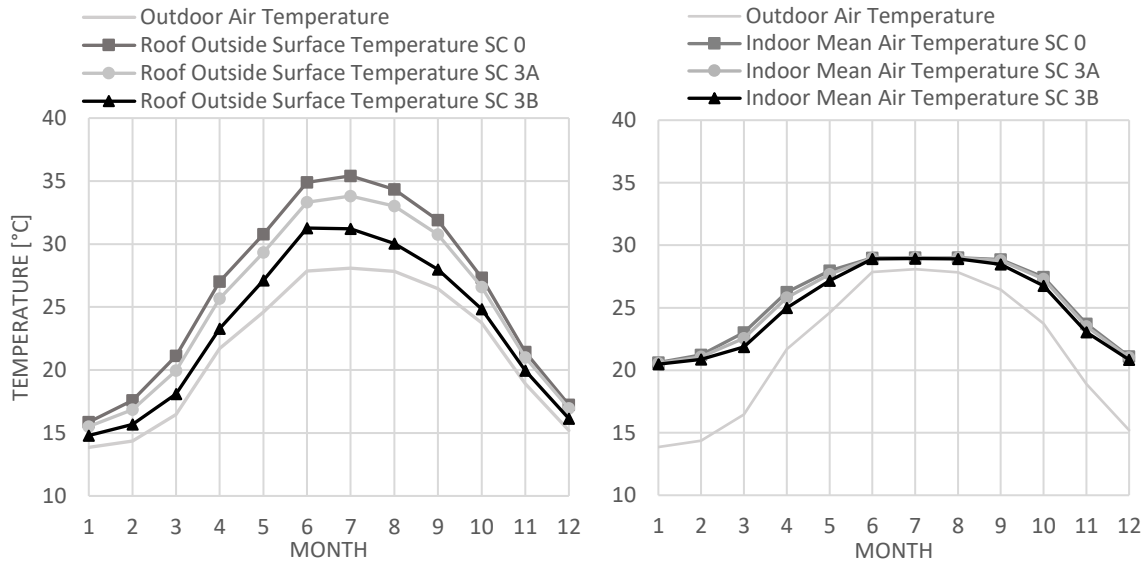
Figure 76: Monthly temperature values. Monthly simulation. Cooling On. *Left*: Roof Surface Temperature of SC 3A (transversal oriented lattice) and 3B (longitudinal orientation) compared to SC 0. *Right*: Indoor Air Temperatures of SC 3A and 3B compared to SC 0.

5.7.2.3. *Discomfort*

The overheating temperatures for June, when the cooling setpoint is set off, are illustrated in **Figure 77**. The comparison between both orientations shows once again the advantage of the longitudinal shading lattice which is oriented perpendicular to the South-North orientation and shades therefore in a more efficient way. SC 3B shows a peak temperature reduction of up to 3.1°C while SC 3A reduces the temperature by maximum 1.4°C.

Figure 77: Risk of overheating. Indoor Mean Air Temperature with Cooling Setpoint Off. Hourly value simulation. June. Left: SC 3A (Transversal oriented shading lattice) compared to SC 0. *Right*: SC 3B (longitudinal lattice) compared to SC 0.

5.8. Scenario 3.1: Self-shading on naturally vented cavity

For this variation of the self-shading roof typology, the same combination with SC 1 is applied as in SC 2.1. As such, the shading lattice proposed in previous paragraph is now applied on the baffle of the ventilated roof. However, although the potential for improvement by combination is present, the main issue is the modelling of this configuration. Indeed, the parameters of the exterior natural vented cavity only specify the characteristics of the baffle material but no geometry can be assigned to it. Therefore, another methodology is applied for this case and enables to approach the results mathematically.
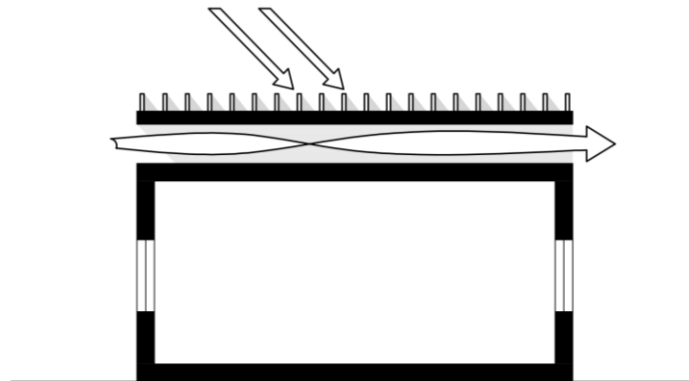
Figure 78: Performance scheme of the combined self-shaded roof and naturally vented cavity as roof design strategy. SC 3.1.

5.8.1. Mathematical approach

Unlike the previous scenarios, the combined use of the self-shading design with the ventilated roof will have to be calculated mathematically instead of by simulation in EnergyPlus. Therefore, the results will be entirely hypothetical and should be taken carefully. However, it will be based accordingly on a simulation performed in the scope of this thesis for the same building and parameters i.e. SC 2.1 that similarly applied SC 2 on a ventilated roof design.

5.8.1.1. Theoretical methodology

The approach used for this design variation of the self-shading strategy is based on the simulation results of SC 2.1. Indeed, the changes in surface properties of the roof studied in SC 2 (cool roof) affect directly the roof temperature analogically to SC 3 with the self-shading. Moreover, the present phase of simulation would then require the transfer of the designed surface properties to the second roof layer such as was performed between SC 2 and SC 2.1.

First of all, the theoretical methodology requires an assessment of the degree of influence of both the surface redesign and the natural vented cavity on the final combined results. In terms of energy demand, these influence factors are calculated iteratively for heating and cooling energy up to the 4th decimal as given in **Table 23**. Accordingly, the annual cooling energy of SC2.1 corresponds to the sum of SC1*0.0380 and SC2*0.9620. The result of the theoretical approach is accurate to the hundred' decimal. Secondly, the same influence factors can be applied to the results of the self-shaded roof scenario of paragraph **5.7**. Although the methodology is explorative but highly hypothetical, this will enable us to approach the real values in a logical way.

Annual Energy needs Academic year	SC 1	factor	SC 2	factor	SC2.1	SC2.1 theory	
Annual Cooling Energy [kWh/m²]	93.11	0.0380	65.73	0.9620	66.769	66.770	**66.77**
Annual Heating Energy [kWh/m²]	9.22	0.6087	19.72	0.3913	13.330	13.330	**13.33**
Total Annual Energy	102.33		85.45		80.099	80.100	**80.10**

Table 23: Theoretical methodology with influence factors applied to SC 1 (Ventilated roof) and 2 (Cool roof), resulting in a theoretical equivalent of SC 2.1 (Cool roof on Ventilated roof). SC 3.1.

5.8.1.2. *Hypotheses*

SC 3 showed an improvement in heating energy need but a slight increase in cooling demand compared to SC 2. In the end, SC 3.1 has a high potential in improving the total energy demand of the school building as was the case for SC 2.1. Indeed, both surface property changes of the cool roof and self-shading roof have similar results as base for the combined design with the ventilated roof. Also, the factor of influence is higher for the improved cooling demand and very low for the unfortunate increase in heating demand. On the other hand, note that the issue of the hot climate regions is mainly the excess need in cooling energy. Therefore, this solution is only interesting if the cooling energy still represents a consequent improvement compared to the reference case, in addition to the better total energy consumption.

5.8.2. Results and discussion

5.8.2.1. *Energy*

In a first instance, only the energy demand will be evaluated with the theoretical results retrieved from the above-described methodology. Indeed, going into monthly values and curves for temperatures with this hypothetical methodology would be unreasonable and inaccurate. However, the yearly energy demand based on influence factors still gives an approached range of results to compare them to the other proposed designs. Followingly, the results for SC 3.1 based on the individual influence of SC 1 and 3 are shown in **Table 24**. For a broader detailing of the calculations, the reader is referred to **Appendix C.5**.

Annual Energy needs Academic year	SC 1	**factor**	SC 3	**factor**	**SC3.1** **theory**
Annual Cooling Energy [kWh/m²]	93.11	0.0380	67.94	0.9620	68.90
Annual Heating Energy [kWh/m²]	9.22	0.6087	16.66	0.3913	12.13
Total Annual Energy	102.33		84.60		81.03

Table 24: Annual Cooling and Heating Energy demand of SC 3.1 calculated from a theoretical methodology.

The total annual energy demand for the school building with application of a combined ventilated and self-shaded roof design shows a decrease of 28.4% compared to the reference design. The cooling energy need decreased by 26% compared to the ventilated roof (SC1) and by 31.3% compared to SC 0. **Table 25** compares the results of the self-shaded ventilated roof design with the self-shaded roof (SC 3), the other hybrid solution of the cool ventilated roof (SC 2.1) and the reference building. As expected, the combined design shows an improvement in heating and total energy demand compared to the self-shaded roof typology. However, the design of the outer layer of a ventilated roof is more effective with the cool roof strategy than with the self-shading for the cooling energy need. This is indeed also the case for a simple roof between SC 2 and SC 3.

Annual Energy needs Academic year	SC 0	SC 2	SC 3	SC 2.1	SC 3.1
Annual Cooling Energy [kWh/m²]	100.33	65.73	67.94	**66.77**	68.90
Annual Heating Energy [kWh/m²]	12.82	19.72	16.66	13.33	**12.13**
Total Annual Energy	113.15	85.45	84.60	**80.10**	81.03
Reduction in Cooling Energy		**34.5%**	**32.3%**	**33.5%**	**31.3%**

Table 25: Annual Cooling and Heating energy need compared to the reference scenario, SC 3 and SC 2.1. SC 3.1.

5.9.   Scenario 4: Living roof

The living roof, also called vegetated roof or green roof, presents the particularities enounced in paragraph **3.2.2.5** of the explorative roof taxonomy. This scenario is slightly more daring than the previous ones because of the combined cooling strategies inherent to the hybrid roof typology. Its effect on energy need, temperature and comfort will be compared to the previous variants of roof designs and assessed in terms of performance. However, the aspect of cost remains the major drawback of this strategy as its installation is very expensive and thus less suitable for the case studied in this thesis.
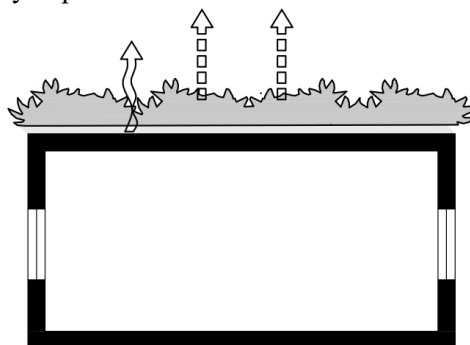
Figure 79: Performance scheme of the living roof design. SC 4.

5.9.1.   Simulation model

Just like for the ventilated cavity in SC 1, the vegetated roof is applied as an external layer to the existing roof above the EnergyPlus file of SC 0. Therefore, despite this layer, the parameters are identical to the reference scenario and suitable for comparison.

5.9.1.1.   Input parameters

In addition to the thermal zone and existing material parameters that remain the same as the reference scenario, a new layer is added to the roof construction as a material property namely Material: RoofVegetation. This object of EnergyPlus takes into account several beneficial aspects already discussed in paragraph **3.2.2.5** of the roof taxonomies. In that chapter, this roof cooling strategy was already defined as hybrid because of its combined action of evapotranspiration and moisture content, shading of the plants, and insulation by the soil layer. The input parameters are detailed in **Table 26**.

Input parameter	Units	Value
Height of the plants	m	0.20
Leaf Area Index	-	1
Leaf Reflectivity	-	0.22
Leaf Emissivity	-	0.95
Minimum Stomatal Resistance	s/m	180
Roughness		Medium Rough
Soil Thickness	m	0.20
Conductivity of Dry Soil	W/mK	0.35
Density of Dry Soil	kg/m³	1100
Specific Heat of Dry Soil	J/kgK	1200
Thermal Absorptance	-	0.90
Solar Absorptance	-	0.70
Visible Absorptance	-	0.75
Saturation Volumetric Moisture Content of the Soil Layer	-	0.3
Residual Volumetric Moisture Content of the Soil Layer	-	0.01
Initial Volumetric Moisture Content of the Soil Layer	-	0.1

Table 26: Input parameters of the Material:RoofVegetation. SC 4.

For the purpose of the present scenario simulation, most of the parameters that require some further knowledge on vegetated roofs are taken at the default values referenced in the U.S. Department of Energy documentation. Moreover, the aspects of the green roof used do not need to be specified further than a default vegetated roof to quantify the effect of it on energy in hot climates. The soil layer is defined with a height of 20 cm and the plants with the same height above that layer. For a broader explanation of these parameters, the reader can consult **Appendix C.4**.

5.9.1.2.   *Output parameters and hypotheses*

The same parameters will be simulated as for the reference scenario. Additionally, the *Material:RoofVegetation* presents output variables that are of interest to understand the functioning of the green roof such as the surface and root moisture ratio of the soil, the soil and vegetation heat transfer rate per area, moisture transfer rate, and evapotranspiration depth. However, the assessment of this roof typology on energy and temperature is more directly dependent on the monthly soil and vegetation temperatures during the year. The output parameters selected for this scenario are shown in the table below.

Ouput parameter	Units
Green Roof Soil Temperature	°C
Green Roof Vegetation Temperature	°C

Table 27: Output parameters for the vegetated roof design. SC 4.

5.9.2.   Results and discussion

5.9.2.1.   *Energy*

Compared to the other scenarios, the vegetated roof improves less the cooling energy (by 3%) although it has the advantage of reducing the heating energy by a factor 3.6 which results in a total energy reduction of 10.8% (**Table 28**). The results for cooling energy reduction is however disappointing compared to the expected cooling performance of such an expensive solution.

Annual Energy needs		
Academic year	SC 0	SC 4
Annual Cooling Energy [kWh/m²]	100.33	97.30
Annual Heating Energy [kWh/m²]	12.82	**3.59**
Total Annual Energy	113.15	100.89

Table 28: Annual Cooling and Heating energy need compared to the reference scenario. Annually value simulation. SC 3. Variants of SC 3: the transversal lattice orientation (3A) and the longitudinal orientation (3B).

Nevertheless, the monthly distribution curve below reveals a decrease in the cooling demand by 2.43 kWh/m² in June and a decrease of the heating demand by 3.43 kWh/m² in January (**Figure 80**).
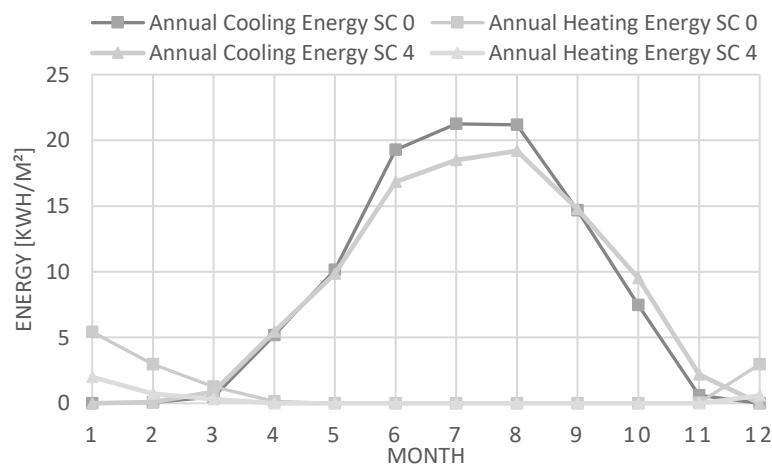
Figure 80: Graph of the annual cooling and heating energy need distributed over the year. SC 4 compared to SC0.

5.9.2.2. Temperature

From the EnergyPlus simulations, data is available for the vegetation and soil temperatures of the green roof. It is interesting to compare the effect of the baffle and cavity in SC 1 to the effect of the plants and soil thickness in SC 4.
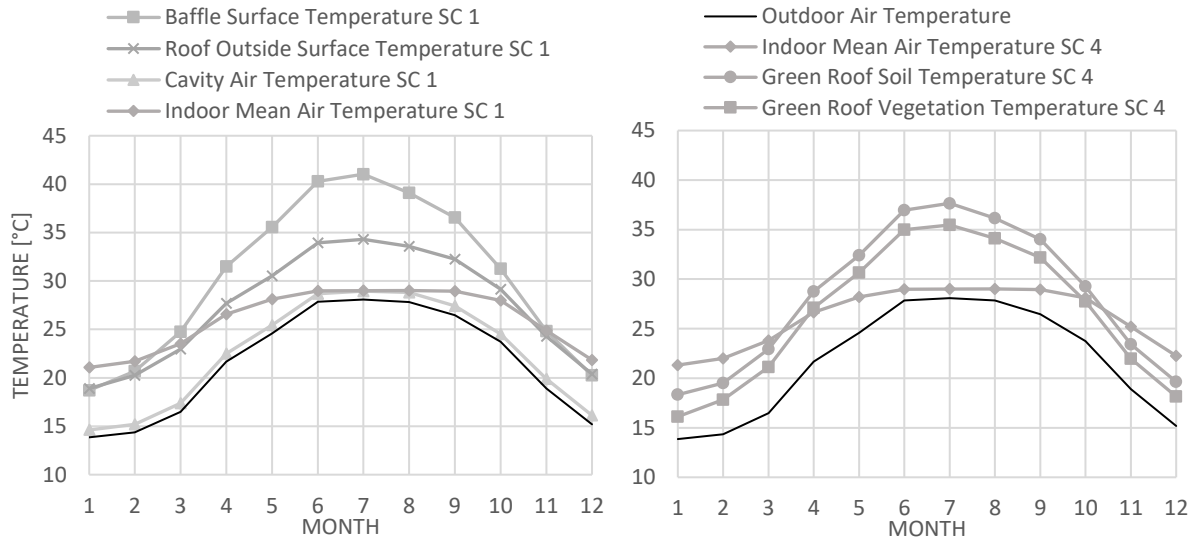
Figure 81: Monthly temperature values. Monthly simulation. Cooling On. *Left*: Surface Temperatures of a ventilated roof with baffle (SC 1). *Right*: Surface Temperatures of a vegetated roof (SC 4).

According to **Figure 81**, the baffle surface temperature as outer layer of the ventilated roof design experiences higher temperatures than the vegetation as outer layer of the green roof typology. In terms of behaviour, whereas the baffle works as a shield to the roof surface which cools down compared to SC 0, the soil temperature of the green roof corresponds to the initial roof surface temperature which is higher than the vegetation. Also, the indoor air temperatures seem to increase which corresponds to a reduced heating need as seen in the discussion above.

5.9.2.3. Discomfort

Nevertheless, the green roof solution minimizes the peak temperatures with a cooling of 4°C in the hottest days of June. The peak value of 40.7°C is pulled down to 38.0°C which is already more acceptable although above comfort values.

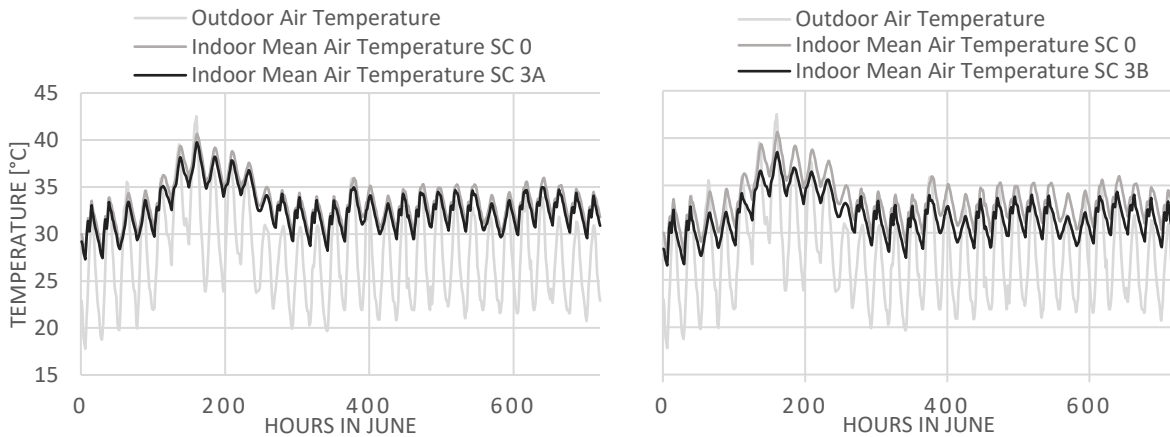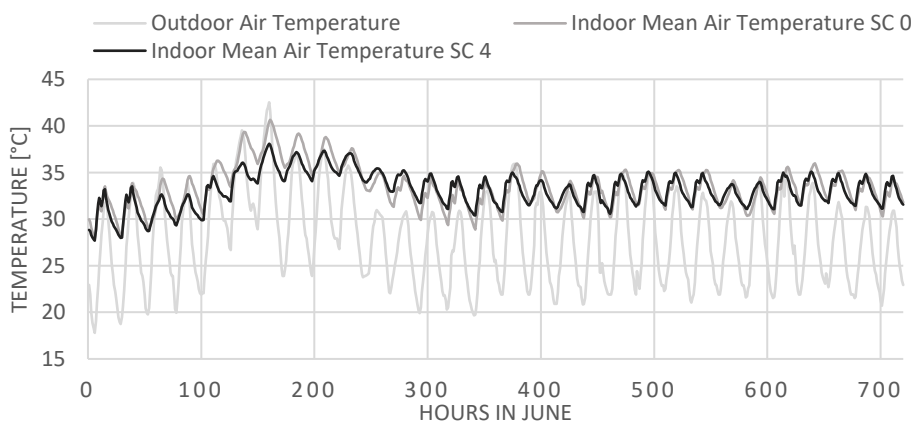**Figure 82**: Risk of overheating. Indoor Mean Air Temperature with Cooling Setpoint Off. Hourly value simulation. June. SC 4 (green roof) compared to SC 0.

Over the hottest day of June, the vegetated roof functions as illustrated in **Figure 83** below. The ceiling temperature inside the classrooms seems to be more constant over the day supposedly thanks to the

effect of the thermal inertia of the soil layer. Hence, the temperature of the ceiling is reduced with a maximum of 5.3°C around 7 PM. The thermal inertia effect is also visible from the curve progression that goes from a fluctuating curve on the outer face to a flat curve with a nearly constant value around 37.4°C.
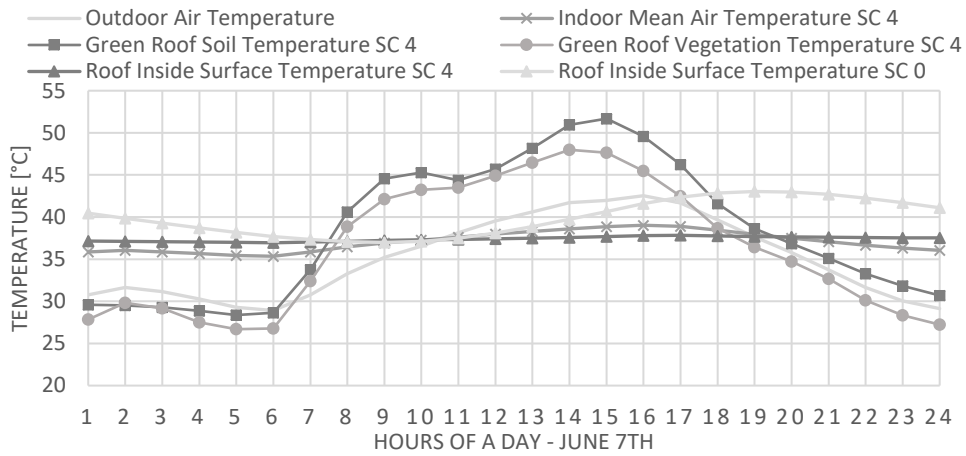
Figure 83: Graph of the roof and air temperature tendencies of a green roof on June 7th. Hourly value simulation. Cooling setpoint Off. SC 4 compared to SC 0.

5.10. Results and discussion

5.10.1. Energy demand

The total and cooling energy demand of the different explored design proposals of this chapter are exposed in the bar charts below. According to the total energy demand results (**Figure 84**), the scenario that performs best would be the ventilated cool roof design analysed more thoroughly in SC 2.1. Also, the combination of the ventilated roof design with a surface property such as the cool roof (SC2.1) and the self-shading strategy (SC3.1) applied on the second roof show encouraging results. However, the heating energy demand reduction achieved by the ventilation space affects the total energy need while the cooling energy need reduction (**Figure 85**) achieved by the combined strategy is worse than without cavity. Yet, the difference in cooling demand is little compared to the improvement the combined design offers for the total energy need. Therefore, the combined roof designs with the ventilated roof typology should still be investigated. Unexpectedly, the roof typology that performed the worst in total energy is the ventilated roof (SC1) which however can be improved significantly with inclination such as shown below. In terms of cooling energy, the vegetated roof (SC4) also showed surprisingly low improvements whereas the theory supported this roof typology.
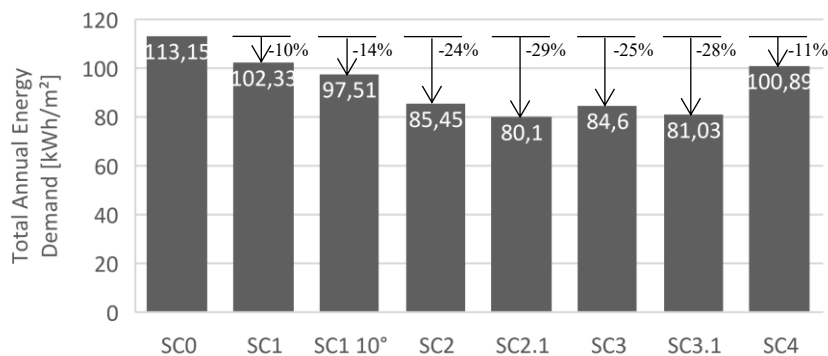
Figure 84: Bar chart of the total annual energy demand of the explored design proposals. SC0: reference scenario, SC1: Ventilated roof, SC1 10°: Inclined ventilated roof, SC2: Cool roof, SC2.1: Ventilated cool roof, SC3: Self-shaded roof (longitudinal lattice), SC3.1: Ventilated self-shaded roof, SC4: Living roof.
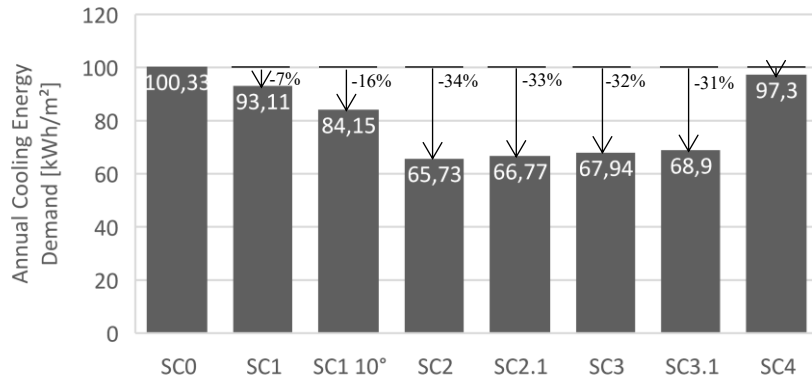
Figure 85: Bar chart of the annual cooling energy demand.

Yet, biomimetic design applied to thermoregulation of roof typologies shows great potential in improving the energy consumption of buildings in a hot and arid climate. First, the inclination of the ventilation space (SC 1 10°) as thought by the black-tailed prairie dog burrows increases significantly the efficiency of the ventilated roof typology. Secondly, the cool roof design (SC2) based on the self-cooling strategy of the desert snail with a high reflective shell surface shows the best results in cooling energy need reduction of the reference building. Finally, the self-shaded roof inspired by the ribbed desert cactus showed similarly great potential. The following graphs are based on the results summarized in **Appendix C.5**.

5.10.2.   Temperature

According to the energy performance of SC 2 and 2.1, the design proposal of the cool roof shows the lowest minimum indoor air temperature according to the summary shown in **Figure 86**. The cool roof combined with the naturally vented cavity also shows the greatest peak temperature reduction and lowest maximum indoor air temperature which comforts the potential of a combined application. The effect of the second roof surface on the existing roof temperature for SC 3.1 also shows a peak reduction of no less than 22.26°C. Note that the ventilated roof typology alone presents fewer improvements than in combination with another roof surface design. Further, the self-shaded roof presents a greater peak temperature reduction for the roof than the cool roof design, although the latter is close but more efficient for indoor air temperature. Finally, the vegetated roof (SC 4) presents a high maximum indoor air temperature reduction whereas on the other hand the maximum surface temperature of the roof is increased compared to the base case.
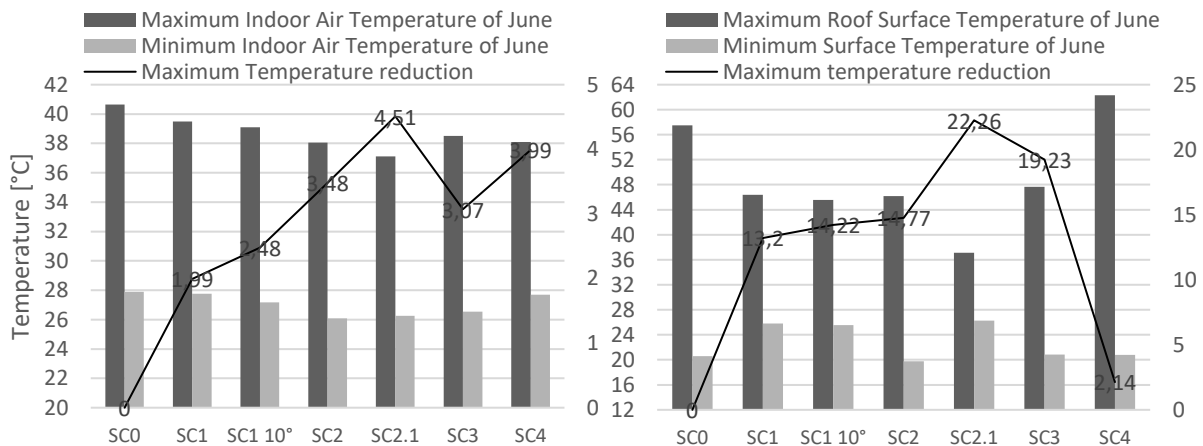
Figure 86: Bar chart of extreme temperatures during June. Hourly Simulation. Cooling Setpoint Off. *Left*: Maximum and minimum indoor mean air temperatures of each scenario with maximum temperature reduction. *Right*: Maximum and minimum outside roof surface temperature of each scenario with maximum temperature reduction compared to the reference situation.

5.10.3. Cost and Life Cycle Analysis

5.10.3.1. Cost

When referring to **Figure 85** and **Figure 85** in previous paragraphs, the dichotomy between cost and performance appears. Whereas every proposed design shows an improvement in terms of energy and temperature minimization, some designs are more costly than others. Therefore, a reasonable consensus should be taken when opting for one design. Concretely, although both the ventilated roof and the vegetated roof have similar added values in terms of energy demand, the first scenario uses free resources, wind, when in fact the last scenario is known to be very expensive both in resources, water and maintenance. However, the ventilated roof design does not perform as consequently as expected and demands the funding of a second roof layer. On the other hand, the inclination of this roof typology increases proportionally the energy performance of the building which is promising. The best results are achieved by the modification of the roof surface itself, both by colour and by form as inspired by nature. The cool roof design, in addition to be the most performant solution, would also presumably be the most economical solution. Indeed, the application of white cool coating on an existing surface is cheap and efficient.

5.10.3.2. Availability

In terms of accessibility and location, the white coating application in SC 2 seems the most suitable solution. The more problematic design proposals although performative, are the self-shaded roof with the lattice and the vegetated roof design. Indeed, the ribbed roof design of SC 3 demands more material resources that will have to be transported on site. Moreover, the material choice for the shading panes will have a direct impact on the availability and transportation energy consumption both altering the total life cycle of the design. The living roof design on the other hand demands water in a hot and arid climate zone which is not evident to supply.

5.10.3.3. Maintenance and longevity

The problem arising from the cool roof solution is the decreasing efficiency resulting from a dusted white surface compared to a newly applied one. Moreover, the coating should resist very high temperatures and moisture deposit, even more when the roof surface is horizontal and flat. White paint for example, would form bubbles and cracks after a while which means the surface should be renewed every other year or five years in the case of high albedo coating. An alternative solution to enhance the longevity of the surface would be to opt for a permanent finishing like white stone, marble or terrazzo. A cheaper solution would even be the installation of a layer of white pebbles or white bathroom tiles in ceramic. The latter has the additional advantage to be lightweight. For the ribbed roof design, drawbacks are identified in terms of maintenance because of the complex roof surface. Nevertheless, the performance of this design is not proportional to the cleanliness of the surface. The ventilated roof design has the other advantage of prolonging the longevity of the existing roof surface thanks to the protection of the second roof layer. Finally, the vegetated roof demands high maintenance as was mentioned before.

Chapter 6

Conclusion

In this last chapter, a general overview of the master thesis concludes the different chapters. Furthermore, the main objectives and research questions introduced in Chapter 1 are confronted with the answers provided in this research with a discussion of the achieved objectives and the ones that could not be reached. The contribution is then delineated and limitations impeding the research discussed. Finally, the thesis is concluded by suggestions for further research based both on the most promising findings and on the limitations encountered.

6.1. General overview

The master thesis was introduced in Chapter 1 by the statement of rising concern for energy consumption observed in the past few decades. The construction sector accounts for one third of the total resource consumption of our continent and the dependency on mechanical cooling systems as a mean to achieve thermal comfort has reached a critical point. Moreover, the building envelope is responsible for nearly half of the heat gains in a building and, in hot and arid climates, half of these gains come directly from the roof surface. Indeed, a link was established between the necessity of improving roof designs and the need for low energy solutions in a context of rising energy costs and excess cooling energy consumption responsible for increasing electricity blackouts. The scarce literature documentation about roof designs for thermal performance however demonstrates the poor consideration for the fifth façade in architectural design. In nature however, thermoregulation of buildings is the feature that most closely links the construction sector with biological organisms. Biomimicry, in addition to being a source of inspiration to sustainable and low-energy solutions, gains interest in the field of architecture and thermoregulation.

In Chapter 2, the state-of-the-art was first introduced by a broader contextualization of the research with a characterization of the hot and arid climate type. Thereafter, biomimetic design was presented as a design solution and the different approaches defined. Finally, the link between thermoregulation, roof design and biomimicry was addressed by a literature research on existing individual relations between the fields. Weaknesses of roof designs in terms of thermoregulation and performance were identified for their composition and orientation in hot climates. Design and biomimicry revealed that the widespread application of biomimicry in architecture remains largely unrealized although a strong connection between the building envelope and nature appeared. At the end of the chapter, the link between biomimicry and thermoregulation led towards the identification of biological role models for the research. The lack of literature documentation about roof classifications led to the elaboration of an explorative roof taxonomy developed in Chapter 3. The existing classical roof taxonomy was expanded towards a more performance-oriented classification resulting in three roof categories further subdivided into roof cooling strategies: the protective, selective and vernacular roof typologies. In this chapter, biological role models were assigned to roof design strategies when relevant. In Chapter 4, the explorative roof taxonomy was applied to case studies of building designs and concepts relevant to the hot climate context, showing a cooling strategy, a biomimetic design or the potential of roof design in

architectural expression. For each case study, a performance scheme was created from a combination of the roof typologies in Chapter 3. Finally, Chapter 5 proposed a research by design approach by computer simulations on EnergyPlus. Hence, the most promising roof designs identified in the precedent chapters and new combinations of them were presented by scenarios and compared to a reference scenario, a typical school building in Egypt. These were compared in terms of performance by energy, temperature and discomfort measurements and then discussed in terms of cost, availability, maintenance and longevity.

6.2.   Discussion of the main objectives

In Chapter 1, the main problem tackled was defined as *the operational energy consumption of buildings in hot climates, tackled by the architectural design of roofs as part of the building envelope through biomimicry of thermoregulation principles.* Accordingly, several research questions were formulated and an attempt was made throughout this thesis to answer these in the most complete manner. Therefore, answers were supported by a thorough literature research, the development of an expanded roof design classification, the analysis of existing buildings and speculations, and finally by experimentation with model simulation.

The first question concerned the design problem of roofs in hot and arid climates: *What is the role of roofs in thermal regulation in the context of hot-arid climate zones?* First, a state-of-the-art of the problem of excess heat load on roofs and high solar altitude in hot climatic regions was presented in Chapter 2 which pointed out the presently unanswered design problem. In Chapter 3, the role of roofs as cooling strategy by specific design for hot and arid climates was developed into an explorative roof design taxonomy. The potential of roofs when designed according to the presented roof typologies, were supported by scientific results rising from their literature documentation. Here, the sub-question: *what are the design strategies that can be applied on roofs in a hot and arid climate?* was answered by the same methodology. Yet, Chapter 5 provided a quantitative answer to the question by assessing the effect of different roof designs on the energy performance of a reference building in Egypt.

Along with the problem of sustainable roof designs, the suggestion was to make use of biomimetic design and find inspiration in biological role models for thermoregulation. The research question went as follows: *How to develop sustainable, energy-efficient roof design principles and strategies using a biomimetic approach?* In Chapter 2, two biomimetic approaches were introduced and completed with an exhaustive list of biological role models relevant to the field of thermoregulation. Although biomimicry was part of the process in both the identification of roof cooling strategies and the analysis of case studies referring to biological organisms, bio-inspired solutions were not the only relevant roof design solutions pointed out in this thesis. However, Chapter 5 confirmed the beneficial effect of three solutions inspired by role models introduced in the state-of-the-art. Indeed, the first scenario showed an increased improvement of the ventilated roof design by inclination of the surface similarly to the cooling strategy applied by the black-tailed prairie dog. Then, the second scenario found inspiration in the desert snail and its white shell colour for the solar reflection of a cool roof surface. Finally, the third scenario was directly influenced by the desert cactus and the notion of self-shading resulting in a ribbed roof surface showing great potential in improving a building's energy performance. On the other hand, it is true that the initial idea of following a clear biomimetic approach as defined in Chapter 2 differed from the methodology used in this thesis, partly because of the scarce knowledge in the field of biology and because the thesis was submitted in the field of architectural engineering. Finally, in Chapter 4, the following question was answered through the analysis of existing buildings and concepts from the literature: *How can attention to roof designs help improve the architectural expression of buildings?* The case studies discussed in this chapter were therefore chosen among others because of the importance of the roof in their architectural expression.

6.3. Contribution

Research on existing classifications of roofs enabling a comparative interpretation of the performance of designs encountered in this master thesis revealed a literature scarcity about the subject, which is in inadequacy with the potential of roof cooling techniques on enhanced building performance in hot and arid climates. Therefore, an explorative roof design classification was conducted based on energy performance and cooling strategies presenting a range of new roof typologies extending the state-of-the-art. Additionally, new assessment criteria of cost, availability and maintenance were introduced in the discussion. These new typologies presented solutions to the problem of excess cooling energy consumption and discomfort distinctive of hot arid climatic regions. Yet, the analysis presented a prospective answer to the increase of the dependency on mechanical cooling systems observed in the construction sector in the past decades.

The research by design offered a new performance evaluation on a reference building, showing the weaknesses of typical school buildings in Egypt. This base case study was the opportunity to compare roof designs applied on the same flat roof and experiencing the same environmental conditions as the roof is the only parameter that is modified throughout the design proposals explored by simulation. From the calculated results of energy and temperature, some roof designs appeared to be overrated compared to their cost and maintenance, others were given a new interest because of their great impact, simplicity and affordability. Existing roof cooling strategies were also enhanced by thermoregulation principles found in nature. The exploration of roof designs by simulation allowed a coherent comparison questioning their state-of-the-art, at the end of which some solutions could be advised above others based on the same parameters.

Biomimicry applied to the field of architecture is known to be largely unrealized. This master thesis introduces a new application for biomimetic design emphasizing the large range of possibilities it offers. In this research, an exhaustive list of biological role models to thermoregulation of buildings was gathered from a thorough literature review enlarging the different existing inventories of the past years. Concretely, the identified role models were applied to roof designs and developed as a cooling strategy, whereunder three were assessed quantitatively through energy and temperature calculations.

6.4. Limitations

A first limitation encountered in this master thesis was the lack of information about roof typologies relevant to the reflection on thermoregulating performance achieved by roof designs. Indeed, the classical roof typologies or archetypes were only based on geometry or surface material. As these characteristics were not satisfactory for the scientific discussion of the roof designs encountered, an additional chapter was conducted introducing an explorative roof design taxonomy on which to base the discussion in this thesis. In Chapter 4 again, relevant case studies showed sometimes a paucity in information about the roof design strategies used. For the research by design in Chapter 5, the simulation program EnergyPlus presented limitations in modelling combined scenarios of roof typologies. Although the component used for the natural vented cavity of SC 1 was very accurate, further detailing of the second roof surface into a ribbed roof revealed to be impossible. The problem was addressed in a more mathematical way, by transfer of the results of a similar scenario available by simulation into the proposed more daring roof design. The default parameters used for the simulations also accounted for a lack of information about the program or existing building used as reference. Finally, the objective of addressing the challenge of cost and life cycle identified in the state-of-the-art was not achieved in a quantitative way as initially intended, by means of results and LCA. This was however performed in a qualitative way in the sense that is has been discussed and has led the assessment of the different design proposals throughout the thesis.

6.5. Further research

In this master thesis, the performance-based roof design classification developed in Chapter 3 is a first contribution that was realized based on existing designs and concepts in an explorative way. The taxonomy could gain interest with further precision and expansion to new designs rising in the future in order to keep it up to date. Although an attempt was made to define case studies based on this taxonomy, a research could be conducted to automatize or regularize the classification of roof designs in the scope of energy performance, possibly based on this classification.

From the results of the research by design and simulation in Chapter 5, roof designs were compared and assessed based on the same parameters, in a quantitative way for energy, temperature and discomfort, and in a yet qualitative way for cost, availability, maintenance and longevity. As was initially intended, it would be interesting to assess the presented design proposals in terms of LCA quantitively. Indeed, as this thesis discusses the operational energy consumption of the building enhanced by redesigning the roof, the embodied energy and resources determined by the LCA can also be determinant in the choice of one proposal above another. Moreover, the use of a more adapted simulation platform should be used to validate the combined design in SC 2.1 of Chapter 5.

In terms of biomimicry, the research derived from the initially defined biomimetic design approaches in the state-of-the-art of Chapter 2. Although biological role models were identified, only a few were used as an inspiration for the proposed designs such as the desert cactus influencing the self-shaded roof design, the desert snail for the cool roof design and the black-tailed prairie dog for the enhancement of the ventilated roof by inclination. Yet, the application of the performative roof typologies gained importance at the expense of biomimetic emulation of the strategies. A broader knowledge in the fields of biology and chemistry combined with architectural engineering would improve the biomimetic potential of thermoregulating designs of roofs in hot and arid climate regions.

Bibliography

5osA. (2009, April 9). [Zoka Zola Architecture + Urban Design] The Rafflesia House. Retrieved Jan. 19, 2020, from https://5osa.com/1219

Abanomi, W., & Jones, P. (2005, May). Passive cooling and energy conservation design strategies of school buildings in hot, arid region: Riyadh, Saudi Arabia. *International Conference "Passive and Low Energy Cooling for the Built Environment"*, 619-630. (C. University, Ed.) Santorini, Greece. Retrieved February 2020, from http://www.inive.org/members_area/medias/pdf/inive/palenc/2005/abanomi.pdf

Abdellfattah Elsayed, A. G. (2016). Parametric design optimization for solar screens: an approach for balancing thermal and daylight performance for office buildings in egypt. (C. U. Faculty of Engineering, Ed.) Giza, Egypt.

Anderson, C. (2012). Esplanade - Theaters on the Bay. *The Master Architect Series: DP Architects*, p. 36-42. Australia: The Images Publishing Group Pty Ltd.

Araujo, A., Haddad, G., & Garcia, G. (n.d.). Votu Hotel. *GCP Arquitetura & Urbanismo*. Retrieved Jan. 5, 2020, from https://www.academia.edu/35928855/Votu_Hotel_hd.pdf

ArchDaily. (2017, November 08). Louvre Abu Dhabi, Ateliers Jean Nouvel. Retrieved December 30, 2019, from https://www.archdaily.com/883157/louvre-abu-dhabi-atelier-jean-nouvel

Archello. (2020). Zero-Energy Home - "Rafflesia House". *Archello*. Retrieved Jan. 19, 2020, from https://archello.com/project/zero-energy-home-rafflesia-house

AskNature Team. (2016, September 14). Shell protects from heat: desert snail. *Ask Nature*. The Biomimicry Institute. Retrieved March 2020, from https://asknature.org/strategy/shell-protects-from-heat/#.XniB94hKhPY

AskNature Team. (2017, July 21). Black-tailed Jackrabbit: Large ears used to cool off. Retrieved March 2020, from https://asknature.org/strategy/large-ears-used-to-cool-off/#.XmOrnqhKhPY

AskNature Team. (2017, August 31). Cactus Family. Shape shades and enhances heat radiation. *AskNature*. Retrieved Dec. 2019, from https://asknature.org/strategy/shape-shades-and-enhances-heat-radiation/#.XhIbB0dKhPZ

AskNature Team. (2017, August 31). Leaf color and shape enhance cooling effect. *Ask Nature*. The Biomimicry Institute. Retrieved March 2020, from https://asknature.org/strategy/leaf-color-and-shape-enhance-cooling-effect/#.XniCiIhKhPY

AskNature Team. (2018, March 5). Black-tailed Prairie Dog. Asymmetric burrow openings create passive ventilation. *AskNature*. Retrieved Dec. 2019, from https://asknature.org/strategy/asymmetric-burrow-openings-create-passive-ventilation/#.XhIZGkdKhPZ

Atelier One. (n.d.). Singapore Arts Centre. *Atelier One, Structural Engineers*. Retrieved Jan. 2020, from http://www.atelierone.com/singapore-arts-centre

Ateliers Jean Nouvel. (n.d.). Le musée et la mer. *Louvre Abou Dabi*. Retrieved from http://www.jeannouvel.com/projets/louvre-abou-dhabi-3/

Aziz, M. S., & El Sherif, A. Y. (2016, November). Biomimicry as an approach for bio-inspired structure with the aid of computation. *Alexandria Engineering Journal, 55*, 707-714. Elsevier B.V.

Azzam, O. A. (n.d.). The development of urban and rural housing in Egypt.

Badarnah, L., Nachman Farchi, Y., & Knaack, U. (2010). Solutions from nature for building envelope thermoregulation. *Design and Nature V, 138*, 251-262. (W. Press, Ed.) Netherlands.

Barozzi, M., Lienhard, J., Zanelli, A., & Monticelli, C. (2016). The sustainability of adaptive envelopes: developments of kinetic architecture. *Procedia Engineering, 155*, 275-284. Elsevier Ltd.

Bass, B., Krayenhoff, E. S., Martilli, A., Stull, R., & Auld, H. (2003, May). The impact of green roofs on Toronto's urban heat island. *Proceedings of the First North American Green Roof Conference: Greening Rooftops for Sustainable Communities*, 292-304. Toronto, Canada: Cardinal Group.

Benyus, J. (1997). *Biomimicry: Innovation Inspired by Nature.* New York: Harper Collins Publishers.

Bhatia, A., Mathur, J., & Garg, V. (2011, April 21). Calibrated simulation for estimating energy savings by the use of cool roof in five Indian climatic zones. *Journal of Renewable and Sustainable Energy, 3*, 1-14. doi:http://dx.doi.org/10.1063/1.3582768

Bianchini, R. (2019, november). Louvre Abu Dhabi. *Inexhibit*. Retrieved december 29, 2019, from https://www.inexhibit.com/mymuseum/louvre-abu-dhabi-jean-nouvel/

Biomimicry Belgium. (n.d.). *What is Biomimicry?* Retrieved from Biomimicry Belgium: http://biomimicry.be/

Biomimicry Institute. (2015). Nature's Unifying Patterns: Learning from nature's overarching design lessons. *Biomimicry Toolbox*. Retrieved March 30, 2020, from https://toolbox.biomimicry.org/core-concepts/natures-unifying-patterns/

Biwole, P. H., Woloszyn, M., & Pompeo, C. (2008). Heat transfers in a double-skin roof ventilated by natural. *Energy and Buildings(40)*, 1487-1497. France: Elsevier B.V. doi:10.1016/j.enbuild.2008.02.004

Butters, C. (2015). A passive cooling retrofit for low cost, hot climate housing. (W. University, Ed.) United Kingdom.

Butters, C. (2015, May 5). Enhancing Air Movement by Passive Means in Hot Climate Buildings. *School of Engineering, University of Warwick*. United Kingdom: ELITH Working Paper.

Castagno, J., & Atkins, E. (2018, November 13). Roof shape classification from LiDAR and satellite image data fusion using supervised learning. *Sensors*. (U. o. Mishigan, Ed.) Mishigan, USA. doi:10.3390/s18113960

Classic Metal Roofing Systems. (2011, August 7). Metal roofing and hot climates. OH. Retrieved Feb. 2020, from https://www.classicmetalroofingsystems.com/metal-roofing-and-hot-climates/

Craig, S. (2020). Assistant Professor. *Mc Gill University. Faculty of Engineering.* Retrieved Jan. 7, 2020, from https://www.mcgill.ca/engineering/salmaan-craig

Craig, S., Harrison, D., Cripps, A., & Knott, D. (2008). BioTRIZ Suggests Radiative Cooling of Buildings Can Be Done Passively by Changing the Structure of Roof Insulation to Let Longwave Infrared Pass. *Journal of Bionic Engineering, 5*, 55-66.

D+H Mechatronic AG. (2013, October 23). California Academy of Science: D+H Provides the Solution for Complex Ventilation and Climate Control of the Building Complex. New York: PR Newswire Association LLC. Retrieved from https://search.proquest.com/docview/1444136350?accountid=17194

Dabaieh, M., Wanas, O., Amer Hegazy, M., & Johansson, E. (2014). Reducing cooling demands in a hot dry climate: A simulation study study for non-insulated passive cool roof thermal performance in residential buildings. *Energy and Buildings(89)*, 142-152. Elsevier B.V. Retrieved from http://dx.doi.org/10.1016/j.enbuild.2014.12.034

Delaqua, V. (2018, January 30). Aprendendo com a natureza: conheça o projeto do Votu Hotel. *ArchDaily*. Brasil. Retrieved Jan. 2020, from https://www.archdaily.com.br/br/887431/aprendendo-com-a-natureza-conheca-o-projeto-do-votu-hotel?ad_medium=gallery

Dilip, J. (2005). Modeling of solar passive techniques for roof cooling in arid regions. *Building and Environment(41)*, 277-287. Ludhiana, India: Elsevier Ltd. doi:10.1016/j.buildenv.2005.01.023

DP Architects Pte Ltd. (2020). Esplanade - Theaters on the Bay. *DPA*. Retrieved Jan. 17, 2020, from https://www.dpa.com.sg/projects/esplanadetheatresonthebay/

EIA. (2015). Egypt International energy data and analysis.

El-Kabbany, M. F. (2013). Alternative building materials and components for affordable housing in Egypt towards improved competitiveness of modern earth construction. (A. S. Stuttgart, Ed.)

Fahmy, M., Mahdy, M. M., & Nikolopoulou, M. (2013, November 10). Prediction of future energy consumption reduction using GRC envelope optimization for residential buildings in Egypt. *Energy and Buildings, 70*, 186-193. Elsevier B.V.

Fantom, N., & Serajuddin, U. (2016, January). The World Bank's Classification of Countries by Income. *Policy research working paper*. (W. B. Group, Ed.)

Fisher, A., & Craig, S. (2017). Large, complex, perforated enclosures in extreme environments. Control of structural & thermodynamic behaviour, from micro- to nano-scale. *Fabricate 2011, Making digital architecture*. UCL Press.

Future Architecture. (n.d.). A Hotel designed with biomimicry, inspired by prairie dogs for ventilation system, toucan peak for thermal exchange and cactus for self-shading. *Architecture Inspired by Nature*. Retrieved Jan. 5, 2020, from http://futurearchitectureplatform.org/projects/3cdd032b-bcc4-4e80-b52a-f03375143da7/

Garg, V., Kotharkar, R., Sathaye, J., Rallapalli, H., Kulkarni, N., Reddy, N., . . . Sarkar, A. (2015). Assessment of the impact of cool roofs in rural buildings in India. *Energy and Buildings(114)*, 156-163. Elsevier B.V. Retrieved from http://dx.doi.org/10.1016/j.enbuild.2015.06.043

GCP Arquitetura & Urbanismo. (n.d.). Votu Hotel. Retrieved Jan. 6, 2020, from http://www.gcp.arq.br/projetos/votu-hotel/

Givoni, B. (1998). *Climate Considerations in Building and Urban Design.* USA: John Wiley & Sons, Inc.

Gonchar, J. (2009, January). Sophisticated tools help designers naturally ventilate a voluminous exhibition hall. *197, 1*, 56-56. 1p. Architectural Record. Retrieved December 31, 2019, from http://search.ebscohost.com.ezproxy.ulb.ac.be/login.aspx?direct=true&db=aph&AN=3636233 1&site=ehost-live

Gordon, S. (2019, May 2). Cooling Degree Day (CDD). *Investopedia*. Retrieved Jan. 9, 2020, from https://www.investopedia.com/terms/c/colddegreeday.asp

Grange, S. (2014, July). Context, architectural design, and ambition. *Exhibit, Louvre Abu Dhabi*. France.

Gupta, V. (n.d.). Natural cooling of buildings - A review. Innovative Informations Incorporated. Retrieved February 2020, from http://space-design.com/wp-content/uploads/2018/04/natural-cooling-of-buildings.pdf

Hanley, W. (2012, March). Public Projects. *200, 3*, 77-77. 1p. Architectural Record. Retrieved Dec. 2019, from http://search.ebscohost.com.ezproxy.ulb.ac.be/login.aspx?direct=true&db=aph&AN=7400174 5&site=ehost-live

Harris, C. M. (2000). Flat roof. *Harris dictionary of architecture & construction*. New York: McGraw-Hill.

Hwang, J., Jeong, Y., Min Park, J., Hong Lee, K., Wook Hong, J., & Choi, J. (2015, September 8). Biomimetics: forecasting the future of science, engineering, and medicine. *Int J Nanomedicine*, 5701-5713. doi:10.2147/IJN.S83642

Imbert, F., Frost, K. S., Fisher, A., Witt, A., Tourre, V., & Koren, B. (2012). Concurrent Geometric, Structural and Environmental Design: Louvre Abu Dhabi.

Johnson, D. (n.d.). *Solar Mirror*. Retrieved May 2020, from Table of absorptivity and emissivity of common materials and coatings: http://solarmirror.com/fom/fom-serve/cache/43.html

Kamel, S. M., & Ibrahim, M. A.-B. (n.d.). The architectural expression of local climate responsive building. Retrieved February 2020, from https://www.cpas-egypt.com/pdf/Dr-Mohamed-Abdel-Baki/Researches/005-THE%20ARCHITECTURAL%20EXPRESSION.pdf

Kéré Architecture. (n.d.). Gando Primary School. Retrieved December 2019, from http://www.kere-architecture.com/projects/primary-school-gando/

Kéré Architecture. (n.d.). Gando School Library. Retrieved Dec. 2019, from http://www.kere-architecture.com/projects/school-library-gando/

Khan, A. Z. (2017). Chapter 05, Bioclimatic Passive Design. *CNST H-306 Bioclimatic Design*. Brussels: Brussels School of Engineering.

Khan, A. Z. (2017). Chapter 06, Passive Heating, Cooling and Daylighting. *CNST H-306 Bioclimatic Design*. Brussels: Brussels School of Engineering.

Kharrufa, S. N., & Adil, Y. (2007). Roof pond cooling of buildings in hot arid climates. *Building and Environment(43)*, 82-89. Baghdad, Iraq: Elsevier Ltd. doi:10.1016/j.buildenv.2006.11.034

Koren, B. S. (2017). Louvre Abu Dhabi 1:33 light-test prototype. *Fabricate 2011, Make Digital Architecture*. UCL Press. Retrieved December 2019, from https://www.jstor.org/stable/j.ctt1tp3c6d.43

Lemp, D., & Weidner, U. (n.d.). Improvements of roof surface classification using hyperspectral and laser scanning data. Karlsruhe, Germany: Institute of Photogrammetry and Remote Sensing.

Lepik, A. (2017, May). The way by Kéré. *Architectural Review, 241, 1441*, 104-110. Retrieved December 2019, from http://search.ebscohost.com.ezproxy.ulb.ac.be/login.aspx?direct=true&db=aph&AN=1232240 27&site=ehost-live

Lewis, D. A., & Nobel, P. S. (2008, December 13). Thermal Energy Exchange Model and Water Loss of a Barrel Cactus, Ferocactus acanthodes. *Plant Physiology*.

Lu, X., Xu, P., Wang, H., Yang, T., & Hou, J. (2016). Cooling potential and applications prospects of passive radiative cooling in buildings: the current state-of-the-art. *Renewable and Sustainable Energy Reviews(65)*, 1079-1097. China: Elsevier Ltd. Retrieved from http://dx.doi.org/10.1016/j.rser.2016.07.058

Mahmoud Arafa, R. (2012). Energy efficient configuration of perforated solar screens for residential desert buildings. (T. A. Engineering, Ed.)

Marceau, M. L., & VanGeem, M. G. (2008). Solar Reflectance Values of Concrete. (P. C. (PCA), Ed.) *Research & Development Information*.

McIntyre, L. (2009, August). Green roofs, High Maintenance Superstar. *Landscape Architecture Magazine, 99(8)*, 64-66, 68-72, 74-77. American Society of Landscape Architects. Retrieved December 28, 2019, from https://www.jstor.org/stable/44794259

Mohajeri, N., Assouline, D., Guiboud, B., Bill, A., Gudmundsson, A., & Scartezzini, J.-L. (2017). A city-scale roof shape classification using machine learning for solar energy application. *Renewable Energy, 121*, 81-93. Elsevier Ltd.

Mourshed, M. (2016, March). Climatic parameters for building energy applications: A temporal-geospatial assessment of temperature indicators. *Renewable Energy, 94*, 55-71. (C. University, Ed.)

Nour ElDin, N., Abdou, A., & Abd ElGawad, I. (2016). Improving Sustainability Concepts in Developing Countries, Biomimetic Potentials for Building Envelope Adaptation in Egypt. *Procedia Environmental Sciences, 34*, 375-386. (E. B.V., Ed.) doi:10.1016/j.proenv.2016.04.033

Oberndorfer, E., Lundholm, J., Bass, B., Coffman, R. R., Doshi, H., Dunnett, N., . . . Rowe, B. (2007, Nov.). Green Roofs as Urban Ecosystems: Ecological Structures, Functions, and Services. *BioScience, 57(10)*, 823-833. (A. I. Sciences, Ed.) Oxford University Press. Retrieved February 2020, from https://www.jstor.org/stable/10.1641/b571005

Parametric House. (2019). Biomimicry Architecture - Esplanade Theatre. Retrieved Jan. 2020, from https://parametrichouse.com/biomimicry-architecture-3/

Passivhaus Institute. (2019). *Building Envelope*. Retrieved from Passipedia: The Passive House Resource: https://passipedia.org/planning/thermal_protection

Pawlyn, M. (2011). *Biomimicry in Architecture.* London: RIBA Publishing.

Pawlyn, M. (2016). Biomimétisme et Architecture. *Biomimétisme*. Éditions Rue de l'échiquier.

Pearlmutter, D., & Berliner, P. (2017). Experiments with a 'psychrometric' roof pond system for passivecooling in hot-arid regions. *(144)*, 295-302. Israel: Elsevier B.V. Retrieved March 2020, from http://dx.doi.org/10.1016/j.enbuild.2017.03.067

Pearson, C. A. (2009, January). Renzo Piano Designs a living, breathing building in San Francisco's Golden Gate Park. *197, 1*, 48-48. 1p. Architectural Record. Retrieved December 31, 2019, from

http://search.ebscohost.com.ezproxy.ulb.ac.be/login.aspx?direct=true&db=aph&AN=3636232
8&site=ehost-live

Peel, M. C., Finlayson, B. L., & McMahon, T. A. (2007, October 11). Updated world map of the Köppen-Geiger climate classification. *Hydrology and Earth System Sciences, 11*, 1633-1644. (E. G. Union, Ed.) Copernicus Publications.

Philips. (2019). *For professionals: LEDtube 1200mm 16W 765 T8 AP C G.* Retrieved May 2020, from Philips: https://www.lighting.philips.com/main/prof/led-lamps-and-tubes/led-tubes/ecofit-ledtubes-t8/929001184608_EU/product

Rahmes, M., Yates, H., Connetti, S., & O'Neil Smith, A. (2008, January 24). Geospatial modeling system providing building roof type identification features and related methods. *United States Patent*. Melbourne, US: Harris Corporation.

Reid, R. L. (2009, March). Under One Green Roof. *Civil Engineering*, 46-57. American Society of Civil Engineers.

Riajul Islam, M., & Schulze-Makuch, D. (2007, July 9). Adaptations to environmental extremes by multicellular organisms. *International Journal of Astrobiology* .

Runsheng, T., Meir, I. A., & Etzion, Y. (2002). An analysis of absorbed radiation by domed and vaulted roofs as compared with flat roofs. *Energy and Buildings(35)*, 539-548. Elsevier Science B.V.

Saleem, A. A., Abel-Rahman, A. K., Ali, A. H., & Ookawara, S. (2015, May 14). An Analysis of Thermal Comfort and Energy Consumption within Public Primary Schools in Egypt.

Schmidt-Nielsen, K., Taylor, C. R., & Shkolnik, A. (1971). Desert snails: Problems of Heat, Water and Food. *Journal of Experimental Biology, 55(2)*, 385-398. The Company of Biologists Ltd.

Schmitt, O. H. (1969). Some interesting useful biomimetic transforms. *Proceedings of the Third International Biophysics Congress*.

Schumacher, C., Ricketts, L., Finch, G., & Straube, J. (2016). The effect of temperature on insulation performance: considerations for optimizing wall and roof designs. Orlando: ResearchGate. Retrieved March 2020, from https://www.researchgate.net/publication/312054592

SERI, GLOBAL 2000, & Friends of the Earth Europe. (2009, September). Overconsumption? Our Use of the World's Natural Resources.

Sharifi, A., & Yamagata, Y. (2015). Roof ponds as passive heating and cooling systems: A systematic review. *Applied Energy(160)*, 336-357. Japan: Elsevier Ltd. Retrieved March 2020, from http://dx.doi.org/10.1016/j.apenergy.2015.09.061

Slessor, C. (2009, October). Primary School. *Architectural Review, 226, 1352*, 66-69. Retrieved December 2019, from http://search.ebscohost.com.ezproxy.ulb.ac.be/login.aspx?direct=true&db=aph&AN=5083764 6&site=ehost-live

Smith, G. (2009, September). Amplified radiative cooling via optimised combinations of aperture geometry and spectral emittance profiles of surfaces and the atmosphere. *Solar Energy Materials and Solar Cells, 93, 9*, 1696-1701. Australia: Elsevier. Retrieved February 2020, from https://doi.org/10.1016/j.solmat.2009.05.015

Suehrcke, H., Peterson, E. L., & Selby, N. (2008). Effect of roof solar reflectance on the building heat gain in a hot climate. *Energy and Buildings, 40, 12*, 2224-2235. Elsevier Ltd. doi:http://dx.doi.org/10.1016/j.enbuild.2008.06.015

Sun Earth Tools. (2009). Outils pour les consommateurs et les concepteurs de l'énergie solaire. Retrieved March 17, 2020, from https://www.sunearthtools.com/dp/tools/pos_sun.php

T.Y. Lin International Group. (2020). The Esplanade - Theatres on the Bay. Retrieved Jan. 2020, from https://www.tylin.com/en/projects/the_esplanade__theatres_on_the_bay

Tang, R., Meir, I. A., & Wu, T. (2006). Thermal performance of non air-conditioned buildings with vaulted roofs in comparison with flat roofs. *Building and Environment(41)*, 268-276. Elsevier Ltd. doi:10.1016/j.buildenv.2005.01.008

The Esplanade CO LTD. (2019). Architecture & Building Design. *Esplanade, Theatres on the Bay*. Retrieved Jan. 2020, from https://www.esplanade.com/about-us/architecture-and-building-design

The World Bank Group. (2020). The world by income and region. Retrieved March 2020, from http://datatopics.worldbank.org/world-development-indicators/the-world-by-income-and-region.html

TL T8 36W 940 1200mm. (n.d.). Retrieved May 2020, from Gloeilamp Goedkoop - Europa's Gloeilampen specialist: https://www.gloeilampgoedkoop.be/tl-t8-36w-940-1200mm.html?SID=2o5r6pkjh7q92mgncec2n2mauu&___store=nl_be&gclid=EAIaIQobChM IgpaxjanU6QIVE57VCh2syQ34EAQYBCABEgIq6fD_BwE&___from_store=fr_fr

Tributsch, H. (1983, January 1). How life learned to live: Adaptation in nature.

U.S. Department of Energy. (2020, March 27). Engineering reference. *EnergyPlus Version 9.3.0 documentation*.

U.S. Department of Energy. (2020). *Input Output Reference.*

U.S. Department of Energy. (n.d.). *Weather Data.* Retrieved April 2020, from EnergyPlus: https://energyplus.net/weather

UNFCCC. (2017, Oct. 12). Developing countries need urgent support to adapt to climate change. Retrieved March 2020, from https://unfccc.int/news/developing-countries-need-urgent-support-to-adapt-to-climate-change

Vanaga, R. (2019). Climate Adaptive Building Shell for Nearly Zero Energy Buildings: Application of Biomimicry Principles. Riga: Riga Technical University Press.

Verma, S. (2017, October 8). #mydurian. Yours Too. *Connected to India*. Retrieved Jan. 2020, from https://www.connectedtoindia.com/mydurian-yours-too-2868.html

Warton University of Pennsylvania. (2010, May 18). *How Hany El Miniawy designs low-cost homes for Egypt's poor, one community at a time.* Retrieved April 2020, from https://knowledge.wharton.upenn.edu/article/how-hany-el-miniawy-designs-low-cost-homes-for-egypts-poor-one-community-at-a-time/

Wayne, A. (2002, December 3). Singapore Offers an Architectural Symbol for the Arts. *The New York Times*.

Wong, N. H., Chen, Y., Ong, C. L., & Sia, A. (2003). Investigation of thermal benefits of rooftop garden in the tropical environment. *Building and Environment, 38*, 261-270.

Woolley-Barker, T. (2017, September 20). Biomimicry helps nature-lovers and fragile wildlife co-exist at the Votu Hotel in Brazil. *PhD*. Inhabitat. Retrieved Jan. 5, 2020, from

https://inhabitat.com/biomimicry-helps-nature-lovers-and-fragile-wildlife-co-exist-at-the-votu-hotel-in-brazil/

Xue, X., Yang, J., Zhang, W., Jiang, L., Qu, J., Xu, L., . . . Zhang, Z. (2015). The study of an engineering efficientcool white roof coating based on styrene acrylate copolymer and cement for waterproofing purpose - Part I: Optical properties, estimated cooling effect and relevant properties after dirt and accelerated exposures. *Construction and Building Materials*(98), 176-184.

Yannas, S., & Weber, W. (2014). Lessons from Vernacular Architecture. New York: Routledge.

Yannas, S., Erell, E., & Molina, J. L. (2006). Roof Cooling Techniques. A Design Handbook. UK and USA: Earthscan.

Zhang, X., & Chen, X. (2015, January 1). Learning synthetic models for roof style classification using point clouds. Eindhoven (NL): Global B.V. .

Zoka Zola. (2007). Rafflesia. *Zoka Zola Architecture + Urban Design*. Chicago. Retrieved Jan. 19, 2020, from https://www.zokazola.com/bird_island_rafflesia.html

Zomorodian, Z. S., & Nasrollahi, F. (2013, December). Architectural design optimization of school buildings for reduction of energy demand in hot and dry climates of Iran. *International journal of architectural engineering & urban planning, 23(1&2)*.

Appendix

Appendix A
State-of-the-art

A.1. Köppen's Climate Classification

1st	2nd	3rd	Description	Criteria*
A			Tropical	$T_{cold} \geq 18$
	f		- Rainforest	$P_{dry} \geq 60$
	m		- Monsoon	Not (Af) & $P_{dry} \geq 100 - MAP/25$
	w		- Savannah	Not (Af) & $P_{dry} < 100 - MAP/25$
B			Arid	$MAP < 10 \times P_{threshold}$
	W		- Desert	$MAP < 5 \times P_{threshold}$
	S		- Steppe	$MAP \geq 5 \times P_{threshold}$
		h	- Hot	$MAT \geq 18$
		k	- Cold	$MAT < 18$
C			Temperate	$T_{hot} > 10$ & $0 < T_{cold} < 18$
	s		- Dry Summer	$P_{sdry} < 40$ & $P_{sdry} < P_{wwet}/3$
	w		- Dry Winter	$P_{wdry} < P_{swet}/10$
	f		- Without dry season	Not (Cs) or (Cw)
		a	- Hot Summer	$T_{hot} \geq 22$
		b	- Warm Summer	Not (a) & $T_{mon10} \geq 4$
		c	- Cold Summer	Not (a or b) & $1 \leq T_{mon10} < 4$
D			Cold	$T_{hot} > 10$ & $T_{cold} \leq 0$
	s		- Dry Summer	$P_{sdry} < 40$ & $P_{sdry} < P_{wwet}/3$
	w		- Dry Winter	$P_{wdry} < P_{swet}/10$
	f		- Without dry season	Not (Ds) or (Dw)
		a	- Hot Summer	$T_{hot} \geq 22$
		b	- Warm Summer	Not (a) & $T_{mon10} \geq 4$
		c	- Cold Summer	Not (a, b or d)
		d	- Very Cold Winter	Not (a or b) & $T_{cold} < -38$
E			Polar	$T_{hot} < 10$
	T		- Tundra	$T_{hot} > 0$
	F		- Frost	$T_{hot} \leq 0$

*MAP = mean annual precipitation, MAT = mean annual temperature, T_{hot} = temperature of the hottest month, T_{cold} = temperature of the coldest month, T_{mon10} = number of months where the temperature is above 10, P_{dry} = precipitation of the driest month, P_{sdry} = precipitation of the driest month in summer, P_{wdry} = precipitation of the driest month in winter, P_{swet} = precipitation of the wettest month in summer, P_{wwet} = precipitation of the wettest month in winter, $P_{threshold}$ = varies according to the following rules (if 70% of MAP occurs in winter then $P_{threshold} = 2 \times MAT$, if 70% of MAP occurs in summer then $P_{threshold} = 2 \times MAT + 28$, otherwise $P_{threshold} = 2 \times MAT + 14$). Summer (winter) is defined as the warmer (cooler) six month period of ONDJFM and AMJJAS.

Table A - 1: Definition of Köppen climate symbols and defining criteria. (Peel, Finlayson, & McMahon, 2007)

A.2. Levels of biomimicry

Levels of biomimicry	Example: Building that mimics termites	
Organism level (mimicry of a specific organism)	Form	The building looks like a termite
	Material	The building is made from the same material as a termite; a material that mimics termite exoskeleton/skin for example
	Construction	The building is made in the same way as a termite; it goes through various growth cycles for example
	Process	The building works in the same way as an individual termite; it produces hydrogen efficiently through meta-genomics for example
	Function	The building functions like a termite in a larger context; it recycles cellulose waste and creates soil for example
Behavior level (mimicry of how an organism behaves or relate to its large context)	Form	The building looks like it was made by a termite; a replica of a termite mound for example
	Material	The building is made from the same materials that a termite builds with; using digested fine soil as the primary material for example
	Construction	The building is made in the same way that a termite would build in; piling earth in certain places at certain times for example
	Process	The building works in the same way as a termite mound would; by careful orientation, shape, materials selection and NV for example, or the building mimics how termites work together
	Function	The building functions in the same way that it would if made by termites; internal conditions are regulated to be optimal and thermally stable for example. It may also function in the same way that a termite mound does in a larger context
Ecosystem level (mimicry of an ecosystem)	Form	The building looks like an ecosystem (a termite would live in)
	Material	The building is made from the same kind of materials that (a termite) ecosystem is made of; it uses naturally occurring common compounds, and water as the primary chemical medium for example
	Construction	The building is assembled in the same way as a (termite) ecosystem; principles of succession and increasing complexity over time are used for example
	Process	The building works in the same way as a (termite) ecosystem; it captures and converts energy from the sun, and stores water for example
	Function	The building is able to function in the same way that a (termite) ecosystem would and forms part of a complex system by utilizing the relationships between processes; it is able to participate in the hydrological, carbon, nitrogen cycles, etc. in a similar way to an ecosystem for example

Table A - 2: Levels of biomimicry (Aziz and El sherif 2016).

A.3. Sun paths
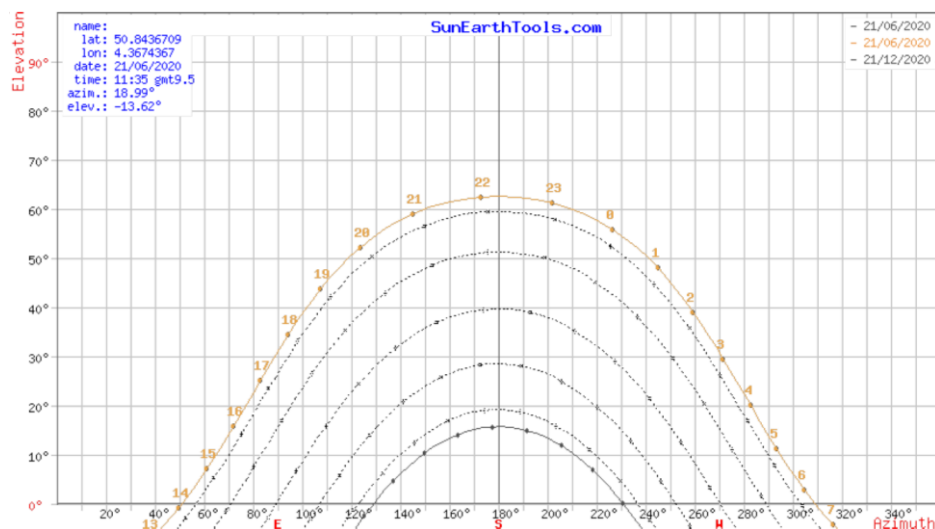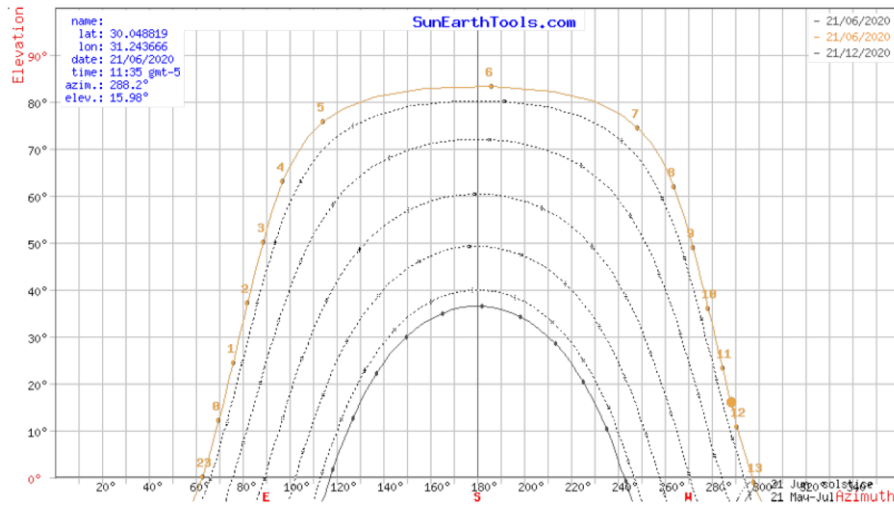
Figure A - 1: *Top*: Solar position path of Brussels, Belgium. *Bottom*: Solar position path Cairo, Egypt. (Sun Earth Tools 2009)

A.4. Biological role models
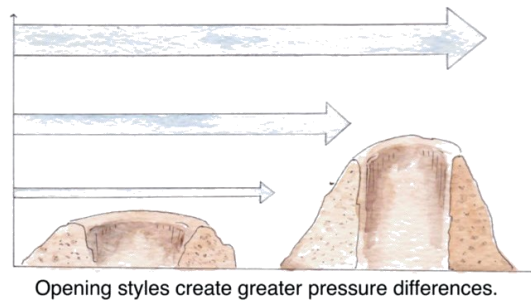
Figure A - 2: Biomimicry Institute principle scheme of the Black-tailed prairie dog as biological role model for thermoregulation. Opening styles create greater pressure differences. (AskNature Team, 2018)
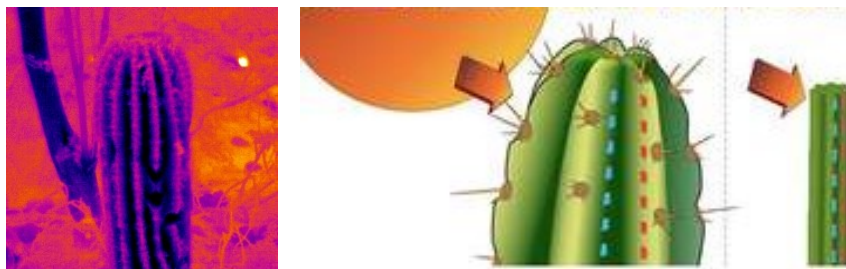
Figure A - 3: Biomimicry Institute principle scheme of the desert cactus as a biological role model for thermoregulation. Self-shading. (AskNature Team, 2017)
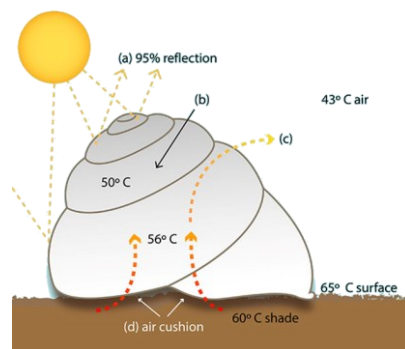
Figure A - 4: Biomimicry Institute principle scheme of the desert snail as a biological role model for thermoregulation. Cool, white and reflective surface. (AskNature Team, 2016)

Appendix B
Innovative roof designs – Case studies

B.1. Louvre Abu Dhabi
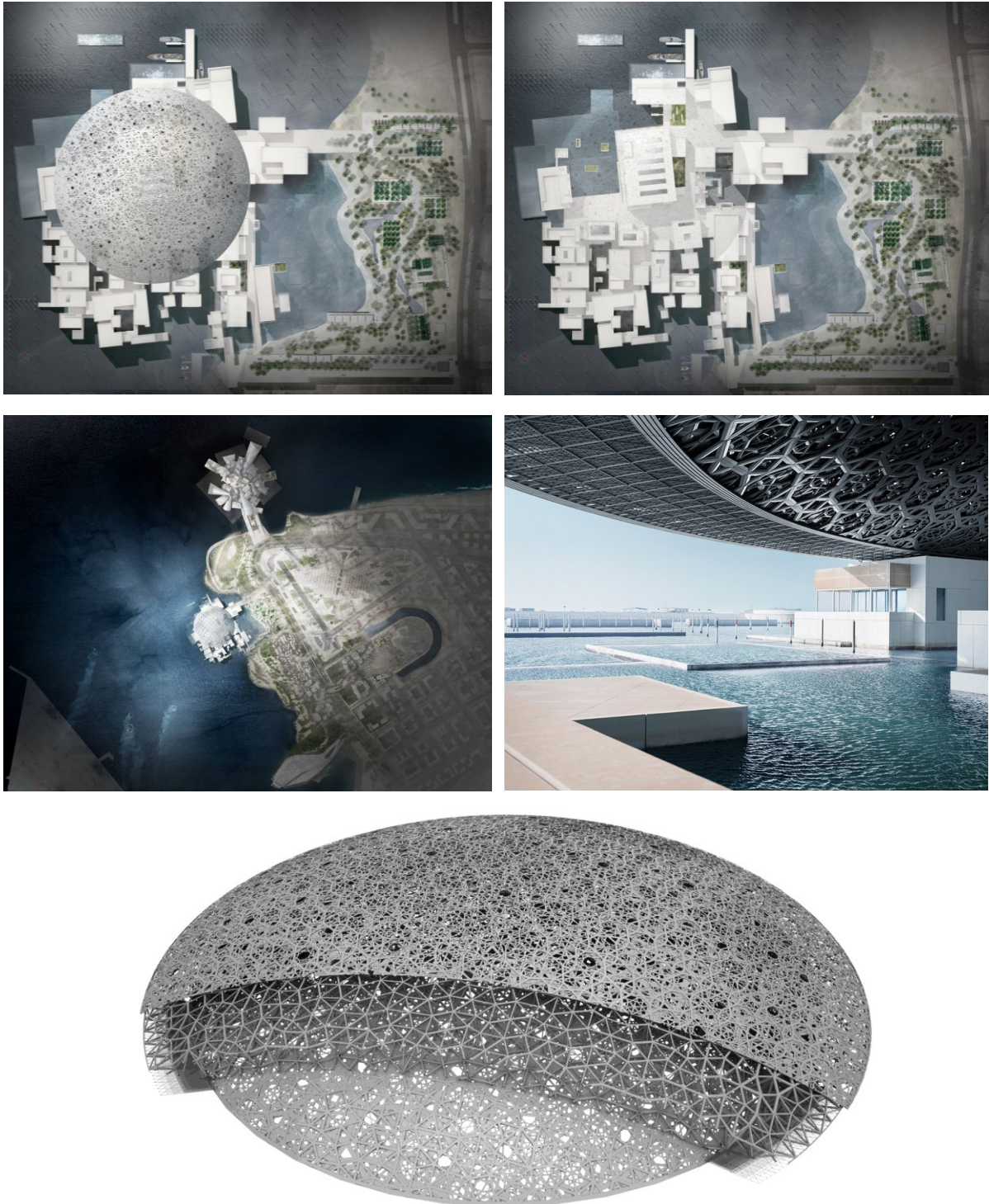
Figure B - 1: Additional documentation of the Louvre Abu Dhabi Museum. *From top to bottom, left to right*: Plan of the Louvre Abu Dhabi Museum with dome. Plan of the Louvre Abu Dhabi Museum without dome. Situation plan of the museum. View from the inside of the museum towards the dome perimeter. 3-Dimenal layering of the dome. (Ateliers Jean Nouvel)

B.2. California Academy of Sciences
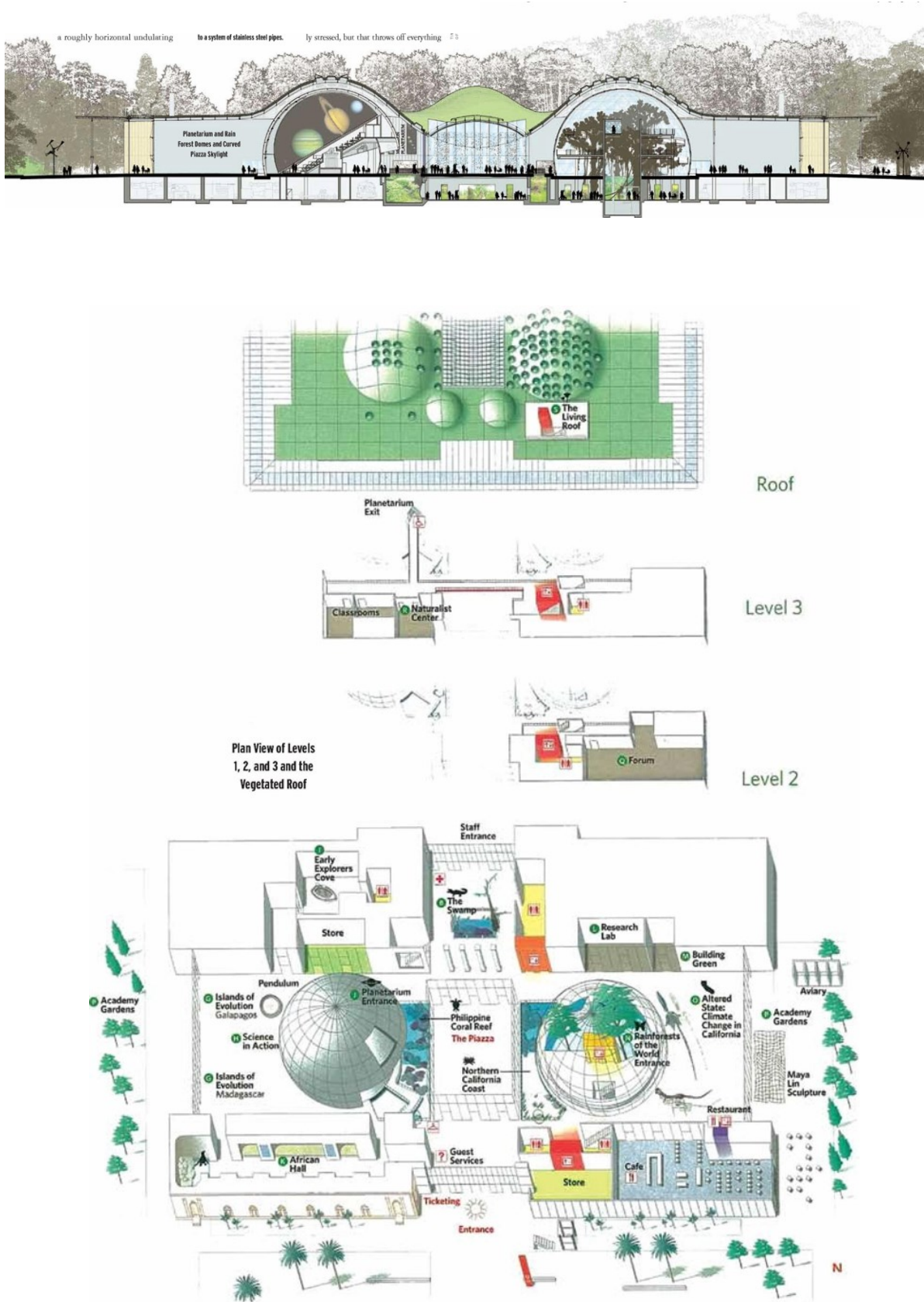
Figure B - 2: Additional documentation of the California Academy of Sciences. *Top*: Section of the building showing the sinuous roof shape. *Bottom*: Roof plan sketch and axonometry of the building. (Reid, 2009)

B.3. Gando Primary School
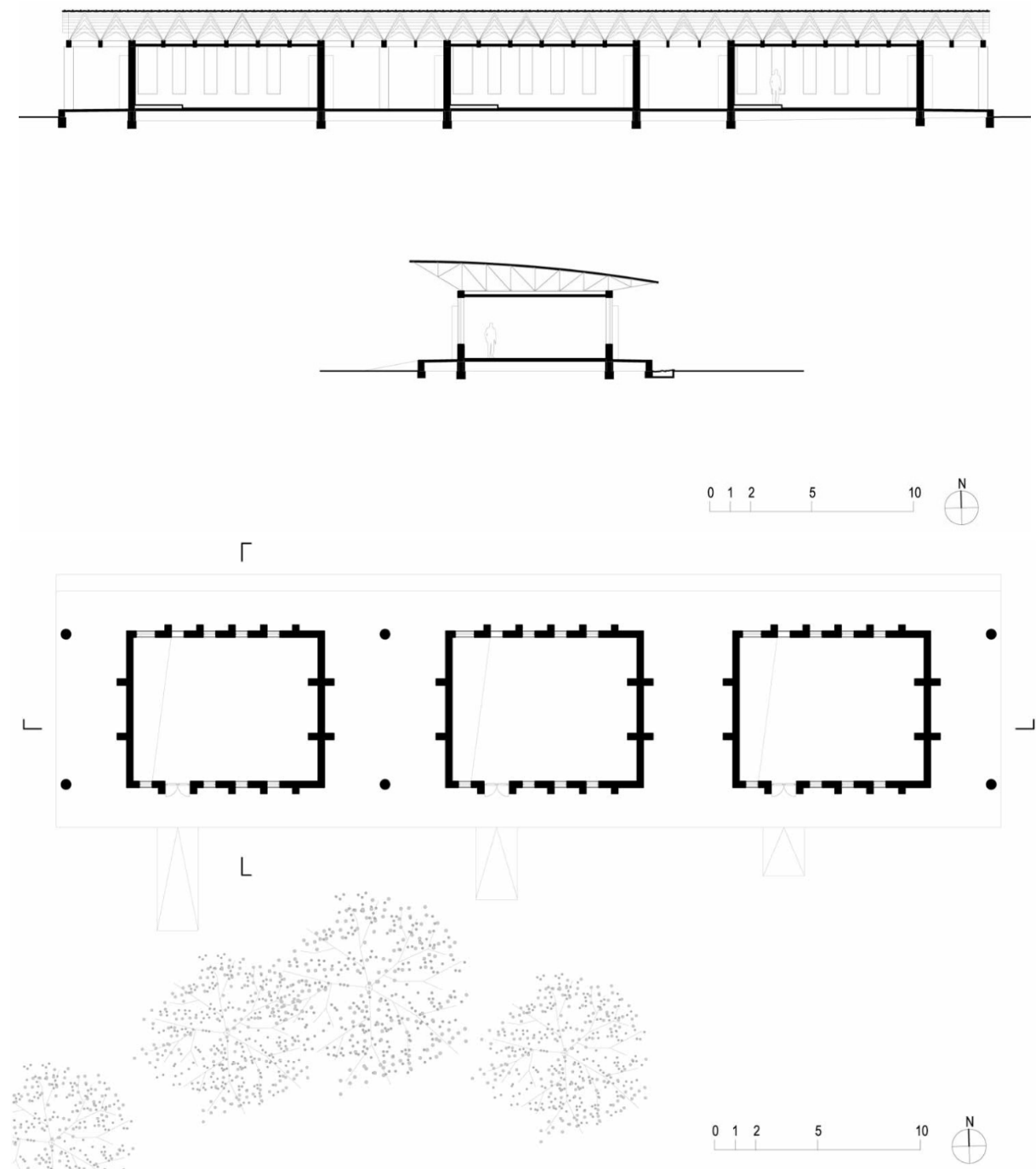
Figure B - 3: Additional documentation of the Gando Primary School. *Top*: longitudinal architectural section of the school building. *Centre*: Transversal architectural section of the school building. *Bottom*: Architectural ground plan of the school building. (Kéré Architecture)

B.4. Votu Hotel
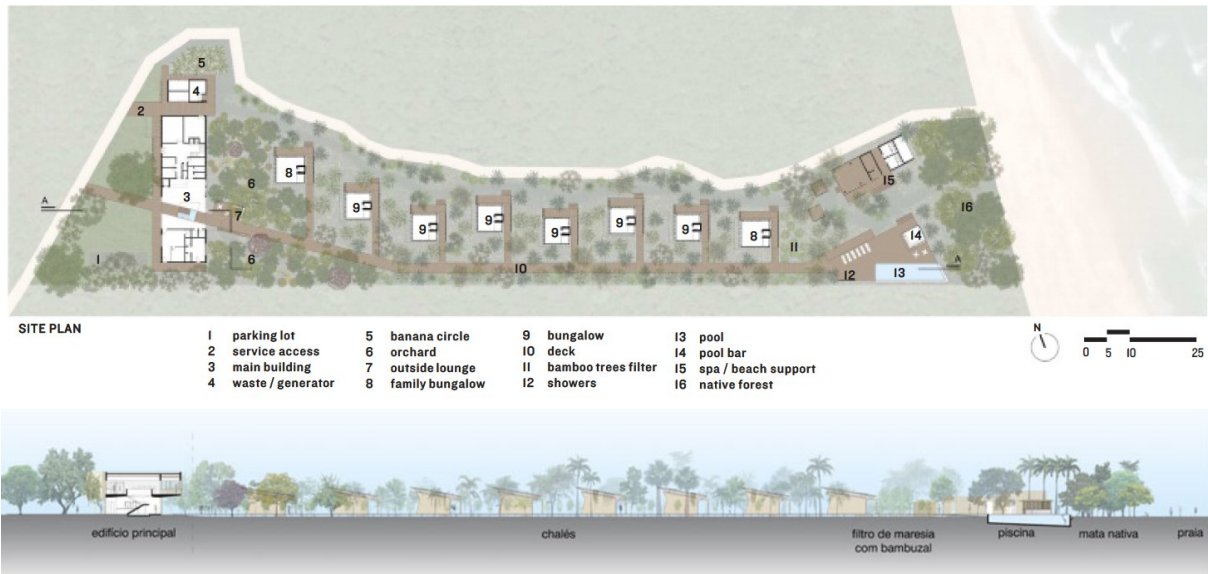
Figure B - 4: Additionnal documentation of the Votu Hotel. *Top*: Site plan. Water management, waste- and nutrient cycles. *Bottom*: Longitudinal contextual section. The water is filtered –before entering the site from the sea side– by bamboo acting as a living filter against salinity, bacteria, or pollutants. Greywater is redirected to the banana circle, introducing food production amongst the sustainability features of the site. Blackwater is also managed by passing through a biodigester and biofilter, ending in a compost pile that successively fertilizes an orchard, providing fruit for the guests (Araujo, Haddad, & Garcia). (GCP Arquitetura & Urbanismo)
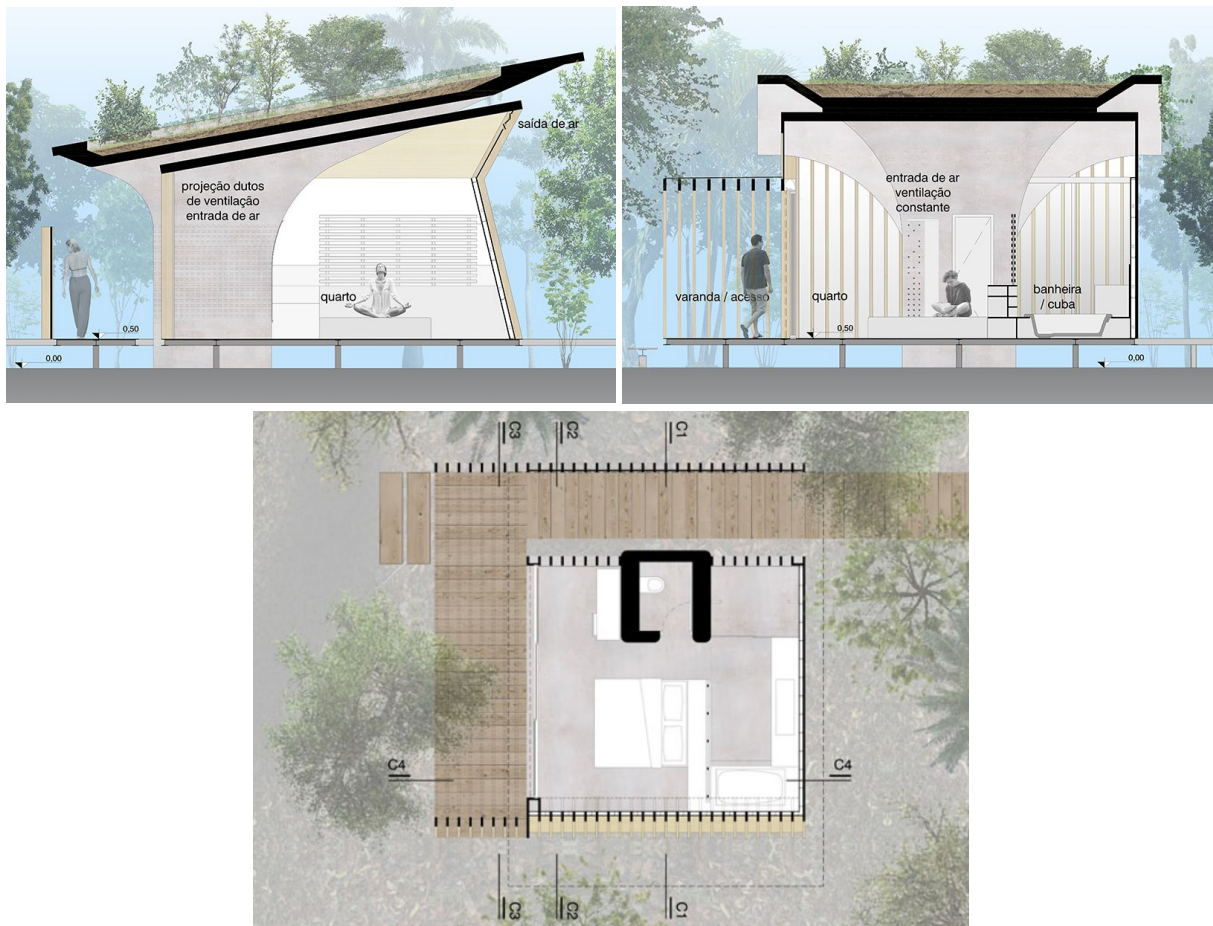
Figure B - 5: Additionnal documentation of the Votu Hotel. *Top*: architectural sections C2 and C4. *Bottom*: Architectural ground plan of a bungalow. (GCP Arquitetura & Urbanismo)

93

B.5.   Esplanade Theaters on the Bay

Figure B - 6: *Left*: Inside view on the shell structure and glazed envelope with shading. *Right*: View on the two rounded envelopes by night (DP Architects Pte Ltd. 2020).

Figure B - 7: Additional documentation of the Esplanade Theaters on the Bay. Situation by sky view on the site. (Parametric House, 2019)
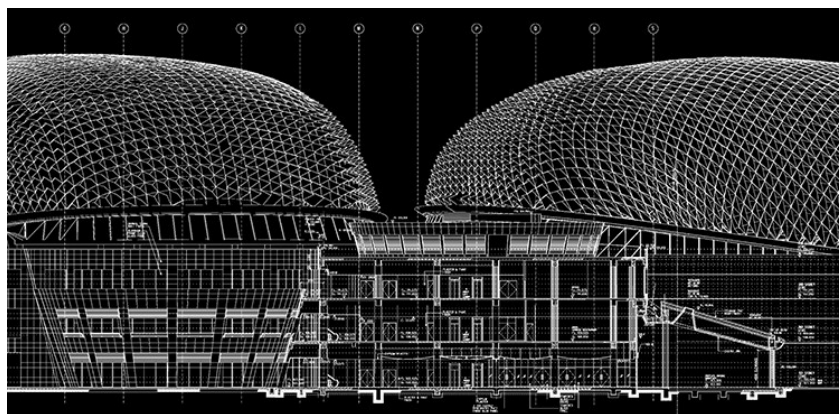
Figure B - 8: Additional documentation of the Esplanade Theaters on the Bay. Technical section of the buildings. (The Esplanade CO LTD, 2019)

B.6. Rafflesia House
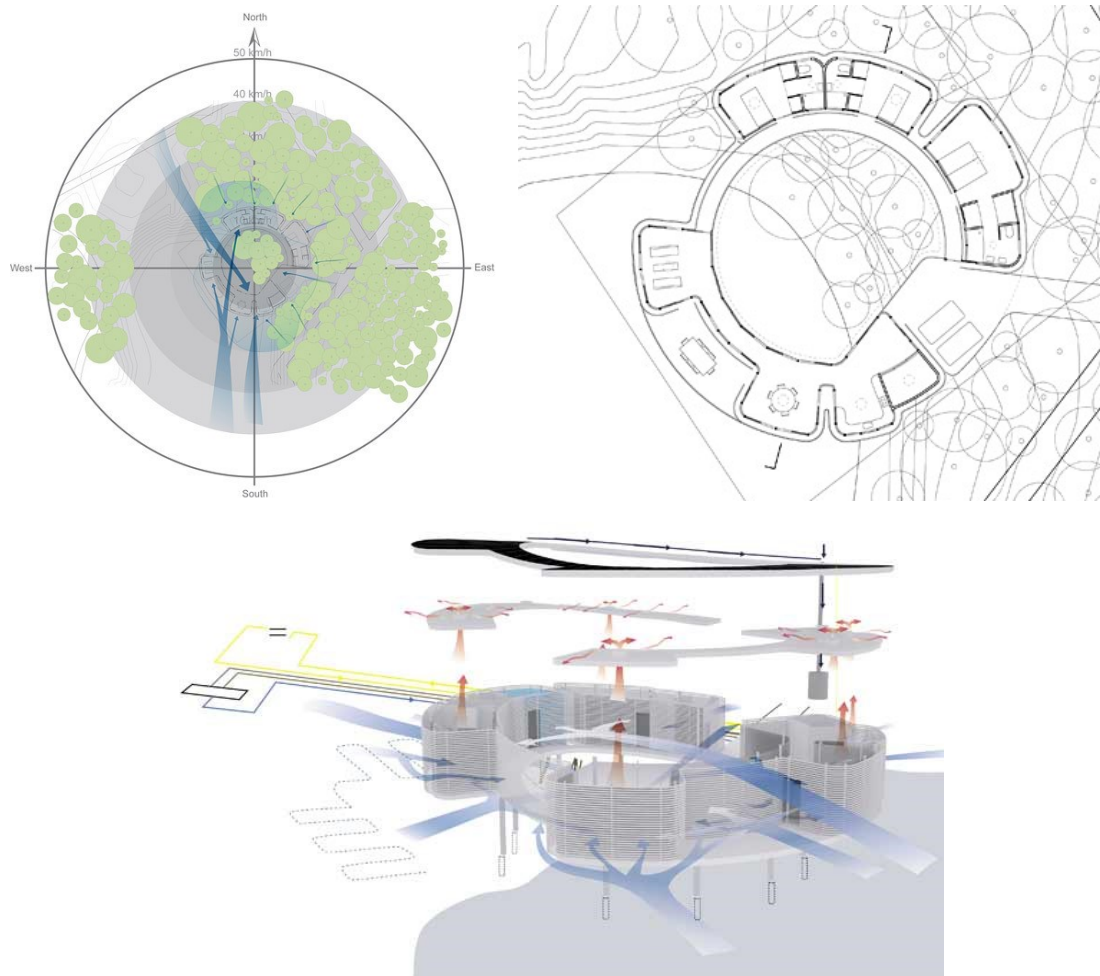
Figure B - 9: Additional documentation of the Refflesia House. *Top left*: situation plan and wind orientation. *Top right*: Architectural ground plan. *Bottom*: Schematic representation of the cooling strategies. (5osA, 2009)

B.7. BioTRIZ
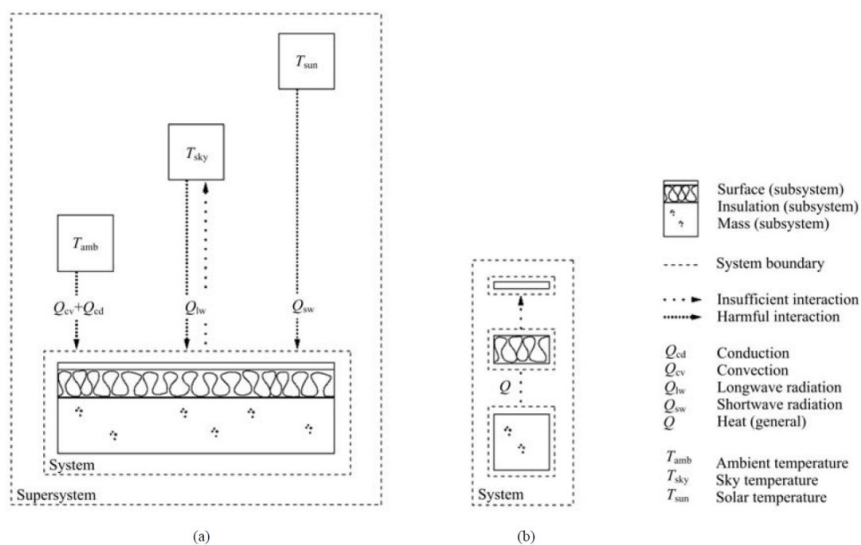
Figure B - 10: A roof and its thermal interaction with the sun, sky and external ambient temperature. Insufficient interactions are shown between the roof and its environment (a), and between the roof subsystems (b) (Craig, Harrison, Cripps, & Knott, 2008).

Appendix C
Research by design and simulations

C.1.   Chapter 5 outline
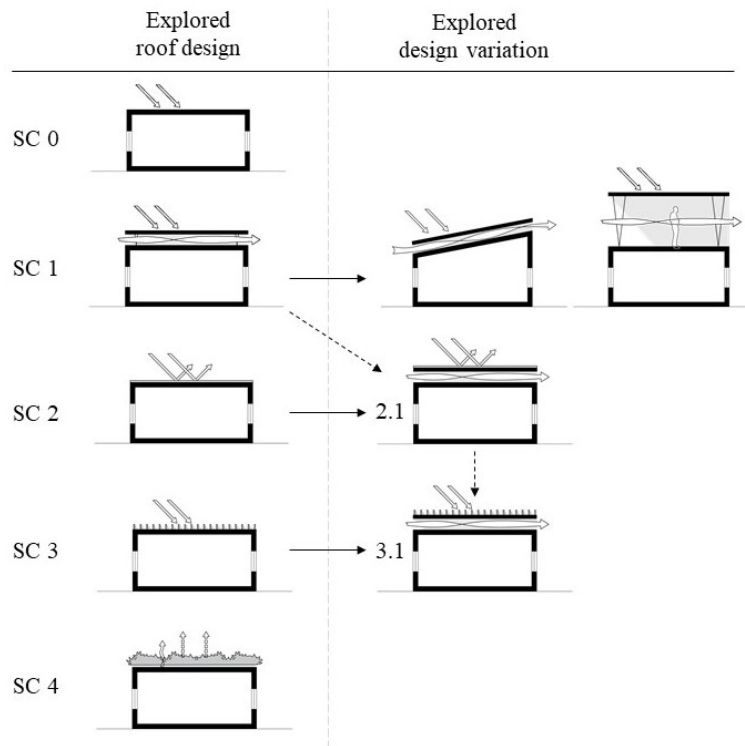
Table C - 1: Outline scheme of the research by design and simulation chapter. Explored scenarios with design variations.

C.2.   Reference building – Scenario 0

Figure C - 1: Map of the available weather data for EnergyPlus. Cairo International Airport. (U.S. Department of Energy).

Figure C - 2: Views inside a classroom of the reference building in Egypt for SC 0 and further. Assyut Prototype Distinct Language School. (Saleem, et al. 2015)

C.3.   Grasshopper script – DIVA for Rhino
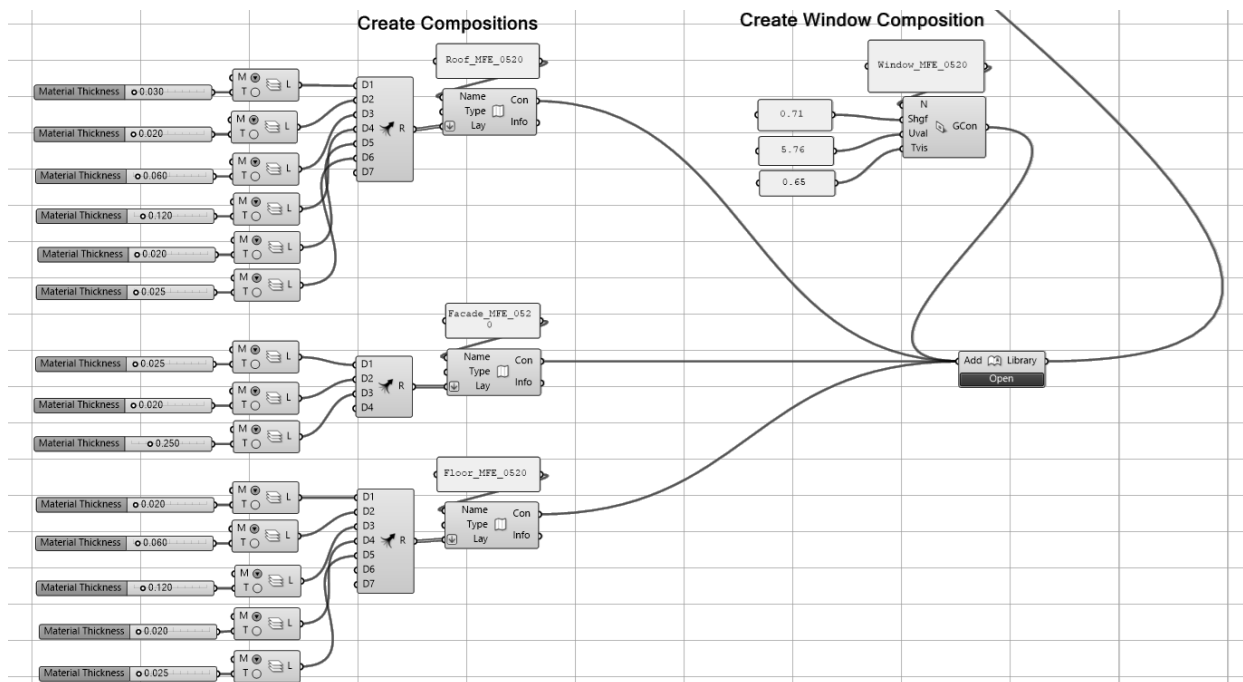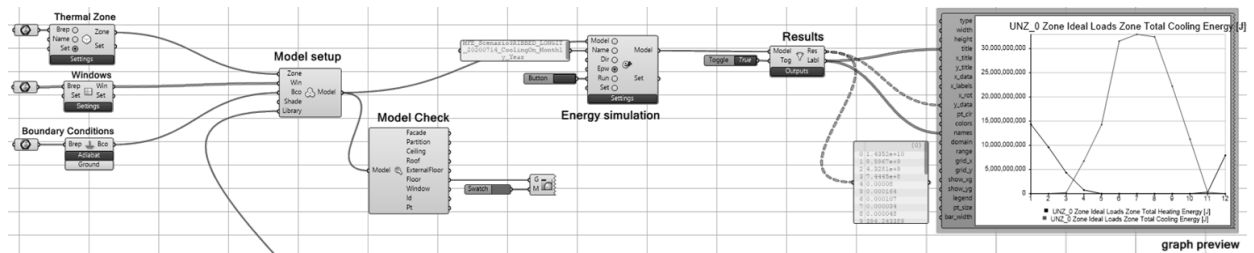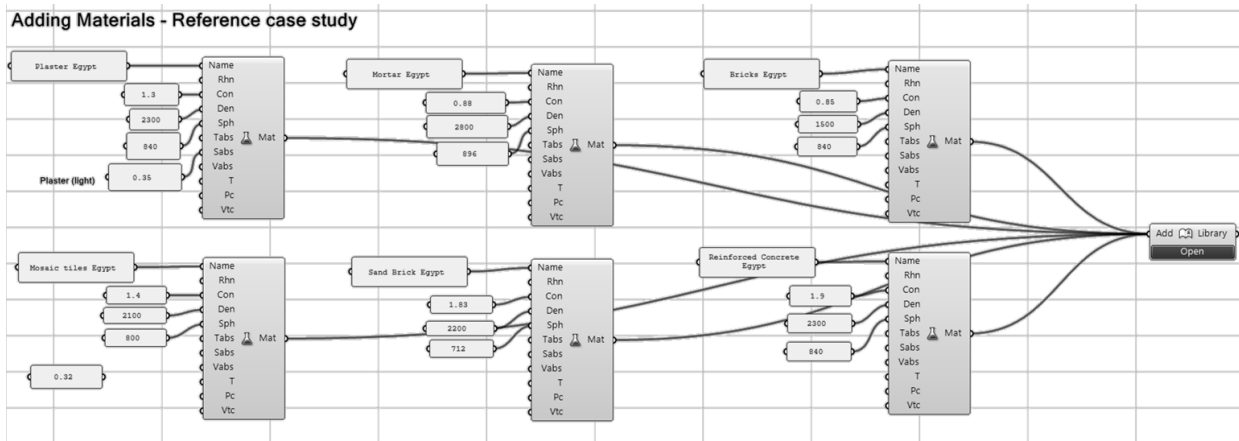
Figure C - 3: Grasshopper script for the energy simulation in DIVA for Rhino. *Top*: Model setup and EnergyPlus simulation component of DIVA for Rhino. Preview of the results in graph on the right. Definition of last level of the building as thermal zone on the left. *Centre*: Library linked to the model setup. Roof, external walls and floor compositions with layers of materials. *Bottom*: Material definition by conductivity, density, specific heat, thermal, solar and visible absorptance. These materials are referenced in the compositions above.
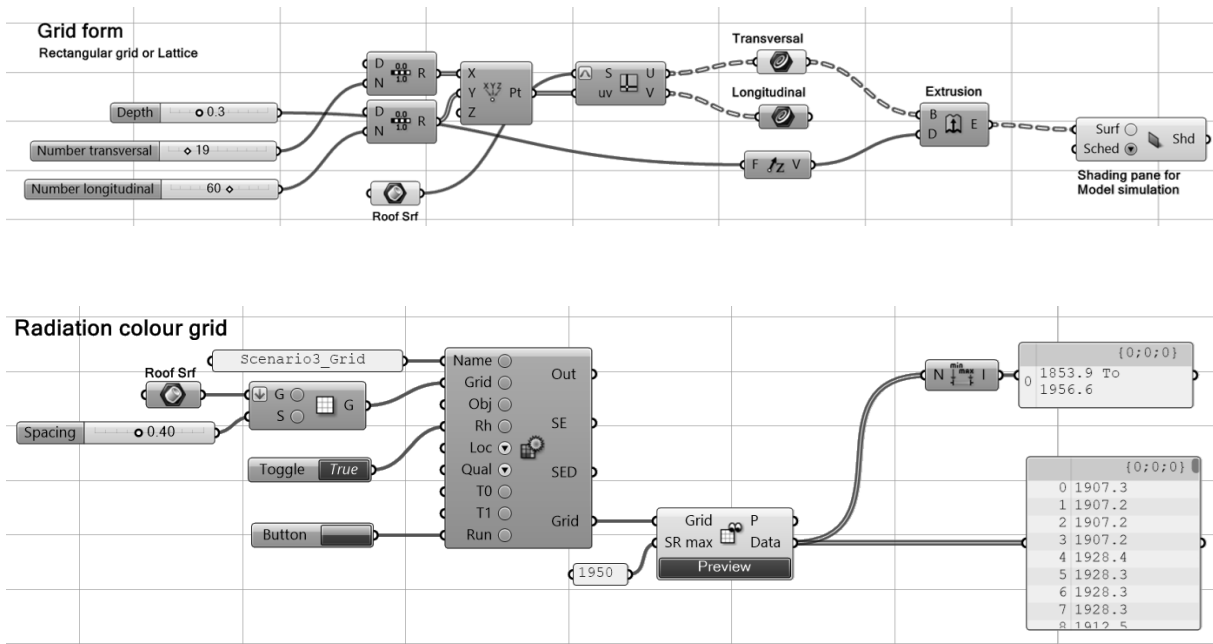
Figure C - 4: Grasshopper script of the shading lattice definition and assimilation in the simulation model. *Top*: Parametric geometry (depth, number and orientation) of the shading lattice. Transversal or longitudinal. The shading surface is defined and linked to the model setup for SC 3. *Bottom*: preliminary visualization of the solar irradiance of the roof surface with shading lattice. Radiation map (Rad Map) component with range maximum value defined at 1950 kWh/m².

C.4. EnergyPlus documentation

1.11.21 SurfaceProperty:ExteriorNaturalVentedCavity

This object is used to model a multi-skin exterior heat transfer surface. This is a special case where the outside face is a slightly detached layer forming a naturally ventilated cavity. The actual outer surface is referred to as the baffle. The modeling here assumes that the heat capacity in the outer baffle can be neglected since it is much lower than the underlying mass surface. This object is used with the Building-Surface:Detailed object where the Heat Transfer surfaces are referred to as the underlying surfaces. The constructions and materials for the BuildingSurface:Detailed object should reflect the construction of just the underlying surface. The SurfaceProperty:ExteriorNaturalVentedCavity object is used to describe the decoupled layer, or baffle, and the characteristics of the cavity and openings for natural ventilation. This object is also used in conjunction with the OtherSideConditionsModel.

The area and orientation are obtained from **BuildingSurface:Detailed** objects, which are referenced by name. This object can be used to model certain types of photovoltaic mounting configurations such as interlocking roof pavers. If the baffle covers only part of a surface, then that surface should be split into separate **BuildingSurface:Detailed** objects where one matches the size of the baffle. A single baffle can be associated with as many **BuildingSurface:Detailed** objects as desired (although if you need to use more than 10 surfaces, then the IDD will need to be extended). The base heat transfer surfaces need not be contiguous nor have the same orientation, but the program will issue warnings if surfaces have widely ranging tilts and azimuths.

Note that the model involves predicting the rates that ambient air moves in and out of the cavity. Accurate modeling of these air flows would be extremely challenging and so the models provided through this object are simplistic engineering models based on discharge coefficients that are sensitive to wind and buoyancy effects. The accuracy depends on the values for, and applicability of, the discharge coefficients and unfortunately little research is available to help characterize these. The models should be considered rudimentary and the user is encouraged to explore different values for the coefficients in attempts to bound the importance of natural ventilation for the cavities. See the Engineering Reference for more details.

1.11.21.1 Inputs

1.11.21.1.1 Field: Name
This field contains a unique name for the ventilated cavity.

1.11.21.1.2 Field: Boundary Conditions Model Name
This field contains the name of an SurfaceProperty:OtherSideConditionsModel object declared elsewhere in the input file. This will connect the baffle and ventilated cavity to the exterior boundary conditions for the underlying heat transfer surface.

1.11.21.1.3 Field: Area Fraction of Openings
This field is used to enter an area fraction for what part of the baffle consists of openings. The area of the openings will set to the product of this field and the sum of the area of the underlying surfaces.

1.11.21.1.4 Field: Thermal Emissivity of Exterior Baffle Material
This field is used to enter the thermal emissivity of the baffler. This surface property is for longwave infrared radiation. The property is used for both sides of collector. Most painted materials have an emissivity of 0.9.

1.11.21.1.5 Field: Solar Absorptivity of Exterior Baffle
This field is used to enter the solar absorptivity of the baffle. This surface property is for shortwave, solar radiation. The property is used for the front side of the baffle that faces the environment. Darker colors have a higher absorptivity. While black is the highest performance, other colors might be used to match the color scheme of the rest of the façade.

1.11.21.1.6 Field: Height Scale for Buoyancy-Driven Ventilation
This field is used to enter a nominal height scale (m) for prediction of ventilation induced by buoyancy. This value (ΔH_{NPL}) is defined as the height from the midpoint of the lower opening to the neutral pressure level. Increasing the value will increase the ventilation rate due to buoyancy.

1.11.21.1.7 Field: Effective Thickness of Cavity Behind Exterior Baffle
This field is used to enter a nominal gap thickness (m) for the collector. If the baffle is corrugated, use the average depth. This distance value is only used when the collector is near horizontal to determine a length scale in the vertical direction for buoyancy calculations. For example, if the collector is mounted on a flat roof, its tilt-adjusted height is zero and the program will use this gap thickness as a length scale rather than the height from the previous field.

1.11.21.1.8 Field: Ratio of Actual Surface Area to Projected Surface Area
This field is used to enter a factor that accounts for the extra surface area resulting from and uneven baffle surface. Corrugations may be present to help stiffen the baffle or ventilated roofing tiles may have more surface are for convection heat transfer than the underlying surface. The projected surface area is obtained by the program from the (flat) underlying surfaces. If the baffle is flat then this ratio is 1.0. If the baffle is corrugated, then this ratio will be greater than one with a typical value might be 1.165.

1.11.21.1.9 Field: Roughness of Exterior Surface
This field is used to describe the relative roughness of the baffle material. This field is similar to one in the **Material** object. This parameter only influences the convection coefficients, more specifically the exterior convection coefficient. A special keyword is expected in this field with the options being

"VeryRough", "Rough", "MediumRough", "MediumSmooth", "Smooth", and "VerySmooth" in order of roughest to smoothest options.

1.11.21.1.10 Field: Effectiveness for Perforations with Respect to Wind
This field is used to enter a value for the coefficient used to determine natural air exchanges from wind. Wind will cause exterior air to move in and out of the cavity. Cv is an arbitrary coefficient used to model the effectiveness of openings and depends on opening geometry and the orientation with respect to the wind. Cv should probably be in the range 0.05 to 0.65. Increasing Cv will increase the amount of natural ventilation. The following equation shows how Cv is used in the program to predict the volumetric flow rate due to wind:

$$\dot{V}_{\text{wind}} = C_v A_{\text{in}} U_\infty \tag{1.21}$$

1.11.21.1.11 Field: Discharge Coefficient for Openings with Respect to Buoyancy Driven Flow

This field is used to enter a value for the coefficient used to determine natural air exchanges from buoyancy. Stack or buoyancy effects will cause exterior air to move in and out of the cavity. Cd is an arbitrary discharge coefficient that depends on the geometry of the opening. Cd should probably be in the range 0.1 to 1.0. Increasing Cd will increase the amount of natural ventilation. The following equations show how Cd is used in the program to predict the volume flow rate due to buoyancy:

$$\dot{V}_{thermal} = C_D A_{in} \sqrt{2g \Delta H_{NPL} \left(T_{a,cav} - T_{amb}\right)/T_{a,cav}} \text{ (if } T_{a,cav} > T_{amb})$$
$$\dot{V}_{thermal} = C_D A_{in} \sqrt{2g \Delta H_{NPL} \left(T_{amb} - T_{a,cav}\right)/T_{amb}} \text{ (if } T_{amb} > T_{a,cav} \text{ and baffle is vertical)}$$

where ΔH_{NPL} is the value input into the field above for the height scale for buoyancy-driven ventilation.

1.11.21.1.12 Field(s): Surface <1 thru x> Name

The remaining fields are used to name the **BuildingSurface:Detailed** objects that are associated with the exterior naturally vented cavity. These are the underlying heat transfer surfaces and are defined elsewhere in the input file. These surfaces should all specify OtherSideConditionsModel as their exterior environment. The input object can currently accommodate up to ten surfaces, but it is extensible by modifying the Energy+.idd entry.

An example IDF entry is

```
SurfaceProperty:ExteriorNaturalVentedCavity,
  PVRoofPaverExtVentCav1 ,   ! Name
  PVRoofPaverSystem1,        ! OtherSideConditionsModel Object Name
  0.02,    ! Area Fraction of Openings
  0.9,     ! Thermal Emissivity of Exterior Baffle Material
  0.92,    ! Solar Absorbtivity of Exterior Baffle
  0.05,    ! Height scale for buoyancy-driven ventilation
  0.05,    ! Effective Thickness of Cavity Behind Exterior Baffle
  0.97,    ! Ratio of Actual surface area to projected surface area
  Smooth , ! Roughness of collector
  0.1 ,    ! Cv, Effectiveness for perforations with respect to Wind
  0.5 ,    ! Cd, Discharge Coefficient for Openings with respect to buoyancy-driven flow
  Zn001:Roof001 ;   ! Surface Name
```

1.11.21.2 Outputs

In addition to related output that can be obtained for all surfaces, these outputs are available for exterior naturally vented cavity configurations:

- HVAC,Average, Surface Exterior Cavity Air Drybulb Temperature [C]
- HVAC,Average, Surface Exterior Cavity Baffle Surface Temperature [C]
- HVAC,Average, Surface Exterior Cavity Total Natural Ventilation Air Change Rate [ACH]
- HVAC,Average, Surface Exterior Cavity Total Natural Ventilation Mass Flow Rate [kg/s]
- HVAC,Average, Surface Exterior Cavity Natural Ventilation from **W**ind Mass Flow Rate [kg/s]
- HVAC,Average, Surface Exterior Cavity Natural Ventilation from Buoyancy Mass Flow Rate [kg/s]

Figure C - 5: Extract of the EnergyPlus documentation files: Input Output Reference p. 431-434. SurfaceProperty:ExteriorNaturalVentedCavity used for SC 1: Ventilated Cavity. (U.S. Department of Energy, 2020)

1.9.38 Material:RoofVegetation

This definition must be used in order to simulate the green roof (ecoroof) model. The material becomes the outside layer in a green roof construction (see example below). In the initial release of the green roof model, only one material may be used as a green roof layer though, of course, several constructions using that material may be used. In addition, the model works only with the ConductionTransferFunction heat balance solution algorithm. This model was developed for low-sloped exterior surfaces (roofs). It is not recommended for high-sloped exterior surfaces (e.g., walls).

1.9.38.1 Inputs

1.9.38.1.1 Field: Name

This field is a unique reference name that the user assigns to a particular ecoroof material. This name can then be referred to by other input data.

1.9.38.1.2 Field: Height of Plants

This field defines the height of plants in units of meters. This field is limited to values in the range $0.005 <$ Height < 1.00 m. Default is .2 m.

1.9.38.1.3 Field: Leaf Area Index

This is the projected leaf area per unit area of soil surface. This field is dimensionless and is limited to values in the range of $0.001 <$ LAI < 5.0. Default is 1.0. At the present time the fraction vegetation cover is calculated directly from LAI (Leaf Area Index) using an empirical relation. The user may find it necessary to increase the specified value of LAI in order to represent high fractional coverage of the surface by vegetation.

1.9.38.1.4 Field: Leaf Reflectivity

This field represents the fraction of incident solar radiation that is reflected by the individual leaf surfaces (albedo). Solar radiation includes the visible spectrum as well as infrared and ultraviolet wavelengths. Values for this field must be between 0.05 and 0.5. Default is .22. Typical values are .18 to .25.

1.9.38.1.5 Field: Leaf Emissivity

This field is the ratio of thermal radiation emitted from leaf surfaces to that emitted by an ideal black body at the same temperature. This parameter is used when calculating the long wavelength radiant exchange at the leaf surfaces. Values for this field must be between 0.8 and 1.0 (with 1.0 representing "black body" conditions). Default is .95.

1.9.38.1.6 Field: Minimum Stomatal Resistance

This field represents the resistance of the plants to moisture transport. It has units of s/m. Plants with low values of stomatal resistance will result in higher evapotranspiration rates than plants with high resistance. Values for this field must be in the range of 50.0 to 300.0. Default is 180.

1.9.38.1.7 Field: Soil Layer Name

This field is a unique reference name that the user assigns to the soil layer for a particular ecoroof. This name can then be referred to by other input data. Default is **Green Roof Soil**.

1.9.38.1.8   Field: Roughness

This alpha field defines the relative roughness of a particular material layer. This parameter only influences the convection coefficients, more specifically the exterior convection coefficient. A keyword is expected in this field with the options being "VeryRough", "Rough", "MediumRough", "MediumSmooth", "Smooth", and "VerySmooth" in order of roughest to smoothest options. Default is MediumRough.

1.9.38.1.9   Field: Thickness

This field characterizes the thickness of the material layer in meters. This should be the dimension of the layer in the direction perpendicular to the main path of heat conduction. This value must be a positive number. Depths of .10m (4 inches) and .15m (6 inches) are common. Default if this field is left blank is .1. Maximum is .7m. Must be greater than .05 m.

1.9.38.1.10   Field: Conductivity of Dry Soil

This field is used to enter the thermal conductivity of the material layer. Units for this parameter are W/(m-K). Thermal conductivity must be greater than zero. Typical soils have values from .3 to .5. Minimum is .2 (specified in IDD). Default is .35 and maximum (in IDD) is 1.5.

1.9.38.1.11   Field: Density of Dry Soil

This field is used to enter the density of the material layer in units of kg/m^3. Density must be a positive quantity. Typical soils range from 400 to 1000 (dry to wet). Minimum is 300, maximum is 2000 and default if field is left blank is 1100.

1.9.38.1.12   Field: Specific Heat of Dry Soil

This field represents the specific heat of the material layer in units of J/(kg-K). Note that these units are most likely different than those reported in textbooks and references which tend to use kJ/(kg-K) or J/(g-K). They were chosen for internal consistency within EnergyPlus. Only positive values of specific heat are allowed.

1.9.38.1.13   Field: Thermal Absorptance

The thermal absorptance field in the Material input syntax represents the fraction of incident long wavelength (>2.5 microns) radiation that is absorbed by the material. This parameter is used when calculating the long wavelength radiant exchange between various surfaces and affects the surface heat balances (both inside and outside as appropriate). For long wavelength radiant exchange, thermal emissivity and thermal emittance are equal to thermal absorptance. Values for this field must be between 0.0 and 1.0 (with 1.0 representing "black body" conditions). Typical values are from .9 to .98. The default value for this field is 0.9.

1.9.38.1.14   Field: Solar Absorptance

The solar absorptance field in the Material input syntax represents the fraction of incident solar radiation that is absorbed by the material. Solar radiation (0.3 to 2.537 microns) includes the visible spectrum as well as infrared and ultraviolet wavelengths. This parameter is used when calculating the amount of incident solar radiation absorbed by various surfaces and affects the surface heat balances (both inside and outside as appropriate). If solar reflectance (or reflectivity) data is available, then absorptance is equal to 1.0 minus reflectance (for opaque materials). Values for this field must be between 0.0 and 1.0. Typical values are from .6 to .85. The default value for this field is 0.7.

1.9.38.1.15   Field: Visible Absorptance

The visible absorptance field in the Material input syntax represents the fraction of incident visible wavelength radiation that is absorbed by the material. Visible wavelength radiation (0.37 to 0.78 microns weighted by photopic response) is slightly different than solar radiation in that the visible band of wavelengths is much more narrow while solar radiation includes the visible spectrum as well as infrared and ultraviolet wavelengths. This parameter is used when calculating the amount of incident visible radiation absorbed by various surfaces and affects the surface heat balances (both inside and outside as appropriate) as well as the daylighting calculations. If visible reflectance (or reflectivity) data is available, then absorptance is equal to 1.0 minus reflectance (for opaque materials). Values for this field must be between 0.5 and 1.0. The default value for this field is 0.75.

1.9.38.1.16   Field: Saturation Volumetric Moisture Content of the Soil Layer

The field allows for user input of the saturation moisture content of the soil layer. Maximum moisture content is typically less than .5. Range is [.1,.5] with the default being .3.

1.9.38.1.17   Field: Residual Volumetric Moisture Content of the Soil Layer

The field allows for user input of the residual moisture content of the soil layer. Default is .01, range is [.01,.1].

1.9.38.1.18   Field: Initial Volumetric Moisture Content of the Soil Layer

The field allows for user input of the initial moisture content of the soil layer. Range is (.05, .5] with the default being .1.

1.9.38.1.19   Field: Moisture Diffusion Calculation Method

The field allows for two models to be selected: **Simple** or **Advanced**. EnergyPlus Currently supports only the **Simple** *Moisture Diffusion Calculation Method*.

Simple is the original Ecoroof model - based on a constant diffusion of moisture through the soil. This model starts with the soil in two layers. Every time the soil properties update is called, it will look at the two soils moisture layers and asses which layer has more moisture in it. It then takes moisture from the higher moisture layer and redistributes it to the lower moisture layer at a constant rate.

Advanced is the later Ecoroof model. The model requires higher number of timesteps in hour for the simulation with a recommended value of 20. This moisture transport model is based on a project which looked at the way moisture transports through soil. It uses a finite difference method to divide the soil into layers (nodes). It redistributes the soil moisture according the model described in:

Marcel G Schaap and Martinus Th. van Genuchten, 2006, 'A modified Maulem-van Genuchten Formulation for Improved Description of the Hydraulic Conductivity Near Saturation', Vadose Zone Journal 5 (1), p 27-34. However, currently **Advanced** *Moisture Diffusion Calculation Method* is not supported in EnergyPlus.

An IDF example:

```
Material:RoofVegetation,
    BaseEco,                !- Name
    0.5,                    !- Height of Plants {m}
    5,                      !- Leaf Area Index {dimensionless}
    0.2,                    !- Leaf Reflectivity {dimensionless}
    0.95,                   !- Leaf Emissivity
    180,                    !- Minimum Stomatal Resistance {s/m}
    EcoRoofSoil,            !- Soil Layer Name
    MediumSmooth,           !- Roughness
    0.18,                   !- Thickness {m}
    0.4,                    !- Conductivity of Dry Soil {W/m-K}
    641,                    !- Density of Dry Soil {kg/m3}
```

```
1100,                      !- Specific Heat of Dry Soil {J/kg-K}
0.95,                      !- Thermal Absorptance
0.8,                       !- Solar Absorptance
0.7,                       !- Visible Absorptance
0.4,                       !- Saturation Volumetric Moisture Content of the Soil Layer
0.01,                      !- Residual Volumetric Moisture Content of the Soil Layer
0.2,                       !- Initial Volumetric Moisture Content of the Soil Layer
Simple;                    !- Moisture Diffusion Calculation Method

Material:RoofVegetation,
LowLAI,                    !- Name
0.5,                       !- Height of Plants {m}
0.5,                       !- Leaf Area Index {dimensionless}
0.2,                       !- Leaf Reflectivity {dimensionless}
0.95,                      !- Leaf Emissivity
180,                       !- Minimum Stomatal Resistance {s/m}
EcoRoofSoil,               !- Soil Layer Name
MediumSmooth,              !- Roughness
0.18,                      !- Thickness {m}
0.4,                       !- Conductivity of Dry Soil {W/m-K}
641,                       !- Density of Dry Soil {kg/m3}
1100,                      !- Specific Heat of Dry Soil {J/kg-K}
0.95,                      !- Thermal Absorptance
0.8,                       !- Solar Absorptance
0.7,                       !- Visible Absorptance
0.4,                       !- Saturation Volumetric Moisture Content of the Soil Layer
0.01,                      !- Residual Volumetric Moisture Content of the Soil Layer
0.2,                       !- Initial Volumetric Moisture Content of the Soil Layer
Simple;                    !- Moisture Diffusion Calculation Method
```

And construction using the ecoroof material:

```
Construction,
    ASHRAE 90.1-2004_Sec 5.5-2_Roof,  !- Name
    BaseEco,                          !- Outside Layer
    ASHRAE 90.1-2004_Sec 5.5-2_Roof Insulation_1,  !- Layer \#2
    ASHRAE 90.1-2004_Sec 5.5-2_MAT-METAL;  !- Layer \#3
```

1.9.39 Ecoroof / RoofVegetation outputs

The following outputs are available for the Roof Vegetation surface.

- Zone,Average,Green Roof Soil Temperature [C]
- Zone,Average,Green Roof Vegetation Temperature [C]
- Zone,Average,Green Roof Soil Root Moisture Ratio []
- Zone,Average,Green Roof Soil Near Surface Moisture Ratio []
- Zone,Average,Green Roof Soil Sensible Heat Transfer Rate per Area [W/m2]
- Zone,Average,Green Roof Vegetation Sensible Heat Transfer Rate per Area [W/m2]
- Zone,Average,Green Roof Vegetation Moisture Transfer Rate [m/s]
- Zone,Average,Green Roof Soil Moisture Transfer Rate [m/s]
- Zone,Average,Green Roof Vegetation Latent Heat Transfer Rate per Area [W/m2]
- Zone,Average,Green Roof Soil Latent Heat Transfer Rate per Area [W/m2]
- Zone,Sum,Green Roof Cumulative Precipitation Depth [m]
- Zone,Sum,Green Roof Cumulative Irrigation Depth [m]
- Zone,Sum,Green Roof Cumulative Runoff Depth [m]
- Zone,Sum,Green Roof Cumulative Evapotranspiration Depth [m]
- Zone,Sum,Green Roof Current Precipitation Depth [m]
- Zone,Sum,Green Roof Current Irrigation Depth [m]
- Zone,Sum,Green Roof Current Runoff Depth [m]
- Zone,Sum,Green Roof Current Evapotranspiration Depth [m]

Figure C - 6: Extract of the EnergyPlus documentation files: Input Output Reference p.227-231. Material:RoofVegetation used for SC 4: Vegetated roof. (U.S. Department of Energy 2020)

4.1 Exterior Naturally Vented Cavity

The input object "SurfaceProperty:ExteriorNaturalVentedCavity" allows modeling a special case for the outside boundary conditions of heat transfer surfaces with a multi-skin exterior that is opaque. From the thermal envelope's point of view, the presence of a vented cavity on the outside of the surface modifies the conditions experienced by the underlying heat transfer surfaces. This exterior cavity acts as a radiation and convection baffle situated between the exterior environment and the outside face of the underlying heat transfer surface. The actual outer surface is referred to as the "baffle". The modeling here assumes that the heat capacity in the outer baffle can be neglected since it is much lower than the underlying mass surface. This object is used with the BuildingSurface:Detailed object where the heat transfer surfaces are referred to as the underlying surfaces. The constructions and materials for the heat transfer surfaces should reflect the construction of just the underlying surface. The SurfaceProperty:ExteriorNaturalVentedCavity object is used to describe the detached layer, or baffle, and the characteristics of the cavity and openings for natural ventilation. This model uses the SurfaceProperty:OtherSideConditionsModel object to pass boundary conditions to the heat transfer modeling for the underlying surfaces.

4.1.1 Baffle Heat Balance

The baffle is assumed to be sufficiently thin and high-conductivity so that it can be modeled using a single temperature (for both sides and along its area). This temperature $T_{s,baff}$ is determined by formulating a heat balance on a control volume that just encapsulates the baffle surface. The baffle is assumed to completely cover the underlying surface such that it is opaque to shortwave and longwave radiation. This assumption means that even though the baffle will have some open area for ventilation, no solar energy passes through these openings. The heat balance is diagrammed in the following figure.

The heat balance on the baffle surface's control volume is:

$$q''_{asol} + q''_{LWR,Env} + q''_{conv,Env} + q''_{LWR,cav} + q''_{conv,cav} + q''_{source} = 0 \qquad (4.1)$$

where:

q''_{asol} is absorbed direct and diffuse solar (short wavelength) radiation heat flux.

$q''_{LWR,Env}$ is net long wavelength (thermal) radiation flux exchange with the air and surroundings.

$q''_{conv,Env}$ = surface convection flux exchange with outside air.

$q''_{LWR,cav}$ is net long wavelength (thermal) radiation flux exchange with the outside face of the underlying surface(s).

$q''_{conv,cav}$ = surface convection flux exchange with cavity air.

q''_{source} is a source/sink term that accounts for energy exported out of the control volume when the baffle is a hybrid device such as a photovoltaic panel.

All terms are positive for net flux to the baffle. Each of these heat balance components is introduced briefly below.

4.1.1.1 External SW Radiation

q''_{asol} is calculated using procedures presented elsewhere in this manual and includes both direct and diffuse incident solar radiation absorbed by the surface face. This is influenced by location, surface facing angle and tilt, shading surfaces, surface face material properties, weather conditions, etc. The baffle blocks all shortwave radiation from reaching the underlying surface.

4.1.1.2 External LW Radiation

$q''_{LWR,Env}$ is a standard radiation exchange formulation between the surface, the sky, the ground, and the atmosphere. The radiation heat flux is calculated from the surface absorptivity, surface temperature, sky, air, and ground temperatures, and sky and ground view factors. Radiation is modeled using linearized coefficients. The baffle blocks all longwave radiation.

4.1.1.3 External Convection

$q''_{conv,env}$ is modeled using the classical formulation: $q''_{conv} = h_{co}(T_{air} - T_o)$ where h_{co}, is the convection coefficient. The h_{co} is treated in the same way as an outside face with ExteriorEnvironment conditions. In addition, when it is raining outside, we assume the baffle gets wet and model the enhanced surface heat transfer using a large value for h_{co} .

4.1.1.4 Cavity LW Radiation

$q''_{LWR,cav}$ is a standard radiation exchange formulation between the baffle surface and the underlying heat transfer surface located across the cavity. Radiation is modeled using linearized coefficients.

4.1.1.5 Cavity Convection

$q''_{conv,cav}$ is modeled using the classical formulation: $q''_{conv} = h_{cp}(T_{air} - T_o)$ where h_{cp}, is the convection coefficient. The value for h_{cp} is obtained from correlations used for window gaps from ISO (2003) standard 15099.

Substituting models into Equation 4.1 and solving for $T_{s,baff}$ yields the following equation:

$$T_{s,baff} = \frac{(I_s\alpha + h_{co}T_{amb} + h_{r,atm}T_{amb} + h_{r,sky}T_{sky} + h_{r,gnd}T_{amb} + h_{r,cav}T_{so} + h_{c,cav}T_{a,cav} + q''_{source})}{(h_{co} + h_{r,air} + h_{r,sky} + h_{r,gnd} + h_{r,cav} + h_{c,cav})}$$

(4.2)

where,

I_s is the incident solar radiation of all types [W/m²],

α is the solar absorptivity of the baffle [dimensionless],

$h_{r,atm}$ is the linearized radiation coefficient for the surrounding atmosphere [W/m² · K],

T_{amb} is the outdoor drybulb from the weather data, also assumed for ground surface [ºC],

$h_{r,sky}$ is the linearized radiation coefficient for the sky [W/m² · K],

T_{sky} is the effective sky temperature [ºC],

$h_{r,gnd}$ is the linearized radiation coefficient for the ground [W/m² · K],

$h_{r,cav}$ is the linearized radiation coefficient for the underlying surface [W/m² · K],

T_{so} is the temperature of the outside face of the underlying heat transfer surface [ºC],

h_{co} is the convection coefficient for the outdoor environment [W/m² · K],

$h_{c,cav}$ is the convection coefficient for the surfaces facing the plenum [W/m² · K], and

$T_{a,cav}$ is the drybulb temperature for air in the cavity [ºC].

4.1.2 Cavity Heat Balance

The *cavity* is the volume of air located between the baffle and the underlying heat transfer surface. The cavity air is modeled as well-mixed. The uniform temperature of the cavity air, $T_{a,cav}$, is determined by formulating a heat balance on a control volume of air as diagrammed below.
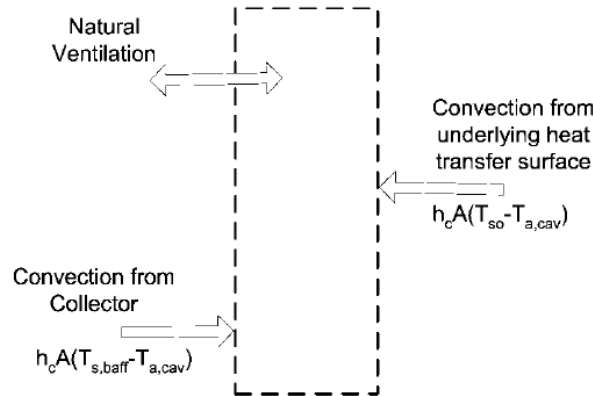
Figure 4.2: Cavity Air Heat Balance

The heat balance on the cavity air control volume is:

$$\dot{Q}_{vent} + \dot{Q}_{co} + \dot{Q}_{c,baff} = 0$$

(4.3)

where,

$\dot{Q}_{vent}$ is the net rate of energy added from natural ventilation – where outdoor ambient air exchanges with the cavity air.

$\dot{Q}_{co}$ is the net rate of energy added by surface convection heat transfer with the underlying surface.

$\dot{Q}_{c,baff}$ is the net rate of energy added by surface convection heat transfer with the collector.

And substituting into Equation 4.3 yields the following equation:

$$T_{a,cav} = \frac{(h_{c,cav} A \, T_{so} + \dot{m}_{vent} c_p T_{amb} + h_{c,cav} A \, T_{s,baff})}{(h_{c,cav} A + \dot{m}_{vent} c_p + h_{c,cav} A)} \quad (4.4)$$

where,

$\dot{m}_{vent}$ is the air mass flow from natural forces [kg/s]

Modeling natural ventilation air exchanges in a general way is challenging. Simplistic engineering models are used to model $\dot{m}_{vent}$ resulting from natural buoyancy and wind forces. Reasoning that the configuration is similar to single-side natural ventilation, we elect to use correlations for natural ventilation presented as equations (29) and (30) in Chapter 26 of ASHRAE Handbook of Fundamentals (2001).

$$\dot{m}_{vent} = \rho \dot{V}_{tot} \quad (4.5)$$

where,

ρ is the density of air [kg/m³], and

$\dot{V}_{tot} = \dot{V}_{wind} + \dot{V}_{thermal}$ is the total volumetric flow rate of air ventilating in and out of the cavity.

$\dot{V}_{wind} = C_v A_{in} U_\infty$

$\dot{V}_{thermal} = C_D A_{in} \sqrt{2g \Delta H_{NPL} (T_{a,cav} - T_{amb})/T_{a,cav}}$ (if $T_{a,cav} > T_{amb}$)

$\dot{V}_{thermal} = C_D A_{in} \sqrt{2g \Delta H_{NPL} (T_{amb} - T_{a,cav})/T_{amb}}$ (if $T_{amb} > T_{a,cav}$ and baffle is vertical)

C_v is the effectiveness of the openings that depends on opening geometry and the orientation with respect to the wind. ASHRAE HoF (2001) indicates values ranging from 0.25 to 0.6. This value is available for user input.

C_D is the discharge coefficient for the opening and depends on opening geometry. This value is available for user input.

Mass continuity arguments lead to modeling the area of the openings as one half of the total area of the openings, so we have:

$$A_{in} = \frac{A}{2} \quad (4.6)$$

g is the gravitational constant taken as 9.81 [m/s²].

ΔH_{NPL} is the height from midpoint of lower opening to the Neutral Pressure Level. This is value is available for user input.

If the cavity is horizontal and $T_{amb} > T_{a,cav}$ then $\dot{V}_{thermal} = 0$ because this is a stable situation.

4.1.3 Underlying Heat Transfer Surface

The exterior baffle and cavity are applied to the outside of a heat transfer surface. This surface is modeled using the usual EnergyPlus methods for handling heat capacity and transients – typically the CTF method. These native EnergyPlus heat balance routines are used to calculate T_{so}. The exterior baffle and cavity system is coupled to the underlying surface using the SurfaceProperty:OtherSideConditionsModel mechanism. The exterior naturally vented cavity model provides values for $h_{r,cav}$, $T_{s,baff}$, $h_{c,cav}$, and $T_{a,cav}$ for use with the heat balance model calculations for the outside face of the underlying surface (described elsewhere in this manual).

Figure C - 7: Extract of the EnergyPlus documentation files: Engineerign Reference p.169-174. Exterior Naturally Vented Cavity used for SC 1: Vented cavity. (U.S. Department of Energy, 2020)

C.5. Results Output data EnergyPlus

MONTHLY: JANUARY - DECEMBER		Cooling:	ON											
	GAINS AND LOSSES								TEMPERATURES				ENERGY NEED	
Date/Time	UNZ_0:Zone People Total Heating Energy [J](Monthly)	UNZ_0:Zone Lights Total Heating Energy [J](Monthly)	UNZ_0:Zone Windows Total Heat Gain Energy [J](Monthly)	UNZ_0:Zone Windows Total Heat Loss Energy [J](Monthly)	UNZ_0:Zone Opaque Surface Inside Faces Total Conduction Heat Gain Energy [J](Monthly)	UNZ_0:Zone Opaque Surface Inside Faces Total Conduction Heat Loss Energy [J](Monthly)	UNZ_0:Zone Infiltration Total Heat Loss Energy [J](Monthly)	UNZ_0:Zone Infiltration Total Heat Gain Energy [J](Monthly)	UNZ_0:F0: Surface Inside Face Temperature [C](Monthly)	UNZ_0:F0: Surface Outside Face Temperature [C](Monthly)	UNZ_0:Zone Outdoor Air Drybulb Temperature [C](Monthly)	UNZ_0:Zone Mean Air Temperature [C](Monthly)	UNZ_0 IDEAL LOADS AIR:Zone Ideal Loads Zone Total Heating Energy [J](Monthly)	UNZ_0 IDEAL LOADS AIR:Zone Ideal Loads Zone Total Cooling Energy [J](Monthly)
January	28004796040	841032720	14420867963	5498170190	2064714735	3.2925E+10	1.5102E+10	224597.509	18.1469515	**15.8601803**	13.8576273	20.6161314	1.21E+10	2.76E-04
February	25458905491	764575200	15260250857	5333434193	3961134610	2.8344E+10	1.4931E+10	6304011.46	19.5888426	17.5982076	14.3589564	21.2153762	6.62E+09	1.40E+08
March	29277741315	879261480	16040446794	5917723322	7769363190	2.7849E+10	1.7325E+10	9800835.31	22.3955542	21.1162248	16.4697408	23.0086313	2.84E+09	1.06E+09
April	25458905491	764575200	15143341443	5688930055	9503081456	1.8811E+10	1.3115E+10	50022861.3	27.0860244	27.0221772	21.6918197	26.2402186	3.23E+08	1.16E+10
May	29277741315	879261480	14905235640	5756511542	13696019314	1.5749E+10	1.3436E+10	684846556	29.9937936	30.7898088	24.5940016	27.9663708	1.55E+03	2.27E+10
June [J]	28004796040	841032720	14031400423	4568094225	18857631426	7272316849	6521679305	406449605	33.0886012	34.8842603	27.8643371	28.9854415	3.41E-04	4.31E+10
June [kWh/m²]	12.53	0.38	6.28	2.04	8.44	3.25	2.92	0.18					0.00	19.29
July	26731850766	802803960	14166198204	4488940811	20285325895	6646714769	3684117608	1042899283	33.3418602	**35.4122861**	28.0835009	28.9976975	2.17E-04	4.75E+10
August	29277741315	879261480	15241044900	4615239062	18995072148	9154139388	3731878942	1176133990	32.8552115	34.3484007	27.8369955	28.9978716	9.04E-05	4.73E+10
September	26731850766	802803960	17858420117	4937200229	14181441232	1.4758E+10	6796193440	406614081	31.3604426	31.8858077	26.4575141	28.8522339	1.43E-04	3.28E+10
October	28004796040	841032720	17007773315	5226696581	9002616214	1.9884E+10	1.1292E+10	109572329	28.0729186	27.3304362	23.737214	27.4549936	3.28E-05	1.67E+10
November	28004796040	841032720	16277172592	5079293501	7113537142	2.5776E+10	1.4771E+10	27750987.8	23.0438787	21.4286925	18.8989725	23.7058547	1.05E+08	1.34E+09
December	26731850766	802803960	16417075500	5461133576	4456833659	3.0868E+10	1.4302E+10	10756943.2	19.3552009	17.236996	15.1981347	21.1060696	6.65E+09	1.50E-04
									MAX roof	**35.4122861**		Annual [J]	28661420871	2.24307E+11
									MIN roof	**15.8601803**		Annual [kWh/m²]	**12.82**	**100.33**

Table C - 2: Monthly simulation results for SC 0. Gains and losses used for the Sankey diagram, surface and air temperatures, monthly energy need for cooling and heating summed up for the annual energy need.

Scenario	SC1 10 cm						SC1 50 cm						SC1 270 cm					
Date/Time	VENTCAV_S C1: Surface Exterior Cavity Baffle Surface Temperature [C](Monthly)	VENTCAV_S C1: Surface Exterior Cavity Air Drybulb Temperature [C](Monthly)	VENTCAV_S C1: Surface Exterior Cavity Total Natural Ventilation Mass Flow Rate [kg/s](Monthly)	VENTCAV_S C1: Surface Exterior Cavity Natural Ventilation from Wind Mass Flow Rate [kg/s](Monthly)	UNZ_0 IDEAL LOADS AIR:Zone Ideal Loads Zone Total Heating Energy [J](Monthly)	UNZ_0 IDEAL LOADS AIR:Zone Ideal Loads Zone Total Cooling Energy [J](Monthly)	VENTCAV_S C1: Surface Exterior Cavity Baffle Surface Temperature [C](Monthly)	VENTCAV_S C1: Surface Exterior Cavity Air Drybulb Temperature [C](Monthly)	VENTCAV_S C1: Surface Exterior Cavity Total Natural Ventilation Mass Flow Rate [kg/s](Monthly)	VENTCAV_S C1: Surface Exterior Cavity Natural Ventilation from Wind Mass Flow Rate [kg/s](Monthly)	UNZ_0 IDEAL LOADS AIR:Zone Ideal Loads Zone Total Heating Energy [J](Monthly)	UNZ_0 IDEAL LOADS AIR:Zone Ideal Loads Zone Total Cooling Energy [J](Monthly)	VENTCAV_S C1: Surface Exterior Cavity Baffle Surface Temperature [C](Monthly)	VENTCAV_S C1: Surface Exterior Cavity Air Drybulb Temperature [C](Monthly)	VENTCAV_S C1: Surface Exterior Cavity Total Natural Ventilation Mass Flow Rate [kg/s](Monthly)	VENTCAV_S C1: Surface Exterior Cavity Natural Ventilation from Wind Mass Flow Rate [kg/s](Monthly)	UNZ_0 IDEAL LOADS AIR:Zone Ideal Loads Zone Total Heating Energy [J](Monthly)	UNZ_0 IDEAL LOADS AIR:Zone Ideal Loads Zone Total Cooling Energy [J](Monthly)
January	15.50076489	14.09980181	6.17297064	6.04477661	9335405289	2.12E-04	15.51341912	13.85466465	30.78969069	30.22388305	9149857713	1.96E-04	15.51555958	13.81127746	165.3416334	162.5726762	9112427341	2.09E-04
February	17.40754168	14.78774847	7.677780114	7.511573907	4635679644	101130037.5	17.42282666	14.394467	38.30906588	37.55786954	4497191933	105841849.6	17.42475223	14.31935602	205.766626	202.0218035	4469222628	106858718.9
March	20.96424575	17.02090096	7.248917855	7.058629942	1966936989	902672586.5	20.99141337	16.53814576	36.14805726	35.29314971	1908811463	959284800.1	20.9949516	16.44225354	194.0752383	189.8399947	1896519567	971320305.9
April	27.27398932	22.24715682	8.131396775	7.951155651	154606043.8	11085031736	27.31942754	21.77165965	40.51296159	39.75577826	144434501.5	11297408338	27.32936031	21.69315339	217.4786468	213.8442388	142383850.9	11341086000
May	31.07890874	25.23118665	8.282291033	8.097462716	113.6452114	20894869881	31.12484762	24.69887892	41.26028568	40.48731358	494.3183453	21237612728	31.13400631	24.60379708	221.4645628	217.7791288	558.3443717	21310786697
June	35.37506706	28.49896081	7.408249165	7.218531078	2.72E-04	39153013318	35.43904979	27.95000171	36.86258616	36.09265539	2.80E-04	39668417614	35.45364312	27.86705266	197.7395965	194.1404937	2.80E-04	39787721810
July	35.8600427	28.75259406	6.31896162	6.121809277	1.58E-04	42879542133	35.9296247	28.17493136	31.41237332	30.60904639	1.56E-04	43469528936	35.94547308	28.0897769	168.4134244	164.6444495	1.68E-04	43605799310
August	34.4897525	28.53750932	6.19526429	5.997220459	7.08E-05	43292218108	34.53232382	27.95252619	30.84378026	29.98610229	7.36E-05	43743618450	34.54072602	27.84714359	165.4381243	161.293666	7.02E-05	43840891046
September	32.02236504	27.06699379	6.369338485	6.185056598	1.11E-04	31020915602	32.05916702	26.56799361	31.74169776	30.92528299	1.13E-04	31372510685	32.0643757	26.47056414	170.3014509	166.3454695	1.05E-04	31440896201
October	27.38382926	24.17260451	6.617296876	6.462731027	234.9333372	17296974087	27.4182289	23.79939435	32.97051621	32.31365514	2873.947169	17556367091	27.42570662	23.7391421	176.9554942	173.8134503	3089.086154	17609760678
November	21.05889721	19.25851062	5.279470567	5.138984899	35484265.66	1521492698	21.07350638	18.95703715	26.33215389	25.6949245	31325042.13	1615041339	21.07523052	18.90011996	141.3655191	138.2116465	30450625.97	1632734478
December	16.75233808	15.48097124	5.227310878	5.097248226	4486259155	1.07E-04	16.76082194	15.23193341	26.07543421	25.48624113	4374803506	9.47E-05	16.76199051	15.18635712	140.0160725	137.0891497	4352779696	9.53E-05
Annual [J]					20614371735	2.08148E+11					20106427526	2.11026E+11					20003787356	2.11648E+11
Annual [kWh/m²]					9.22	93.11					8.99	94.39					8.95	94.67

Table C - 3: Monthly simulation results for SC 1. Comparison of the three cavity thicknesses 10 cm, 50 cm and 270 cm. Baffle and Cavity temperatures, mass flow rate due to wind and buoyancy, and mass flow rate due to wind (higher for respectively 270 cm > 50cm > 10cm). Annual energy need calculated from the monthly values.

ANNUAL ENERGY DEMAND	Heating	Cooling	Total
SC0	12.82	100.33	113.15
SC1 10cm	9.22	93.11	102.33
		7.20	9.57 % reduc
SC1 10°	13.36	84.15	97.51
		16.13	13.83 % reduc
SC2 cool	19.72	65.73	85.45
		34.49	24.48 % reduc
SC2.1	13.33	66.77	80.10
		33.45	29.21 % reduc
SC3	16.66	67.94	84.60
		32.29	25.23 % reduc
SC 3.1	9.74	69.10	78.84
		31.13	30.33 % reduc
SC4	3.59	97.30	100.89
		3.02	10.84 % reduc

Table C - 4: Summary of the simulation results of SC 0 to 4. Annual heating, cooling and total energy need. Reduction achieved by each scenario compared to SC 0.

TEMPERATURES	overheating			Roof temperature			Roof temperature Monthly year		
	MAX indoor air temperature June	MIN indoor air temperature June	MAX temperature reduction	Max roof temperature Cooling Off June	Min roof temperature Cooling Off June	MAX temperature reduction June	Max roof temperature Cooling On	Min roof temperature Cooling On	MAX temperature reduction
SC0	40.65	27.89	0	57.51	20.6	0	35.41	15.86	0
SC1	39.49	27.76	1.99	46.37	25.8	13.2	34.17	17.02	1.24
SC1 10°	39.09	27.18	2.48	45.57	25.55	14.22	33.83	16.47	3
SC2	38.06	26.08	3.48	46.16	19.74	14.77	30.78	13.9	4.63
SC2.1	37.11	26.25	4.51	37.11	26.25	22.26	30.57	15.69	3.88
SC3	38.52	26.53	3.07	47.68	20.83	19.23	31.27	14.8	4.31
SC4	38.09	27.69	3.99	62.32	20.78	2.14	37.66	18.34	-1.63

Table C - 5: Summary of the simulation results of SC 0 to 4. *Left*: Air temperatures when cooling setpoint is off, hourly values for June. *Centre*: Extreme roof surface temperatures. Hourly values for June. *Right*: Extreme average roof temperatures. Monthly values for all year.

ANNUAL ENERGY DEMAND: COOL ROOF ON VENTILATED CAVITY		Heating	Cooling	Total
	SC0	12.82	100.33	**113.15**
Vent cav	SC1	9.22	93.11	**102.33**
		28.08	7.20	9.57 % reduc
		3.60	7.23	10.83 reduc
Cool roof	SC2	19.72	65.73	**85.45**
		-53.83	34.49	24.48 % reduc
		-6.90	34.60	27.70 reduc
	SC2.1	13.330	66.769	**80.099**
	SC2.1 theory	13.330	66.770	**80.100**
		-3.97	33.45	29.21 % reduc
		-0.51	33.57	33.06 reduc

	Heating	Cooling
factor SC2&3	0.3913	0.962
factor SC1	0.6087	0.038
sum	1	1

ANNUAL ENERGY DEMAND: SELF SHADING ON VENTILATED CAVITY		Heating	Cooling	Total
	SC0	12.82	100.33	**113.15**
Vent cav	SC1	5.29	98.46	**103.75**
		58.72	1.87	8.31 % reduc
		7.53	1.88	9.41 reduc
Self shading	SC3	16.66	67.94	**84.60**
		-29.93	32.29	25.24 % reduc
		-3.84	32.39	28.56
	SC3.1 theory	9.74	69.10	**78.84**
		24.03	31.13	30.33 %reduc SC0
			25.78	22.95 %reduc SC1

Table C - 6: Summary of the methodology for SC 3.1 based on influence factors experienced in SC 2.1.